

**One-Step Ammonia
Using Magnetic Nano-catalyst**

By

Norhasifah Binti Noordin

10919

Dissertation submitted in partial fulfillment of
the requirements for the
Bachelor of Engineering (Hons)
(Chemical Engineering)

SEPTEMBER 2011

Universiti Teknologi PETRONAS
Bandar Seri Iskandar
31750 Tronoh
Perak Darul Ridzuan

**ONE-STEP AMMONIA
USING MAGNETIC NANOCATALYST**

NORHASIFAH BINTI NOORDIN

10919

**CHEMICAL ENGINEERING
UNIVERSITI TEKNOLOGI PETRONAS**

SEPTEMBER 2011

CERTIFICATION OF APPROVAL

CAB4612

FINAL YEAR PROJECT 1

September 2011 Semester

**ONE-STEP AMMONIA
USING MAGNETIC NANO-CATALYST**

BY

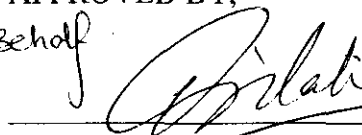
NORHASIFAH BINTI NOORDIN

10919

A project dissertation submitted to the
Chemical Engineering Programme
Universiti Teknologi PETRONAS
in partial fulfillment of the requirement for the
BACHELOR OF ENGINEERING (Hons)
(CHEMICAL ENGINEERING)

APPROVED BY,

On Behalf



Dr. Ku Zilati Ku Shaari
Senior Lecturer
Chemical Engineering Department
Universiti Teknologi PETRONAS

(PROFESSOR DR. NOORHANA YAHYA)

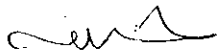
FUNDAMENTAL AND APPLIED SCIENCE

UNIVERSITI TEKNOLOGI PETRONAS
TRONOH, PERAK

SEPTEMBER 2011

CERTIFICATION OF ORIGINALITY

This is to certify that I am responsible for the work submitted in this project, that the original work is my own except as specified in the references and acknowledgements, and that the original work contained herein have not been undertaken or done by unspecified sources or persons.



NORHASIFAH BINTI NOORDIN 10919

ABSTRACT

Ammonia production is a very energy and capital intensive industry as it requires high temperature (400–500°C) and high pressure (150–300 bar) for its daily operations. In order to overcome these drawbacks, application of magnetic nanocatalyst with magnetic induction method is seen as an excellent solution. By introducing nano-catalyst with the new concept of micro-reactor with magnetic field induction applied, the catalytic activity can be induced and the yield can be enhanced. The magneto-dynamic will be introduced in the ammonia production process in order to replace the concept of thermodynamic in Haber Bosch which require the production of ammonia at high temperature and high pressure. The nanocatalysts have been reduced by using Temperature Reduction Method (TPR) and YIG nanocatalyst has been reduced from $Y_3Fe_5O_{12}$ to Y_3Fe at 960°C temperature. Hematite nanocatalyst has been reduced from Fe_2O_3 to Fe metal at 1025°C temperature while Manganese Oxide nanocatalyst has been reduced from MnO to Mn metal at 470°C temperature. Besides, Manganese Zinc Ferrite nanocatalyst has been reduced from $Mn_{0.8}Zn_{0.2}Fe_2O_4$ to MnZnFe at 736°C temperature. The $Y_3Fe_5O_{12}$ (YIG) catalyst with magnetic induction has been produced 242.56 $\mu\text{mol/h.g-cat}$ yield of ammonia which is 95.88% much higher than ammonia synthesis without magnetic induction (10 $\mu\text{mol/h.g-cat}$). The ammonia yield with magnetic induction method at temperature 0°C is 242.56 $\mu\text{mole/h.g-cat}$ which is 0.90% higher than synthesis at 25°C temperature (240.4 $\mu\text{mol/h.g-cat}$). Ammonia yield at 0.2 Tesla is 249.04 $\mu\text{mole/h.g-cat}$ which is higher than yield at 0.1 Tesla which is 242.56 $\mu\text{mol/h.g-cat}$. It is proven that as more magnetic field applied, more effective the catalytic activity will be as better alignment of the electron spin of the catalyst occur and enhance the adsorption and desorption process. $Y_3Fe_5O_{12}$ (YIG) shows the best catalytic reaction followed by Fe_2O_3 (Hematite) and MnO (Manganese Oxide). By this new route, synthesis of ammonia at low temperature is realized and offers the ammonia producers a potential contender in the market place.

Chapter 1 in this study will discuss about background of the study on current scenario and history of ammonia production, problem statement and objectives and

scope of the study. On chapter 2, the theory is been discussed especially about the ammonia synthesis, ammonia feeds and products properties, followed by the ammonia market data, the concept of energy, concept of thermodynamic on Haber Bosch process, the concept of thermo-magnetic equilibrium reaction, the theory of magnetic induction, Hemholtz coil, atom and magnetic field, application of magnetic nano-catalyst, catalytic reaction. Then, topic discussed is about the micro-reactor, and last but not least about temperature programmed reduction (TPR). Next, the methodology is described in chapter 3 whereas the subtopic is divided into design of experiment which involved four phases that are planning, screening, optimize and verification. Next, sample preparation and sample testing is being discussed. Chapter 4 consists of result and discussion where the result of TPR and result of yield in Experiment 1 to Experiment 8 percentage is calculated. Last but not least, conclusion and recommendation is provided in Chapter 5.

ACKNOWLEDGEMENTS

First of foremost, I am very grateful to Allah for His blessing and inspiration during the whole semester for this project. I am also very grateful and thankful for the consistent encouragement from and knowledge shared by my Final Year Project FYP Supervisor that is Professor Dr.Noorhana Yahya. She is a very talented and brilliant person, without her supervision, concern and support, this particular project would not be as complete as it is today.

My gratitude is extended to FYP2 coordinator, Dr.Lukman Ismail for his time and commitment in arranging various seminars to provide support and knowledge in assisting me. Not forgotten, I also would like to thank Miss Poppy Puspitasari, a PhD candidates for her full support, help and contribution along the process of preparing the catalyst and provide guidance in doing the experiments and theory.

Never forget to my family and friends who always give me support to finish this project. I really appreciate all the supports and guidance that I receive from all party during this project. Thank you.

TABLE OF CONTENTS

LIST OF TABLES	viii
LIST OF FIGURES.....	ix
CHAPTER 1 INTRODUCTION	1
1.1 Background of Study	1
1.1.1 Current Scenario.....	1
1.1.2 History of Ammonia Production	3
1.1.3 Haber Bosch Process.....	4
1.2 Problem Statements	6
1.3 Objectives and Scope of Study	7
CHAPTER 2 LITERATURE REVIEW AND THEORY.....	9
2.1 Ammonia Synthesis	9
2.1.1 Feed Properties.....	15
2.1.2 Product Properties	16
2.2 Ammonia Market Data	20
2.3 The Concept of Energy	23
2.3.1 Law of Thermodynamics	26
2.3.2 The Thermodynamic Concept in Haber Bosch Process.....	28
2.3.3 The Concept of Thermo-Magnetic Induction Equilibrium Reaction	31
2.4 Theory of Magnetic Induction	35
2.4.1 Domains and Hysteresis	37
2.4.2 Magnetization versus Temperature	38
2.4.3 Ferromagnetism.....	39
2.4.4 The Magnetic Field Effects in Chemical Reaction	40
2.4.5 Magneto-Thermodynamic Effect in Chemical Reaction.....	47
2.5 Hemholtz Coil.....	49
2.6 Atom and Magnetic Field	53
2.7 Application of Magnetic Nano-catalyst.....	54
2.8 Catalytic Reaction.....	62
2.8.1 Catalyst and Magnetism	62
2.8.1 Adsorption Process.....	63

2.8.2 Desorption	65
2.9 Micro-Reactor	66
2.10 Kjeldahl Method	67
2.11 Temperature Programmed Reduction (TPR)	75
CHAPTER 3 METHODOLOGY	76
3.1 Design of Experiments	76
3.2 Elements Determination	78
3.3 Sample Preparation	78
3.3.1 Experiment 1: Find the Trend of the Optimum Catalytic Induction	78
3.3.2 Experiment 2: Synthesis of Ammonia at Different Magnetic Conditions	79
3.3.3 Experiment 3: Synthesis of Ammonia Using Different Type of Catalysts	80
3.3.4 Experiment 4: Synthesis of Ammonia at Different System's Temperature	81
3.3.5 Experiment 5: Synthesis of Ammonia at Different Temperature of Inlet Gas	82
3.3.6 Experiment 6: Synthesis of Ammonia at Different TPR Condition	84
3.3.7 Experiment 7: Synthesis of Ammonia at Different Magnetic Strength	85
3.3.8 Experiment 8: Synthesis of Ammonia with Different Magnetic Strength Using Helmholtz Coil	86
CHAPTER 4 RESULT AND DISCUSSION	88
4.1 Data Gathering & Analysis	88
4.2 Results and Discussion	92
CHAPTER 5 CONCLUSION AND RECOMMENDATION	106
5.1 Conclusion	106
5.2 Recommendations	107
REFERENCES	108
Appendix A Calculations of Yield Percentage	113
Appendix B Micro-Reactor	115
Appendix C Testing of Ammonia Produced at PETRONAS Fertilizer Kedah by Using Dragger Pump	116
Appendix D Field Trip to PETRONAS Fertilizer Kedah	117

LIST OF FIGURES

Figure 1 : Urea requirement for Bio-Fuel Cultivation (Historical and 2020 Forecast) [1].....	1
Figure 2 : Ammonia Consumption by Application [1]	2
Figure 3 : Urea Trade Flow Pattern [1].....	3
Figure 4 : Fritz Haber and Carl Bosch[2].....	4
Figure 5 : Flow Scheme of Haber Bosch Process[3].....	5
Figure 6 : World Ammonia Supply and Demand[21].....	21
Figure 7 : Example of Energy Transformations and Their Uses[23].....	26
Figure 8 : Equilibrium State	27
Figure 9 : Gibbs Free Energy as function of r for $H_2 \rightarrow 2H$	29
Figure 10 : Synthesis of Ammonia.....	31
Figure 11 : Magnetic Field	31
Figure 12 : Electrically Charged Particle[28].....	36
Figure 13 : Force between Electric Current[28].....	36
Figure 14 : Variation in Magnetization and Domains under an External Field [30].....	38
Figure 15 : M-T Curve for Magnetic Material[31]	38
Figure 16 : Schematic Illustration of the Mutual Alignment of Atomic Dipole for a Ferromagnetic Material after External Magnetic Field is Applied[33]	40
Figure 17 : Magnetic Strength versus Alignment of Atomic Spin [Source: http://www.chem1.com/CQ/magscams.html].....	40
Figure 18 Recent trends in spin chemistry research analyzed by year and by country, measured as citations of the landmark review of spin chemistry. Data from ISI Web of Knowledge 2008	41
Figure 19 : Radical Pair Mechanism [41]	42
Figure 20 : Typical MFEs in Organic RPs From Zero Field Up to A Few Tesla.....	44
Figure 21 : Reaction-Diffusion in Liquids	44
Figure 22 : Regularization Methods Allow Details of the Diffusive Motion of RPs to be recovered From Experimental MFE Data [35]	46
Figure 23 : Characterizing MARY curves[37].....	47
Figure 24 : Hemholtz Coil.....	50
Figure 25 : Magnetic Field Applied by Hemholtz Coil	51
Figure 26 : Magnetic Strength, B	52
Figure 27 :Mechanism of chemisorption on the iron metal surface.....	63

Figure 28 : Mechanism of migration on the iron metal surface	64
Figure 29 : Mechanism of desorption on the iron metal surface.....	65
Figure 30 : Ammonia Micro-Reactor.....	67
Figure 31 : Estimation of Nitrogen by Kjeldahl Method	67
Figure 32 : Distillation	69
Figure 33 : Titration	70
Figure 34 : Calculation	71
Figure 35 : Temperature Program Reduction Equipment	75
Figure 36 : TPR Profile of Fe_2O_3 (Hematite) Nanocatalyst	88
Figure 37 : TPR Profile of MnO (Manganese Oxide) Nanocatalyst.....	89
Figure 38 : TPR Profile of $\text{MnZnFe}_2\text{O}_4$ (Manganese Zinc Ferrite) Nanocatalyst.....	90
Figure 39 : TPR Profile of $\text{Y}_3\text{Fe}_5\text{O}_{12}$ (YIG) Nanocatalyst	91
Figure 40 : Trend of Catalytic Induction.....	93
Figure 41 : Yield of Ammonia at Different Magnetic Induction Condition	95
Figure 42 : Trend of Ammonia at Different System Temperature.....	96
Figure 43 : Yield of Ammonia by Using Different Type of Catalyst	98
Figure 44 : Yield of Ammonia at Different Temperature of Inlet Gas	100
Figure 45 : Ammonia Synthesis at Different TPR Condition	102
Figure 46 : Yield of Ammonia at Different Magnetic Strength.....	104
Figure 47 : Synthesis of Ammonia at Different Magnetic Field Adding Helmholtz Coils.....	105

LIST OF TABLES

Table 1 : Literature Review Summary of Ammonia Synthesis	14
Table 2 : Data and Initial Condition for $H_2 \rightarrow 2H$	28
Table 3 : Data and initial conditions for $N_2 + 3H_2 \leftrightarrow 2NH_3$	30
Table 4 : Thermodynamic Table	33
Table 5 : Curie temperature of Various Materials.....	39
Table 6 : Literature Review Summary of Application of Nano-catalyst in Chemical Industry	58
Table 7 : Literature Review Summary of Kjeldahl's Method.....	72
Table 8 : Reduction Mechanism of Fe_2O_3 (Hematite) Nanocatalyst.....	88
Table 9 : Reduction Mechanism of MnO (Manganese Oxide) Nanocatalyst.....	89
Table 10 : Preparation of 5-substituted 1H-tetrazoles with various catalysts [72]	99

CHAPTER 1

INTRODUCTION

1.1 Background of Study

1.1.1 Current Scenario

For the current scenario, the ammonia and urea industry is rising significantly as new markets for bio-fuel and NO_x abatement emerges while existing market are challenged. Production restructuring has resulted from the feed stock cost rises while substantial new investment has occurred in others. Capital and logistic cost rises have altered the business decision but despite this upheaval and uncertainty, growth has continued apace.

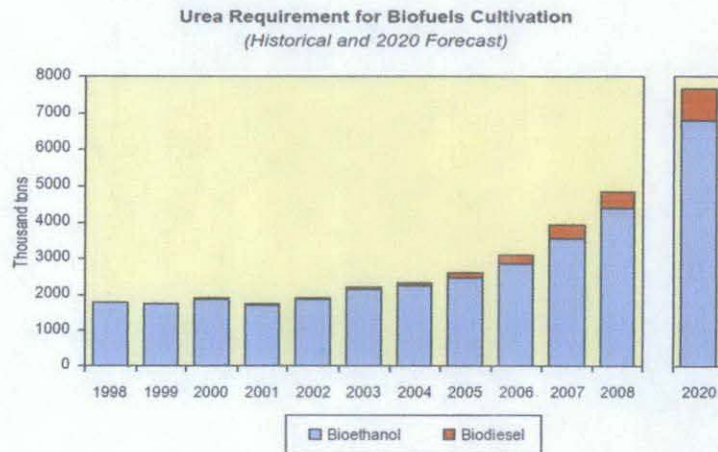


Figure 1 : Urea requirement for Bio-Fuel Cultivation (Historical and 2020 Forecast) [1]

Figure 1 show that almost five million tons of urea applied to crops in 2008 was for bio-fuel use and about 3.5 percent of overall global demand. This forecast is about to increase by 2010 about 7.7 million tons as equal to six world-scale area unit. It

shown that bio-fuel will give a huge impact on global demand for urea into next decade and beyond.

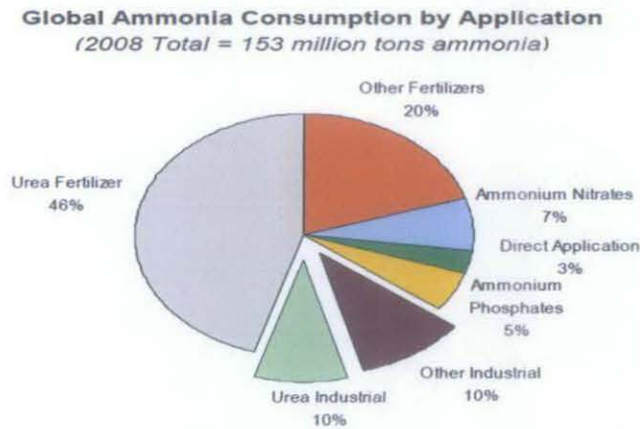


Figure 2 : Ammonia Consumption by Application [1]

On the other hand, ammonia is the largest volume chemical produced from hydrocarbon feedstock and it is a key intermediate for fertilizers production such as urea, ammonium nitrates, ammonium phosphates and compounds as well as a variety of industrial applications includes synthetic resins, synthetic fibers, polyurethanes, explosive and refrigeration fluid.

Population and economic growth is a key driver for increasing fertilizer consumption. These factors result in increasing protein uptake and higher consumption of agriculture products. The greater demands in meat and agriculture products boost fertilizer use in its production. Bio-fuel is also gaining importance due to high fossil fuel prices and environmental legislation. Growing crops in bio-fuel is contributing to nitrogen fertilizer consumption.

Ammonia demand is primarily driven by urea consumption which is mainly a function of fertilizer demand. The highest rate of urea consumption is in regions where agriculture remains a major sector in national economies such as Asia, South America, and Europe as shown in Figure 3. However, with the upward pressure on the natural gas price, producers are focusing on new interest in alternative feedstock of natural gas. [1]

Urea Trade Flow Pattern, 2008

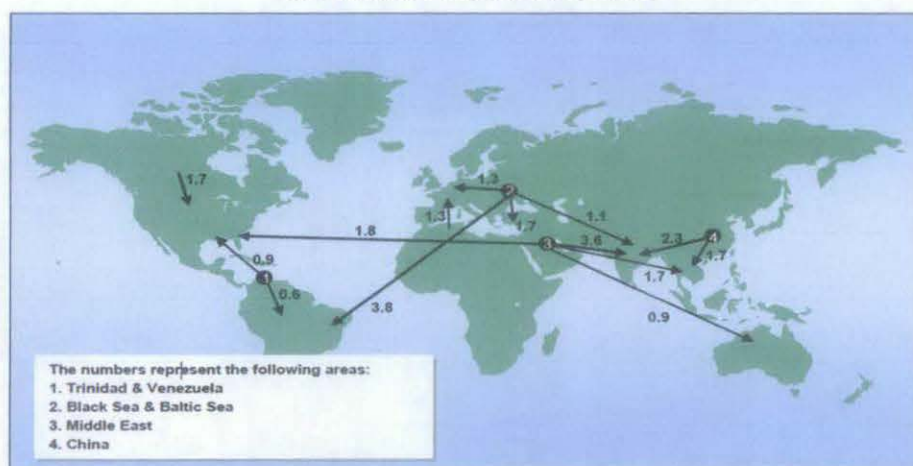


Figure 3 : Urea Trade Flow Pattern [1]

1.1.2 History of Ammonia Production

As the nineteenth century drew to a close, a number of prominent scientists expressed the belief that a rapidly increasing world population threatened to outrun the food supply. The most promising solution was to boost the world's crop yields with resulting to the increasing use of fertilizers. Large quantities of ammonia which is used in fertilizer production were needed. The appalling prospect of a starving world underscored the opportunity to make huge financial gains should the problem of how to artificially synthesis ammonia be solved.

Ammonia contains nitrogen, which gives it the properties that promote plant growth. Traditionally farmers supplied that nitrogen by using manure to fertilize their crops. As the world's population grew and higher yields were needed, scientists began to search for new sources of fertilizer. Chile mined a seemingly plentiful supply of natural nitrates from the Atacama Desert but there was concern that this resource would soon be depleted. Assured sources of cheap 'fixed' nitrogen, nitrogen combined with oxygen or hydrogen were also needed by dye and explosives manufacturers.

In 1909, Fritz Haber, a young physical chemist in Karlsruhe, Germany, struck the jackpot as he found a way to tap into the atmosphere's vast reservoir of nitrogen gas and combine it with hydrogen to form ammonia using enormous pressures, extremely high temperatures and a catalyst. BASF promptly bought Haber's patents and before

his great discovery could be made profitable, one more step had to be completed whereas BASF had to turn Fritz Haber small-scale laboratory feat into a major industrial operation. On the other hand, Carl Bosch, a talented metallurgical engineer and BASF's future chairman was given the task to design and built an industrial-size installation that could contain the great pressures and high temperatures required in Haber's process. This process was referred as the Haber-Bosch process.

The Haber-Bosch process went on-stream in September 1913 and it was considered one of the greatest innovations of the twentieth century. Many alternative techniques have been developed since but none have proved more effective. The Haber-Bosch process gave farmers access to cheap nitrogenous fertilizer and enabling them to grow more crops. World production of cereals increased seven-fold during the twentieth century allowing humanity to survive a quadrupling of the population from 1.6 billion in 1900 to over 6 billion in 2000. [2]



Figure 4 : Fritz Haber and Carl Bosch[2]

1.1.3 Haber Bosch Process

The Haber process combines nitrogen from the air with hydrogen derived mainly from natural gas into ammonia. The reaction is reversible and the production of ammonia is exothermic. [3]



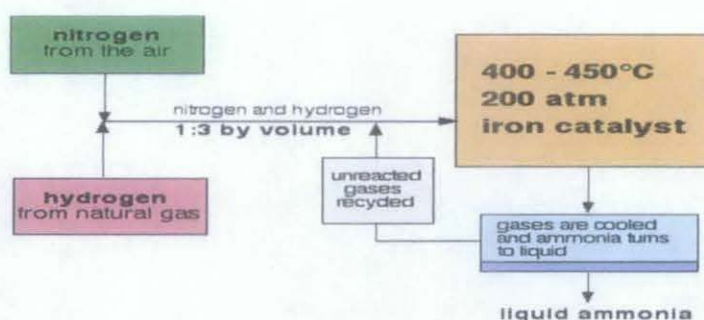


Figure 5 : Flow Scheme of Haber Bosch Process[3]

There are two major considerations for traditional ammonia process that is the position of the equilibrium and the reaction rate. As the temperature increases, the equilibrium will be shifted and hence, the amount of products will drop drastically. The position of the equilibrium must be shifted as far as possible to the right in order to produce the maximum possible amount of ammonia in the equilibrium mixture.

According to Le Chatelier's Principle, this will be favored by lowering the temperature. In order to get as much ammonia as possible in the equilibrium mixture, one might suppose that a low temperature to be used and some other means to increase rate. Theoretically a low temperature would give a high yield of ammonia but nitrogen is very stable molecule and not very reactive, so the rate of reaction is too slow at low temperatures. However as lowering the temperature, the reaction also will become slower. The gases should reach equilibrium within the very short time so that they will be in contact with the catalyst in the reactor. Temperature of 400°C - 450°C is a compromise temperature producing a proportion of ammonia in the equilibrium mixture of about 15%.

Le Chatelier's Principle also state that by increasing the pressure, the system will respond by favoring the reaction which produces fewer molecules. Increasing the pressure brings the molecules closer together. In this particular instance, it will increase their chances of hitting and sticking to the surface of the catalyst where they can react. As pressure increase, the rate of a gas reaction also will increase. However, very high pressures are very expensive to produce. The plant need to build extremely strong pipes and containment vessels to withstand the very high pressure. This will resulting to a high capital costs for the plant design. The maintenance cost also will be

very high. As a result, a pressure of 100bar-200bar is a compromise pressure chosen on economic grounds. [4]

In the absence of a catalyst the reaction is so slow that virtually no reaction happens in any sensible time. The catalyst ensures that the reaction is fast enough for a dynamic equilibrium to be set up within the very short time that the gases are actually in the reactor. These conditions are applied industrially to produce yield of ammonia around 10% to 20%.

1.2 Problem Statements

The current technology of ammonia production is only capable to generate small yield of product from huge amount of feedstock which is only about 10% to 20% of ammonia yields with high capital and energy intensive consumption. As for example, many Indian ammonia plants struggle with high feedstock prices, high maintenance and high energy consumption for the plant in order to maintain at high temperature and high pressure. In order to survive in competition from new plants in areas with low cost gas, many plant owners of existing plants have decided to revamp their plant to reduce the energy consumption and/or increase the capacity. New development needed to fulfill these needs of the markets. [5]

In order to overcome these drawbacks, magnetic nanotechnology is seen as an excellent solution by introducing nano-catalyst applied with the new concept of magnetic induction method to induce the catalytic activity and at the same time enhancing the production yield. By applying the concept from the First Law of Thermodynamics that energy cannot be created or destroyed, but can be converted from one form to another, magneto-dynamic has been introduced to replace the concept of thermodynamic from Haber Bosch process which require the production of ammonia at high temperature and high pressure.

1.3 Objectives and Scope of Study

As energy cannot be created or destroyed but can be converted from one form to another, the objective the study is to introduce the application of conversion of magnetic energy to chemical energy instead of using the conversion of heat and mechanical energy to chemical energy in ammonia production which require high capital and energy intensive in the production of ammonia.

The potential energy is needed to do useful work. So, the magnetic energy is needed to replace the thermal energy which required in the conventional Haber-Bosch process to affect the reaction equilibrium. The technique of replacing the thermal energy by magnetic energy will be explored in this project. This is a new area of research and will lead to a new approach for the driving force of chemical reactions.

With this new concept, a high yield of ammonia (30%-100% conversion) at ambient temperature and ambient pressure can be produced since catalytic activity is induced and the yield can be enhanced. The hypothesis is ammonia synthesis can occur at ambient or lower than ambient temperature with magnetic field induction to produce high yield of ammonia.

The proper scope of study is vital to the accomplishment of this project. Hence, the following scopes of work had been clarified:

- Identify the problem statements
- Conducting literature survey on ammonia synthesis, ammonia market data, the concept of energy, theory of magnetic induction, hemholtz coil, atom and magnetic field, application of magnetic field, catalytic reaction, micro-reactor, and temperature programmed reduction
- Conduct design of experiments
- Observe the reaction of ammonia synthesis with nano-catalyst at different temperature
- Observe the reaction of ammonia synthesis with nano-catalyst by lowering the temperature as low as possible

- Observe the reaction of ammonia synthesis with nano-catalyst at different type of catalyst
- Observe the reaction of ammonia synthesis with nano-catalyst at different TPR condition
- Observe the reaction of ammonia synthesis with nano-catalyst by at different magnetic field strength
- Making the necessary decisions, judgments and assumptions in design problem

CHAPTER 2

LITERATURE REVIEW AND THEORY

2.1 Ammonia Synthesis

Fixed nitrogen from the air is the major ingredient of fertilizers which makes intensive food production possible. During the development of inexpensive nitrogen fixation processes, many principles of chemical and high-pressure processes were clarified and the field of chemical engineering emerged. (G Austin, 1984) states that, before synthetic nitrogen fixation, wastes and manures of various types or their decomposition products, and ammonium sulfate which is a by-product from the coking of coal were the primary sources of agricultural nitrogen. Chilean saltpetre, saltpetre from human and animal urine, and later, ammonia recovered from coke manufacture were some of the important sources of fixed nitrogen. [6]

During the first decade of the twentieth century, the worldwide demand for nitrogen based fertilizers far exceeded the existent supply. The largest source of the chemicals necessary for fertilizer production was found in a huge guano deposit (essentially sea bird droppings) that was 220 miles in length and five feet thick, located along the coast of Chile. Scientists had long desired to solve the problem of the world's dependence on this fast disappearing natural source of ammonia and nitrogenous compounds. Priestly and Cavendish passed electric sparks through air and produced nitrates by dissolving the oxides of nitrogen thus formed in alkalis. Commercial development of this process had proved elusive, for much electrical energy was consumed at low efficiency. Nitrogen had been fixed as calcium cyanamide, but the process was too expensive except for producing chemicals requiring the cyanamide configuration. Other processes, such as thermal processing to mixed oxides of nitrogen (NO_x), cyanide formation, aluminum nitride formation and decomposition to ammonia showed little commercial promise although they were

technically possible. It was Fritz Haber, along with Carl Bosch, who finally solved this problem.

Haber invented a large-scale catalytic synthesis of ammonia from elemental hydrogen and nitrogen gas, reactants which are abundant and inexpensive. By using high temperature (around 500°C high pressure (approximately 150-200 atm), and an iron catalyst, Haber could force relatively unreactive gaseous nitrogen and hydrogen to combine into ammonia. This furnished the essential precursor for many important substances, particularly fertilizers and explosives used in mining and warfare. Bosch, with his technical ingenuity, developed suitable high-pressure equipment and production methods for large-scale production of ammonia. The collaborative efforts of Haber and Bosch made the commercial high-pressure synthesis of ammonia possible by 1913. The first commercial plant with a capacity of 30 tons/day was set up by the German chemical giant BASF (Badische Anilin und Soda Fabrik) in Oppau, Germany. [7] (Dr.H.L Roy, 1986)

This energy-intensive process has undergone considerable modification in recent years, resulting in prices which have not escalated as rapidly as energy prices in general. (Bakemeier and others, 1997) Today, synthetic ammonia produced from reaction between nitrogen and hydrogen is the base from which virtually all nitrogen-containing products are derived. (Chemical and Engineering News, 1996) state that the worldwide production of ammonia exceeds 130 million tonnes and is the sixth largest chemical produced. [8]

The technological improvements in the past 90 years has resulted in significant improvement in the yield of ammonia and modern plants usually produce 1000-1500 T/day of ammonia. The plants employ gas velocities of about 10000-20000m³/m³ catalyst per hour and typical conversions obtained are in the range of 8-15% depending on the catalyst. The iron-based industrial ammonia synthesis process utilises, in the majority of cases, a triply promoted catalyst operating at temperatures between 400-700°C and pressures over 300 atm. These severe conditions require enormous energy input. There has been a decrease in the synthesis pressure conditions from -300 to 80atm, but this has been due to engineering advances in the construction of the plant.

The dominance of iron based catalyst has recently been challenged by promoted ruthenium catalyst deposited on active graphite. Since ruthenium shows a marked improvement in activity, it has enabled the lowering of ammonia synthesis temperatures, and consequent lowering of the operating pressures. Operation at synthesis pressures as low as 40atm is thus technically feasible.[9] (Z.Kowalczyk, S.Jodiz and J.Sentek, 1996)

Synthesis of ammonia is the most important industrial process for isolation of nitrogen as well as further production of nitrogen compounds of vital importance (urea, nitric acid and fertilizers). This process is nearly a hundred years old, discovered in the beginning of the 20th century by Fritz Haber and developed for industrial production by Carl Bosch. [10]

The reaction between gaseous N_2 and H_2 ($N_2 + 3H_2 \leftrightarrow 2NH_3$) is exothermic, carried out at high pressures and temperatures and occurs with large yields when iron catalysts are present. The iron catalyst consists of reduced magnetite ore (Fe_3O_4) which is enriched ("promoted") most frequently with Al- and K- (or Ca, Mg, Si)-oxides while its optimal performance requires reaction temperatures around 400°C and pressures from 150-300 atmospheres. [11, 12] Being a transition metal with partially occupied d-bands iron represents a surface suitable for adsorption and dissociation of N_2 molecules.

Studies of catalytic processes are difficult mainly because of pressure and temperature differences between synthesis and study conditions, since synthesis occurs at high temperatures and pressures, while characterization of surfaces needs an UHV environment. Studies of ammonia synthesis on iron catalysts require specially designed chambers and often inspection of surfaces of industrial catalysts occurs. [12] (Sandra Bencic, 2001)

During the past decades, there has been a considerable progress in a field of low-temperature ammonia synthesis from dinitrogen and dihydrogen. New types of catalysts precursors, supports and electron promoters for this process have been developed and novel impressive examples of synergistic effects in ammonia synthesis

have been described. Important information on the mechanism of the dinitrogen activation and its hydrogenation has been obtained. As a result of these studies, new efficient catalysts exhibiting an increased activity in ammonia synthesis in the low-temperature region have been found.

It has been reported that the first supported catalysts for this process based on potassium derivatives of anionic metal carbonyl clusters ($K_2[Ru_4(CO)_{13}]$, $K_2[Os_3(CO)_{11}]$, $K_2[Fe_2(CO)_8]$). A remarkable feature of such clusters is their ability to serve as precursors of both catalytically active metal particles and potassium promoter. Based on this approach, $K_2[Ru_4(CO)_{13}]$, $K_2[Os_3(CO)_{11}]$ and $K_2[Fe_2(CO)_8]$ clusters is applied for creating the first systems on carbon supports capable of catalyzing the dinitrogen hydrogenation in the absence of a specially added electron promoter [13,14]. The highest activity among these supported “single-component” ammonia synthesis catalysts was observed for the $K_2[Ru_4(CO)_{13}]$ samples which turned out to be active in the ammonia synthesis starting from 250°C (1 atm).

Further increase in the ammonia synthesis rate has been achieved on the replacement of carbon supports by highly basic magnesium oxide [14]. It has also been found that particularly effective ammonia synthesis catalysts can be obtained when the $K_2[Ru_4(CO)_{13}]$, $K_2[Os_3(CO)_{11}]$ and $K_2[Fe_2(CO)_8]$ based systems on carbon supports are treated with metallic potassium as an additional electron promoter [15]. (S.M. Yunusov, E.S. Kalyuzhnaya, B.L. Moroz, A.S. Ivanova, T.V. Reshetyenko, L.B. Avdeeva, V.A. Likholobov, V.B. Shur.,2004)

Alumina-supported rhenium catalysts were prepared and tested for ammonia synthesis. Ammonium perrhenate was used as the precursor of the supported rhenium catalysts and $\gamma-Al_2O_3$ ($100m^2g^{-1}$) was impregnated with this compound in an aqueous solution. NH_4ReO_4/Al_2O_3 was reduced with pure hydrogen at 823K for 2 hours, and then the sample was activated with the reactant gas or pure hydrogen prior to ammonia synthesis. The catalyst, which was activated with the reactant gas, was found to contain not only Re metal, but also Re nitride, which is more active than Re metal. The cesium promoter (Cs:Re=1:1) was added to the catalyst by the impregnation method; the resulting activity was significantly higher than that of the non-promoted catalyst. H_2 chemisorption and $Na_{ds} + H_2$ TPSR experiments revealed

that the Re area was decreased by the addition of cesium, whereas the onset of NH_3 formation during the TPSR experiment was not affected. XRD and elemental analyses revealed that the alkali addition has some drawbacks: the formation of cesium perrhenate and the decomposition of rhenium nitride. The ammonia synthesis rates over supported rhenium catalysts were found to increase under high-pressure. Kinetic studies based on power-law rate expressions indicated that the unpromoted Re surfaces were covered by H_{ads} and $\text{NH}_{x,\text{ads}}$. By the addition of cesium, the degree of ammonia poisoning was not changed, but the inhibition by hydrogen was removed. Hence, cesium is identified as a very efficient promoter for supported Re catalysts. [16] (R.Kojima, H. Enomoto, M.Muhler, K. Aika, 2003)

Table 1 : Literature Review Summary of Ammonia Synthesis

Author	Catalyst	Temperature	Pressure	Yield NH₃	Ref
Dr.H.L.Roy, 1986	Iron	500°C	150-250atm	-	[7]
Bakemeier and others, 1997	Iron-promoted	400-700°C	300atm	8-15%	[8]
Z.Kowalczyk, S.Jodiz and J.Sentek, 1996)	Ruthenium	-	40atm	-	[9]
Sandra Bencic (2001)	Iron	400°C	150-300atm	-	[12]
S.M. Yunusov, E.S. Kalyuzhnaya, B.L. Moroz, A.S. Ivanova, T.V. Reshetenko, L.B. Avdeeva, V.A. Likhobov, V.B. Shur. (2004)	K ₂ [Ru ₄ (CO) ₁₃]	250°C	1 atm	15.2ml/g.h	[14]
R.Kojima, H. Enomoto, M.Muhler, K. Aika (2003)	20 wt.% Re/Al ₂ O ₃	623K	0.1Mpa	39.4µmol/g	[16]
R.Kojima, H. Enomoto, M.Muhler, K. Aika (2003)	1Cs-20 wt.% Re/Al ₂ O ₃	623K	0.1Mpa	6.8µmol/g	[16]

2.1.1 Feed Properties

This section discussed about the properties of reactants that is nitrogen, hydrogen and carbon dioxide and main product that is ammonia.

Nitrogen

Nitrogen which a chemical symbol of N_2 is a colorless, odorless and tasteless gas. It makes up 78.09% by volume of the air. It has the characteristic of nonflammable, hence not prop up combustion. Nitrogen gas is slightly lighter than air and slightly soluble in water. Normally used as an inert gas; but it is not truly inert. For example; forms nitric oxide and nitrogen dioxide with oxygen, ammonia with hydrogen, and nitrogen sulfide with sulfur. Nitrogen compounds are formed naturally through biological activity. In addition, compounds are also formed at high temperature or at moderate temperature with aid of catalysts. At high temperatures, nitrogen will combine with active metals, such as lithium, magnesium and titanium to form nitrides.

Without doubt, nitrogen is necessary for various biological processes, and is used as a fertilizer, usually in the form of ammonia or ammonia-based compounds. Compounds formed with halogens and certain organic compounds can be explosive. Nitrogen condenses at its boiling point, $-195.8^{\circ}C$, to a colorless liquid that is lighter than water. [17]

Hydrogen

Hydrogen which a chemical symbol of H_2 is a colorless, odorless, tasteless, flammable and non-toxic gas at atmospheric temperatures and pressures. Hydrogen burns in air with a pale blue, almost invisible flame. Hydrogen is the lightest of all gases, approximately one-fifteenth as heavy as air. Furthermore, hydrogen ignites

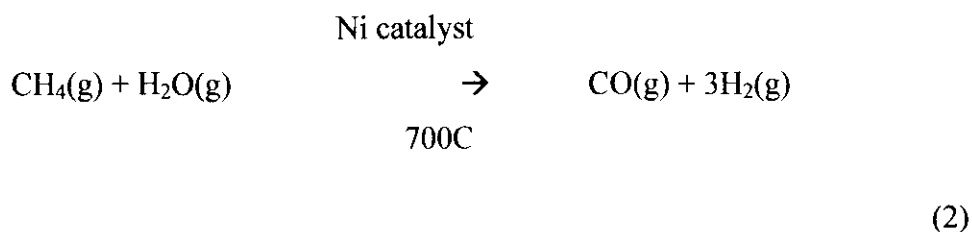
easily and forms, together with oxygen or air, create an explosive gas (oxy-hydrogen).

It has the highest combustion energy release per unit of weight of any commonly occurring material. As a result, makes it the fuel of choice for upper stages of multi-stage rockets. Hydrogen has the lowest boiling point of any element except helium. When cooled to its boiling point, -252.76°C , and hydrogen becomes a transparent, odorless liquid that is only one-fourteenth as heavy as water. Liquid hydrogen is not corrosive or particularly reactive. When converted from liquid to gas, hydrogen expands approximately 840 times. Its low boiling point and low density result in liquid hydrogen spills dispersing rapidly. [18]

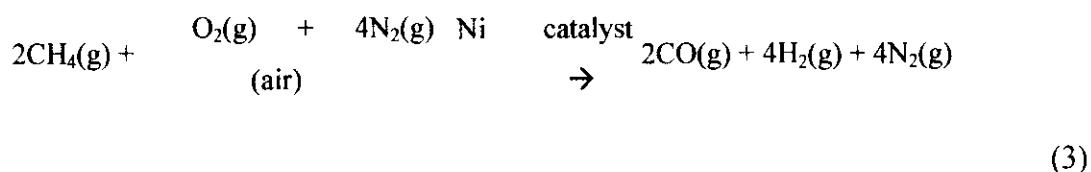
2.1.2 Product Properties

Ammonia

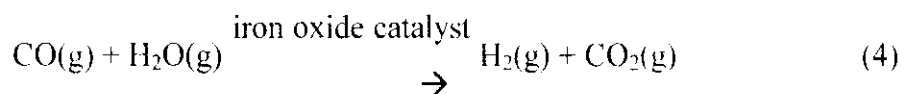
Ammonia is a compound of nitrogen and hydrogen which is covalently bonded with the formula of NH_3 . The first step of ammonia production is hydrogen production by reforming light petroleum fractions or natural gas (methane, CH_4) by adding steam:



Enough steam is used to react with about 45% of the methane (CH_4), the rest of the methane is reacted with air:

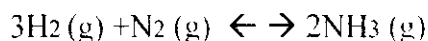


All the carbon monoxide (CO) in the mixture is oxidised to CO₂ using steam and an iron oxide catalyst:



The carbon dioxide (CO₂) is removed using a suitable base so that only the nitrogen gas (N₂) and hydrogen gas (H₂) remain and are used in the production of ammonia (NH₃).

The reaction that occurs is:



Ammonia is a colorless gas with a characteristic of pungent odor. Ammonia contributes significantly to the nutritional needs of terrestrial organisms by serving as as precursor to foods and fertilizers. Either directly or indirectly, ammonia is also a building block for the synthesis of many pharmaceuticals. Ammonia is caustic and hazardous and is been used in commercial cleaning products.

Ammonia, as used commercially, is often called anhydrous ammonia. This term emphasizes the absence of water in the material. Anhydrous ammonia boils at a temperature of -33.33⁰C. In refrigeration systems, the liquid is stored in closed containers under pressure. When the pressure is released, the liquid evaporates rapidly, generally forming an invisible vapor or gas. The rapid evaporation causes the temperature of the liquid to drop until it reaches the normal boiling point of -33.33⁰C, a similar effect occurs when water evaporates off the skin, thus cooling it. This is why ammonia is used in refrigeration systems.

Liquid and gas ammonia expand and contract with changes in pressure and temperature. For example, if liquid anhydrous ammonia is in a partially filled, closed container it is heated from -17.78°C to 20°C , the volume of the liquid will increase by about 10 percent. If the tank is 90 percent full at -17.78°C , it will become 99 percent full at 20°C . At the same time, the pressure in the container will increase from 16 pounds per square inch (psi) to 110 psi. Liquid ammonia will expand by 850 times when evaporating. Anhydrous ammonia gas is considerably lighter than air and will rise in dry air. However, because of ammonia's tremendous affinity for water, it reacts immediately with the humidity in the air and may remain close to the ground.

The odor threshold for ammonia is between 5 - 50 parts per million (ppm) of air. The permissible exposure limit (PEL) is 50 ppm averaged over an 8 hour shift. It is recommended that if an employee can smell it they ought to back off and determine if they need to be using respiratory protection.

Anhydrous ammonia is easily absorbed by water. At -20°C , about 700 volumes of vapor can be dissolved in one volume of water to make a solution containing 34 percent ammonia by weight. Ammonia in water solution is called aqua ammonia or ammonium hydroxide.

Ammonia, especially in the presence of moisture, reacts with and corrodes copper, zinc, and many alloys. Only iron, steel, certain rubbers and plastics, and specific nonferrous alloys resistant to ammonia should be used for fabrications of anhydrous ammonia containers, fittings, and piping. Ammonia will combine with mercury to form a fulminate which is an unstable explosive compound. Anhydrous ammonia is flammable over a narrow range and with extremely high ignition energy but rated as an inflammable liquid by the U.S. Department of Transportation. The fire hazard from ammonia is increased by the presence of oil or other combustible materials. Anhydrous ammonia is an alkali. [19]

The chemical and physical properties of ammonia are described as below:

- **#H bond acceptors:**1
- **#H bond donors:**3
- **Enthalpy of Vaporization:** 23.33 kJ/mol
- **Vapor Pressure:** 5992.52 mmHg at 25°C
- **Boiling Point:** -33.33⁰C
- **Flash Point:** NA (Gas)
- **Freezing Point:** -108°F
- **Specific Gravity:** 0.890
- **Solubility:** 34%
- **Ionization Potential:** 10.18eV
- **Vapor Pressure:** 8.5atm
- **Appearance:** Colorless gas with a pungent, suffocating odor - shipped as a liquefied compressed gas. Easily liquefied under pressure
- **Safety:** DANGER: CORROSIVE, burns skin and eyes
- **First Aid:** Eye: Irrigate immediately (solution/liquid) Skin: Water flush immediately (solution/liquid) Breathing: Respiratory support Swallow: Medical attention immediately (solution)
- **Exposure Routes:** inhalation, ingestion (solution), skin and/or eye contact (solution/liquid)
- **Incompatibilities and Reactivity:** Strong oxidizers, acids, halogens, salts of silver & zinc [Note: Corrosive to copper & galvanized surfaces.]
- **Personal Protection and Sanitation:** Skin: Prevent skin contact Eyes: Prevent eye contact Wash skin: When contaminated (solution) Remove: When wet or contaminated (solution) Change: No recommendation Provide: Eyewash (>10%), Quick drench (>10%)

2.2 Ammonia Market Data

According to the International Fertilizer Industry Association (IFA), the world nitrogen market in 2009 recovered from the depressed demand conditions seen in 2008 in both the fertilizer and industrial sectors. World ammonia production in 2009 remained stable at 153m tonnes NH₃. Global ammonia trade fell 7.4% to an estimated 17.4m tonnes NH₃.

Global ammonia capacity was 153m tonne/year NH₃ in 2009, with the main additions occurring in China, Trinidad, Indonesia, Oman, India and Egypt. The IFA noted that many projects that were slated for commissioning in 2009 have been delayed by six months or more.

According to the IFA 2010 world capacity survey, global ammonia capacity will increase by 20% to 224m tonne/year NH₃ by 2014. The bulk of the growth will be in China, Middle East, Latin America and Africa. IFA estimated global seaborne ammonia availability will be close to 19m tonnes in 2014, a net increase of 1.7m tonnes over 2009. In terms of nitrogen supply, world capacity will reach 184m tonne N in 2014. IFA estimated global nitrogen supply capability (or effective capacity) to grow from 134.8m tonnes N in 2010 to 158.5m tonnes N in 2014.

For the period 2009 to 2014, consumption of nitrogen nutrient fertilizer is projected by the IFA to grow at 2.0%/year to 111.7m tonnes N in 2014, compared to 103.9m tonnes N in 2010. Nitrogen demand in the non-fertilizer sector is forecast to grow at 4.6%/year from 21.6m tonnes N in 2009 to 26.6m tonnes N in 2014. Taking into account distribution losses, IFA estimated global nitrogen demand will reach 142m tonnes N in 2014.

Demand for nitrogen fertilizers in China was soft in 2009 with ammonia production increasing at a moderate rate of 3.8% compared to 2008 to 50.8m tonnes NH₃. Much of the increase was related to higher urea and DAP output. In the

medium term, China's ammonia capacity is projected by the IFA to increase from 62m tonne/year NH₃ in 2009 to 71m tonne/year in 2013.

India is ranked as the world's third largest producer and importers of ammonia. Imports which are estimated at 1.9m tonnes in 2009 are used for phosphate fertilizers since domestic ammonia production is mostly integrated with urea production. Excluding any plant restarts, IFA expected India's ammonia capacity to reach 20m tonne/year in 2014.

In the Middle East, new merchant ammonia capacity is expected in Iran and Saudi Arabia. The IFA estimated the potential for seaborne ammonia exports to grow from 3.1m tonnes in 2009 to 4.2m tonnes in 2014. Trinidad is the world's largest ammonia exporter with a capability close to 4.9m tonnes in 2009. Other Caribbean and Latin American exporters include Venezuela, Mexico, Argentina, Brazil and Colombia. Over the past five years, imports into the US, the world's largest importer, has ranged between 7m-8m tonnes/year, estimated the IFA. Imports come mainly from Trinidad and to some extent from Russia, Ukraine, Venezuela and the Middle East.

According to the IFA, no major change in merchant ammonia capacity is expected in Europe. It is believed that Europe will remain the net importer of seaborne ammonia for the short term. IFA predicts an average import requirement of around 3m tonne/year. [20]

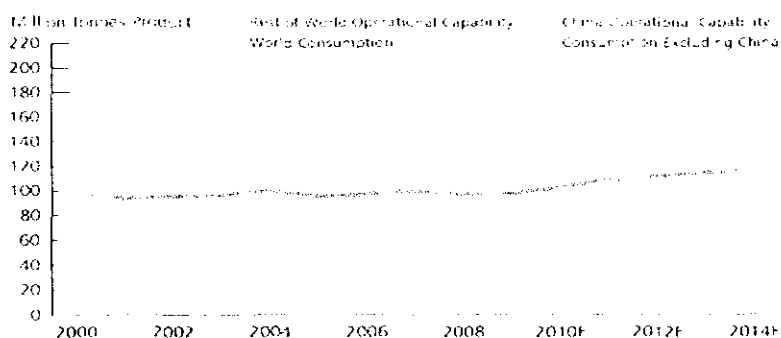


Figure 6 :World Ammonia Supply and Demand[21]

From Figure 6, we can see world ammonia consumption for agriculture and industrial uses has grown at a consistent rate since 2000. The steady growth will continue and the limited planned capacity additions will support a relatively balanced market in the short term. Although several ammonia plants are projected to come online over the medium term, the shorter lead time for such construction makes the number of projects proposed beyond 2012 speculative at this stage. [21]

In domestic perspective, the main user for ammonia is fertilizer as it compose 80% of ammonia in the world. To know the demand for fertilizer, we can observe it through the condition of agriculture in Malaysia. According to Tenth Malaysia Plant (2010), a report been published by The Economic Planning Unit, Prime Minister Department, it had been mentioned regarding agriculture on three main strategy.

Firstly, in National Key Economic Areas (NKEAs), there are two part related with fertilizer. There are on No.2, Palm oil and related products, and No.11, Agriculture. Secondly, in Northern Corridor Economic Region that covers the states of Kedah, Pulau Pinang, Perlis, and the four northern districts in Perak, one of the things that will be focusing is on promoting agriculture. Thirdly, East Coast Economic Region (ECER) that covers the states of Kelantan, Pahang, Terengganu and the district of Mersing in Johor, where the development plan will focus on key initiatives related to petrochemical and agriculture.

Thus, the demand for ammonia production on global region is quiet difficult to enter due to surplus condition. However, some issue not been consider such as some ammonia production plant will be closed due to time limit and the project proposed beyond 2012 been cancelled or delayed. On the other hand, the domestic demand can still be entered. It is been supported by the trend of Malaysia government that emphasize and had positive vision on agriculture. As a result, develop an ammonia production plant in Malaysia is still profitable judge on the steady growth of agriculture in Malaysia.

2.3 The Concept of Energy

Energy is the ability to do work (apply a force through a distance). The many forms of energy include mechanical (including sound), electrical, thermal, light (radiant), chemical, and nuclear. Energy can change from one type to another. This is called an energy conversion or energy transformation. The Law of Conservation of Energy states that energy can change form, but it cannot be created or destroyed. Therefore, the total amount of energy stays the same. In energy transformations, some energy is always lost to the environment as thermal energy.

The Joule (J) is the fundamental unit of energy for both work and heat and is the work done by a force of one Newton acting through a distance of one meter. The joule is also equal to 1/4.184 of a calorie. Energy is often expressed as the calorie (cal) which is the amount of heat needed to raise the temperature of one gram of water by 1°C at pressure of 1 atm. One calorie is equal to 4.184 joules.

Kinetic energy is the energy of a moving object. The amount of kinetic energy depends on the mass and velocity of the moving object. Potential energy is the stored energy of an object based on its position. The chemical energy in fossil fuels is also a form of potential energy. Coal, oil, gasoline, and natural gas have potential energy because of their chemical composition.

Thermal energy is the total kinetic energy of a substance's atoms and molecules. Atoms and molecules are constantly in motion. When thermal energy causes particles to move faster and farther apart, the result is a phase change (or change of state). During a phase change, the thermal energy is being used to break bonds between molecules. Even though thermal energy continues to be absorbed, the temperature does not rise. Thermal energy can be transferred from warmer to colder particles in three ways:

- Conduction is the heating of an object from direct contact between a heat source and the object

- Convection is heating of an object through the movement of a fluid (a gas or liquid)
- Radiation is the heating of an object by radiant energy traveling through space by electromagnetic waves. E.g.; the thermal energy coming to the Earth from the Sun through infrared waves

A wave is a disturbance that transfers energy through matter or space. Sound is a form of mechanical energy produced by vibrations. It travels in longitudinal (compression) waves and moves much slower than the speed of light. In longitudinal waves, matter vibrates in the same direction as the waves are traveling. Sound waves require a medium (solid, liquid, or gas) through which to travel. Longitudinal waves cause molecules of a medium to vibrate “back and forth” in the same direction that the wave is traveling. The speed of sound depends on the type of medium (how dense) it is passing through and the temperature of the medium. Light has properties of both waves and particles. The particle theory states that light energy is made up tiny packets of energy called photons. The wave theory describes light as form of radiant energy that moves in transverse waves which are waves that move particles up and down perpendicular to the direction of the wave. Visible light is a part of the electromagnetic spectrum. The electromagnetic spectrum is an arrangement (model) of electromagnetic waves in order of their wavelengths and frequencies. On the other hand, there is a relationship between electricity and magnetism as electricity can generate magnetic fields and magnetic fields can generate electricity. Examples of relationships between electricity and magnetism are:

- Electromagnets
 - The magnetic field which surrounds the wire
 - Temporary magnets and lose their magnetic properties when the current is removed
- Electromagnetic induction
 - When a magnetic field is passed near a wire that is a good conductor of electricity, an electric current can be “induced” in the wire in a process called electromagnetic induction

- It is believed that the magnetic field exerts a force upon the electrons in the wire, thus causing the flow of electrons
- Motors and Generators
 - When magnetic fields interact, mechanical motion can occur

Electricity is a form of energy produced by moving electrons. Electricity can be static or moving through electrical conductors (electric current). Moving electrons transmit electrical energy from one point to another. [22]

In 1845, Joule performed an experiment that demonstrated energy transformation both qualitatively and quantitatively. Joule placed a paddle wheel in a tank of water and measured the temperature of the water. He cranked the wheel in the water for a period of time, and then read the temperature again. He found that the temperature of the water rose as he cranked the paddle wheel. Joule quantified this observation and discovered that an equal amount of energy was always required to raise the temperature of the water by one degree. He also discovered that it did not have to be mechanical energy; it could be energy in any form. He obtained the same results with electrical or magnetic energy as he did with mechanical energy. Joule's experiments showed that different forms of energy are equivalent and can be converted from one form to another. [23]

These observations led to what is now called the "Law of conservation of energy." This law states that any time energy is transferred between two objects, or converted from one form into another, no energy is created and none is destroyed. The total amount of energy involved in the process remains the same.

Most chemical reactions involve transformations in energy. A chemical reaction is simply the process whereby bonds are broken between atoms and new ones are made. The ultimate example of energy transformation is that of the radiant energy of the Sun. All of the energy on Earth originated from the Sun, energy left over from the formation of Earth (usually thermal energy caused by the gravitational collapse of matter), or energy derived from nuclear decay in Earth's interior.) The thermal

energy in Earth's interior drives plate tectonics and, at the surface, the Sun's radiant energy is converted by plants into chemical energy through the process of photosynthesis. This chemical energy is stored in the form of sugars and starches. When these plants are eaten by animals (i.e., as part of the food chain), this chemical energy is either transformed into another form of chemical energy (fats or muscle) or used for mechanical or thermal energy. With regard to fossil fuels, the fuels used in the modern era derive from the transformations of solar energy over millions of years.









	A television changes electrical energy into sound and light energy.
	A toaster changes electrical energy into thermal energy and light.
	A car changes chemical energy from fuel into thermal energy and mechanical energy.
	A flashlight changes chemical energy from batteries into light energy.
	When you speak into your telephone, sound energy from your voice is changed into electrical energy. The electrical energy is then converted back into sound energy on another phone, allowing someone to hear you.
	Light energy is converted into electrical energy using solar panels.
	Campfires convert chemical energy stored in wood into thermal energy, which is useful for cooking food and staying warm.
	Nuclear energy generates a tremendous amount of thermal energy, which can be converted into electrical energy in a nuclear power plant.

Figure 7 : Example of Energy Transformations and Their Uses[23]

2.3.1 Law of Thermodynamics

The First Law of Thermodynamics state that energy cannot be created or destroyed; it can only change forms. [24] The First Law of Thermodynamics is concerned with the quantity of energy and the transformations of energy. It does not tell us the preferred direction of the process to achieve.

The Second Law of Thermodynamics describes the relationship between entropy and the spontaneity of natural processes which determine the perfection and point out the direction of a process.

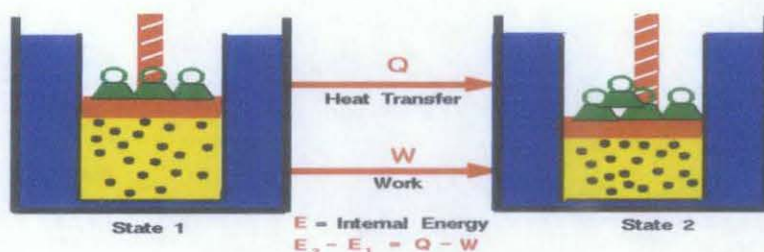


Figure 8 : Equilibrium State

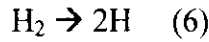
Figure 8 shows that any thermodynamics system in an equilibrium state possesses a state variable called the internal energy (E). Between any two equilibrium states, the change in internal energy is equal to the different of heat transfer into the system and work done by the system. It can be described by the kinetic theory of gases. In observation of work done by or on gas, it is found that the amount of work depends not only on the initial and final states of the gas but also depend on the process or path which produce the final state. Similarly, the amount of heat transferred into or from a gas is also depend on the initial and final states and also on the process or path which produced the final state.

Many observations of real gases have shown that the difference of the heat flow into the gas and the work done by the gas depends only on the initial and final states of the gas and does not depend on the process or path which produces the final state. This suggests the existence of an additional variable, called the internal energy of the gas, which depends only on the state of the gas and not on any process. The internal energy is a state variable, just like the temperature or the pressure. The first law of thermodynamics defines the internal energy (E) as equal to the difference of the heat transfer (Q) into a system and the work (W) done by the system. [25]

$$E_2 - E_1 = Q - W \quad (5)$$

The internal energy is just a form of energy and can be stored in the system. However, the heat and work cannot be stored or conserved independently since they depend on the process.

2.3.2 The Thermodynamic Concept in Haber Bosch Process



Both molecular and atomic hydrogen are ideal gases in the reference state ($P_R=100\text{bar}$ and $T_R=298\text{K}$) so that for a low pressure P and high temperature $T>T_R$, equation 7 is valid. Data and initial conditions may be obtained from Table 2.

$$G(r) - G(0) = \left[\Delta \widetilde{h}_R + \sum_{\alpha=1}^{\nu} \gamma_{\alpha} (z_{\alpha} + 1) R(T - T_R) \right] \frac{R}{A} - T \left[\Delta \widetilde{s}_R + \sum_{\alpha=1}^{\nu} \gamma_{\alpha} (z_{\alpha} + 1) R \ln \frac{T}{T_R} - \sum_{\alpha=1}^{\nu} \gamma_{\alpha} R \ln \frac{P}{P_R} \right] \frac{R}{A} + RT \sum_{\alpha=1}^{\nu} \left[(v_{\alpha}(t_0) + \gamma_{\alpha} \frac{R}{A}) \ln \frac{v_{\alpha}(t_0) + \gamma_{\alpha} \frac{R}{A}}{\sum_{\beta=1}^{\nu} [v_{\beta}(t_0) + \gamma_{\beta} \frac{R}{A}]} - v_{\alpha}(t_0) \ln \frac{v_{\alpha}(t_0)}{\sum_{\beta=1}^{\nu} [v_{\beta}(t_0)]} \right] \quad (7) [26]$$

Table 2 : Data and Initial Condition for $\text{H}_2 \rightarrow 2\text{H}$

	γ_{α}	$v_{\alpha}(t_0)$	$\Delta \widetilde{h}_R$	$\Delta \widetilde{s}_R$	z_{α}
H_2	-1	1 mol	435.8 $\frac{\text{kJ}}{\text{mol}}$	98.6 $\frac{\text{J}}{\text{mol} \cdot \text{K}}$	5/2
H	2	0			3/2

Thus, we obtain equation 7 in the explicit form with $r=R/A$ mol so that the range of r is $0 \leq r \leq 1$:

$$G(r) - G(0) = \left[435.8 \text{ kJ} + \frac{3}{2} 8.314 \frac{\text{J}}{\text{K}} (T - T_R) \right] r - T \left[98.6 \frac{\text{J}}{\text{K}} + \frac{3}{2} 8.314 \frac{\text{J}}{\text{K}} \ln \frac{P}{P_R} \right] r + 8.314 \frac{\text{J}}{\text{K}} T \left[(1 - r) \ln \frac{1-r}{1+r} + 2r \ln \frac{2r}{1+r} \right] \quad (8) [26]$$

Figure 9 shows plots of this function for $T = 298\text{K}$, $P = 1\text{ bar}$ and $T = 3000\text{K}$, $P = 0.01\text{bar}$. We conclude that for low temperature the minimum of G occurs at or near $r = 0$ so that H_2 is stable constituent. At the high temperature there is a mixture of constituents in equilibrium, where G has a minimum at $r \approx 0.7$. The figure also shows the three lines of equation 8 separately. The first line labeled 'energy' has an end-point minimum at H_2 , while the third one labeled 'entropy of mixing' is responsible for the genuine minimum at $r \approx 0.7$, at least for the high temperature. Thus we may say that energy favors the molecules, while entropy favors the atoms and the entropy of mixing favors mixing naturally. The entropy of mixing however cannot be achieved much at low temperature because it is too small. In Figure 9, it cannot be seen because to the naked eyes, its graph coincides with the r axis.

There is a subtle point concerning the energy of mixing for $r \rightarrow 0$ and $r \rightarrow 1$. In both cases its slope is infinite. Therefore- however dominant the linear curves of energy and entropy may be – entropy of mixing enforces a minimum close to an end point. This minimum is so close to the end point and so small that it cannot be seen on the scale of Figure 9a, but it is there. In Figure 9a, it occurs at $r \approx 10^{-8000}$ so that with only 10^{22} molecules, we will not see a single H_2 dissociated into H atoms at the low temperature.

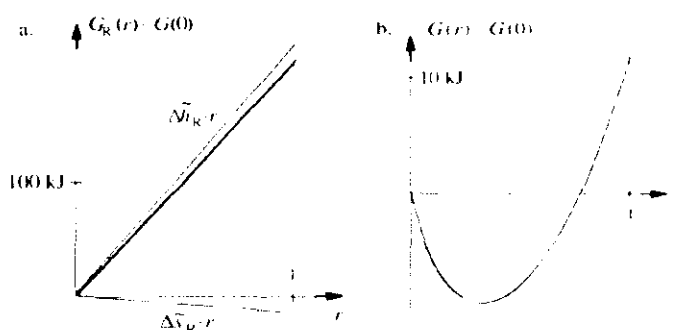


Figure 9 : Gibbs Free Energy as function of r for $\text{H}_2 \rightarrow 2\text{H}$

The minima of the bold curve define the chemical equilibrium

- a. References State
- b. $T=3000\text{K}$, $P=0.01\text{bar}$

For ammonia reaction, the data and initial values are shown in Table 3.

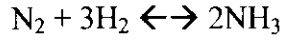


Table 3 : Data and initial conditions for $\text{N}_2 + 3\text{H}_2 \leftrightarrow 2\text{NH}_3$

	γ_{α}	$\nu_{\alpha}(l_0)$	$\Delta \tilde{h}_R$	$\Delta \tilde{s}_R$	z_{α}
N_2	-1	1 mol	$-92.4 \frac{\text{kJ}}{\text{mol}}$	$-178.6 \frac{\text{J}}{\text{mol K}}$	$5/2$
H_2	-3	3 mol			$5/2$
NH_3	2	0			3

For this choice the explicit form of G reads according to equation 7,

$$\begin{aligned}
 G(r) - G = & \left[-92.4\text{kJ} - 6 \times 8.314 \frac{\text{J}}{\text{K}} (T - T_R) \right] r \\
 & - T \left[-178.6 \frac{\text{J}}{\text{K}} + 6 \times 8.314 \frac{\text{J}}{\text{K}} \ln \frac{T}{T_R} - 8.314 \frac{\text{J}}{\text{K}} \ln \frac{P}{P_R} \right] r \\
 & + 8.314 \frac{\text{J}}{\text{K}} T \left[(1-r) \ln \frac{1-r}{4-2r} + 3(1-r) \ln \frac{3(1-r)}{4-2r} \right. \\
 & \left. + 2r \ln \frac{2}{4-2r} + \ln 4 - 3 \ln \frac{3}{4} \right] \quad (9)[26]
 \end{aligned}$$

The range of r is $0 \leq r \leq 1$ according to Equation 8. We plot this function first for $T=T_R, P=P_R$ in Figure 10 and obtain a graph with a minimum very close to $r=0.98$ so that we might expect that ammonia is easily formed. In reality, however there is practically no ammonia since before reaction can occur, the tightly bound molecules H_2 and N_2 must be converted into their atomic forms and this decomposition requires a catalyst. In the Haber Bosch synthesis one use perforated iron sheets. Their effectiveness however requires high temperature of 500°C . But at that temperature the entropic part of G (the second line in equation 9) is emphasized and we obtain a graph whose minimum lies at $r=0$, cf. Figure 10, so that again no ammonia forms. In order to decrease the entropic influence, one may raise the pressure as in equation 9. If the pressure is increased up to 200 bar, a graph for G that has a minimum at about

$r = 0.48$ is obtained, cf Figure 10. Thus ammonia can be produced in quantity at high temperature and high pressure. [26]

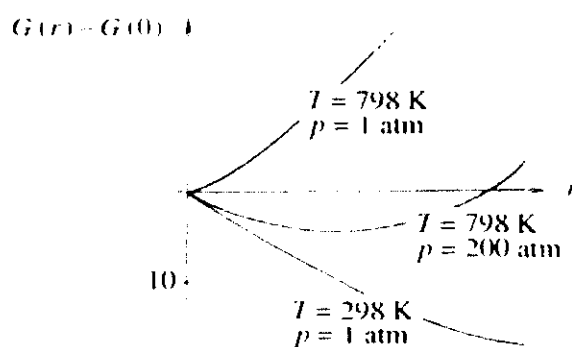


Figure 10 : Synthesis of Ammonia

Figure 10 shows that high temperature is needed for the catalyst to work and high pressure guarantees a good output.

2.3.3 The Concept of Thermo-Magnetic Induction Equilibrium Reaction

Magnetic fields are produced by the motion of charged particles and can be defines as the magnetic field intensity produce by the current I_{net} and dl is a differential element of length the path of integration.

$$\int H \cdot \partial l = I_{net} \tag{10}$$

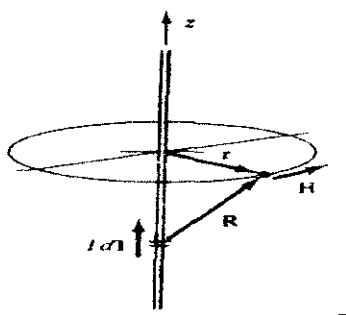


Figure 11 : Magnetic Field

In Figure 11, at each point of the circle, the magnetic field intensity H is tangential and with the same magnitude. Since the strength of the magnetic field flux produced in the core is depended on the material of the core. Hence,

$$B = \mu H \quad (11)$$

Where μ = magnetic permeability of material (H/m)

B = magnetic flux density, tesla (T)

H = magnetic field intensity (A/m)

The magneto-static energy density (in J/m^3) is defines as:

$$w_m = \mu H^2 = \frac{1}{2} B \cdot H = \frac{B^2}{2\mu} \quad (12)$$

Thus the magneto-static energy is

$$W_m = \int w_m \partial v \quad (13)$$

$$W_m = \frac{1}{2} \int B \cdot H \partial v \quad (14)$$

$$W_m = \frac{1}{2} \int \mu H^2 \partial v \quad (15)$$

The change in Gibbs free energy (ΔG°) of the system allows the determination of whether the system is spontaneous or not. It is defined as enthalpy of the system minus the product of the temperature times the entropy of the system.

$$G = H - TS \quad (16)$$

The change in the Gibbs free energy (run at constant temperature) can be defined as

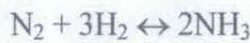
$$\Delta G^\circ = \Delta H^\circ - T\Delta S^\circ \quad (17)$$

Where,

ΔG° = standard-state free energy of reaction

- If, $\Delta H^\circ < 0 \rightarrow$ exothermic, $\Delta H^\circ > 0 \rightarrow$ endothermic
 $\Delta S^\circ < 0 \rightarrow$ atoms or particles become more order
 $\Delta S^\circ > 0 \rightarrow$ increase in the disorder (atoms or particles)
 $\Delta G^\circ < 0 \rightarrow$ exergonic (spontaneous; shift to the right)
 $\Delta G^\circ > 0 \rightarrow$ endergonic (non-spontaneous; shift to the left)

We know that,



Refer to the standard-state enthalpy of formation and absolute entropy data table [27], we find the following information:

Compound	H_f° (kJ/kmol)	S° (kJ/kmol-K)
N ₂	0	191.61
H ₂	0	130.68
NH ₃	-46,190	192.33

Table 4 : Thermodynamic Table

TABLE A-26

Enthalpy of formation, Gibbs function of formation, and absolute entropy at 25°C, 1 atm

Substance	Formula	\bar{h}_f° kJ/kmol	\bar{g}_f° kJ/kmol	S° kJ/kmol-K
Carbon	C(s)	0	0	5.74
Hydrogen	H ₂ (g)	0	0	130.68
Nitrogen	N ₂ (g)	0	0	191.61
Oxygen	O ₂ (g)	0	0	205.04
Carbon monoxide	CO(g)	-110,530	-137,150	197.65
Carbon dioxide	CO ₂ (g)	-393,520	-394,360	213.80
Water vapor	H ₂ O(g)	-241,820	-228,590	188.83
Water	H ₂ O(l)	-285,830	-237,180	69.92
Hydrogen peroxide	H ₂ O ₂ (g)	-136,310	-105,600	232.63
Ammonia	NH ₃ (g)	-46,190	-16,590	192.33
Methane	CH ₄ (g)	-74,850	-50,790	186.16
Acetylene	C ₂ H ₂ (g)	+226,730	+209,170	200.85
Ethylene	C ₂ H ₄ (g)	+52,280	+68,120	219.83
Ethane	C ₂ H ₆ (g)	-84,680	-32,890	229.49
Propylene	C ₃ H ₆ (g)	+20,410	+62,720	266.94
Propane	C ₃ H ₈ (g)	-103,850	-23,490	269.91
n-Butane	C ₄ H ₁₀ (g)	-126,150	-15,710	310.12
n-Octane	C ₈ H ₁₈ (g)	-208,450	+16,530	466.73
n-Octane	C ₈ H ₁₈ (l)	-249,950	+6,610	360.79
n-Dodecane	C ₁₂ H ₂₆ (g)	-291,010	+50,150	622.83
Benzene	C ₆ H ₆ (g)	+82,930	+129,660	269.20
Methyl alcohol	CH ₃ OH(g)	-200,670	-162,000	239.70
Methyl alcohol	CH ₃ OH(l)	-238,660	-166,360	126.80
Ethyl alcohol	C ₂ H ₅ OH(g)	-235,310	-168,570	282.59
Ethyl alcohol	C ₂ H ₅ OH(l)	-277,690	-174,890	160.70
Oxygen	O(g)	+249,190	+231,770	161.06
Hydrogen	H(g)	+218,000	+203,290	114.72
Nitrogen	N(g)	+472,650	+455,510	153.30
Hydroxyl	OH(g)	+39,460	+34,280	183.70

Source: From JANAF, *Thermochemical Tables* (Midland, MI: Dow Chemical Co., 1971); *Selected Values of Chemical Thermodynamic Properties*, NBS Technical Note 270-3, 1968; and *API Research Project 44* (Carnegie Press, 1953).

$$\Delta H^\circ = \Sigma H_f^\circ (\text{product}) - \Sigma H_f^\circ (\text{reactants}) \quad (18)$$

Since $\Delta H^\circ < 0$, which means that it is an exothermic process

$$\Delta S^\circ = \Sigma S^\circ (\text{product}) - \Sigma S^\circ (\text{reactants}) \quad (19)$$

Since $\Delta S^\circ < 0$, which means that the process will lead to cause the molecules arrange in more order form.

Calculated out the ΔG°

$$\text{Where } \Delta G^\circ = \Delta H^\circ - T\Delta S$$

$$T = 25^\circ\text{C} + 273.15$$

$$= 298.15 \text{ K}$$

$$\text{Hence } \Delta G^\circ = -92380 \text{ J} - (298.15 \text{ K}) (-198.99 \text{ J/K})$$

$$= -33051.1315 \text{ J}$$

Since the $\Delta G^\circ < 0$, therefore we can conclude that this is an exergonic process and the reaction is spontaneous at 25°C (ambient temperature). On the other words, the system is shift to the right, converting the reactants into products, before it can reach equilibrium.

The magnitude of ΔG° tells us how far the standard-state is from equilibrium. The larger the value, the further the reaction has to go to get to form the standard-state conditions to equilibrium. When the temperature of the system is increases, the entropy term will become more important. The reaction will become less favorable when the temperature increases.

$$\Delta G^\circ = \Delta H^\circ - T\Delta S^\circ$$

The relationship between ΔG° and equilibrium constant, K is given as

$$\Delta G^\circ = - RT \ln K \quad (20)$$

Where R = gas constant = 8.31447 kJ/kmol-K [16].

This equation allows us to calculate the equilibrium constant for any reaction from the standard-state free energy of reaction or vice versa. For ammonia synthesis, we know that $\Delta G^\circ = -33051.1315$ J at 25°C.

$$\begin{aligned} \Delta G^\circ &= - RT \ln K \\ -33051.1315 \text{ J} &= - (8.31447 \text{ kJ/kmol-K})(298.15 \text{ K}) \ln K \end{aligned}$$

$$\begin{aligned} \ln K &= \frac{33051.1315 \text{ J}}{\left(\frac{8.31447 \text{ kJ}}{\text{kmol} \cdot \text{K}} \right) (298.15 \text{ K})} \\ K &= 6.1702 \times 10^5 \text{ mol} \end{aligned}$$

From the equation, we know that to get ΔG° in negative sign, the value of K must be larger than 1. It is because when $K = 1$, $\Delta G^\circ = 0$. This is indicating that there is no driving force behind the reaction. When $K < 1$, $\Delta G^\circ = \infty$. Not valid

2.4 Theory of Magnetic Induction

A magnetized bar has its power concentrated at two ends which are north (N) and south (S) poles. The N end will repel the N end of another magnet, S will repel S, but N and S attract each other. The region where this is observed is loosely called a magnetic field.

For the matter consists of electrically charged particles: each atom consists of light, negative electrons swarming around a positive nucleus. Objects with extra electrons are negatively (-) charged, while those missing some electrons are positively (+) charged. Experiments have shown that (+) repels (+), (-) repels (-),

while (+) and (-) attract each other. When the ends of a chemical battery were connected by a metal wire, a steady stream of electric charges flowed in that wire and heated it. That flow became known as an electric current. In a simplified view, what happens is that electrons hop from atom to atom in the metal.

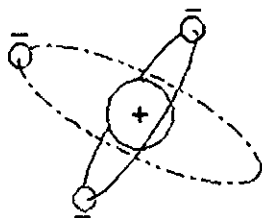


Figure 12 : Electrically Charged Particle[28]

The fundamental nature of magnetism was not associated with magnetic poles or iron magnets, but with electric currents. The magnetic force was basically a force between electric currents as shown in Figure 13 below.

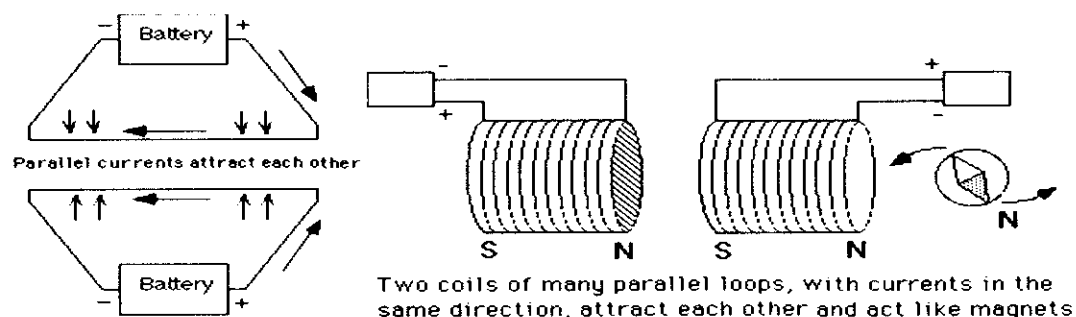


Figure 13 : Force between Electric Current[28]

Each coil acts very much like a magnet with magnetic poles at each end (electromagnet). Ampere guessed that each atom of iron contained a circulating current (magnetic spin), turning it into a small magnet and that in an iron magnet all these atomic magnets were lined up in the same direction, allowing their magnetic forces to add up. [28]

2.4.1 Domains and Hysteresis

In magnetism, a domain wall is an interface separating magnetic domains. It is a transition between different magnetic moments and usually undergoes an angular displacement of 90° or 180° . Although they actually look like a very sharp change in magnetic moment orientation, when looked at in more detail there is actually a very gradual reorientation of individual moments across a finite distance [29].

The energy of a domain wall is simply the difference between the magnetic moments before and after the domain wall was created. This value is more often than not expressed as energy per unit wall area. The width of the domain wall varies due to the two opposing energies that create it: the Magneto-crystalline anisotropy energy and the exchange energy, both of which want to be as low as possible so as to be in a more favorable energetic state. The anisotropy energy is lowest when the individual magnetic moments are aligned with the crystal lattice axes thus reducing the width of the domain wall, whereas the exchange energy is reduced when the magnetic moments are aligned parallel to each other and thus makes the wall thicker, due to the repulsion between them (where anti-parallel alignment would bring them closer - working to reduce the wall thickness). In the end equilibrium is reached between the two and the domain wall's width is set as such. An ideal domain wall would be fully independent of position; however, they are not ideal and so get stuck on inclusion sites within the medium, also known as crystallographic defects. These include missing or different (foreign) atoms, oxides, and insulators and even stresses within the crystal. This prevents the formation of domain walls and also inhibits their propagation through the medium. Thus a greater applied magnetic field is required to overcome these sites. Figure 14 illustrates the domain walls in a magnetic material.

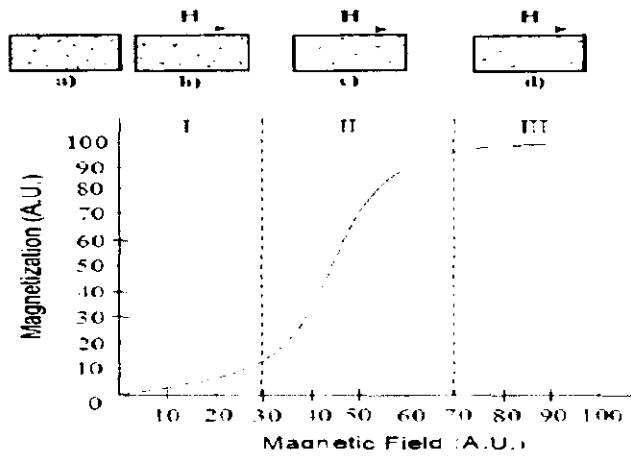


Figure 14 : Variation in Magnetization and Domains under an Eternal Field [30]

2.4.2 Magnetization versus Temperature

The influence of temperature on magnetic material can be determined in the magnetic properties of these materials. Raising the temperature of a solid, results in the increase of the thermal vibrations of atoms, with this the atomic magnetic moments are free to rotate. This phenomenon the atoms tend to randomize the directions of any moments that may be aligned [31]. With increasing temperature, the saturation magnetization diminishes gradually and abruptly drops to zero at what is called the Curie temperature (T_c).

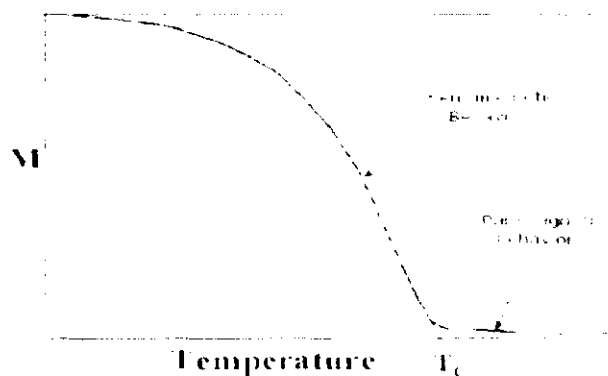


Figure 15 : M-T Curve for Magnetic Material [31]

Figure 15 show that the Curie point of a ferromagnetic material is the temperature above which it loses its characteristic ferromagnetic ability. At temperatures below the Curie point the magnetic moments are partially aligned within magnetic domains in ferromagnetic materials. As the temperature is increased from below the Curie point, thermal fluctuations increasingly destroy this alignment, until the net magnetization becomes zero at and above the Curie point. Above the Curie point, the material is purely paramagnetic. At temperatures below the Curie point, an applied magnetic field has a paramagnetic effect on the magnetization, but the combination of para-magnetism with ferromagnetism leads to the magnetization following a hysteresis curve with the applied field strength. Table 5 shows some examples of Curie temperature for various materials.

Table 5 : Curie temperature of Various Materials

Material	Curie Temperature (K)
Magnetite	858
Iron	1043
Y ₃ Fe ₅ O ₁₂ (YIG)	550
Hematite	1000
Nickel	631
Cobalt	1393

2.4.3 Ferromagnetism

Ferromagnetism is the phenomenon by which materials such as iron in an external magnetic field become magnetized and remain magnetized for a period after the material is no longer in the field. Ferromagnetic materials have atomic magnetic fields that align themselves parallel to externally applied magnetic fields. This creates a total magnetic field within the material much greater than the applied field.

Above a critical temperature known as the Curie temperature, the material becomes paramagnetic. [32] Figure 16 shows the behavior of a ferromagnetic material, which will exist even in the absence of an external magnetic field [33].

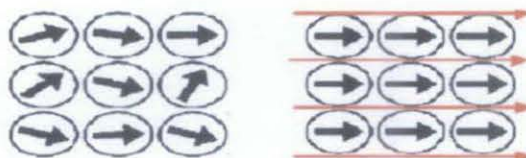


Figure 16 : Schematic Illustration of the Mutual Alignment of Atomic Dipole for a Ferromagnetic Material after External Magnetic Field is Applied[33]

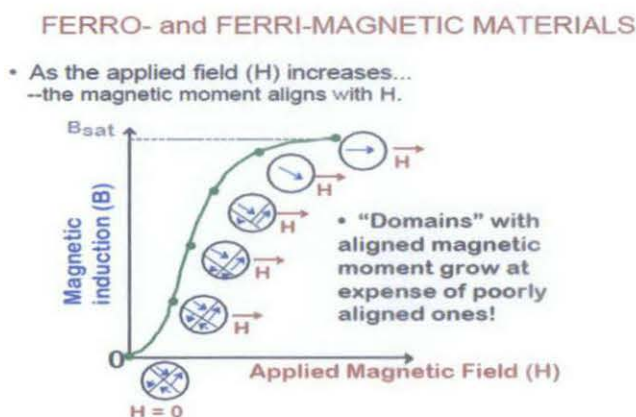


Figure 17 : Magnetic Strength versus Alignment of Atomic Spin
[Source: <http://www.chem1.com/CQ/magscams.html>]

2.4.4 The Magnetic Field Effects in Chemical Reaction

A new approach is done in this project by introducing magnetic energy to replace the thermal energy which required in the conventional Haber-Bosch process to affect the reaction equilibrium. The technique of replacing the thermal energy by magnetic energy will be explored in this project. This is a new area of research and will lead to a new approach for the driving force of chemical reactions.

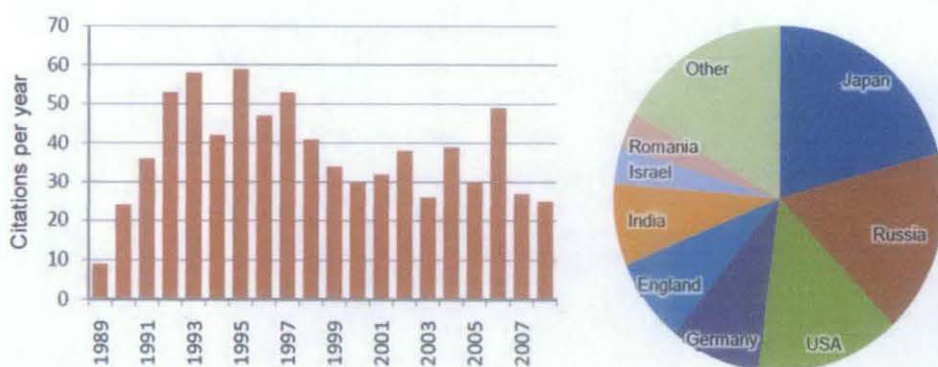


Figure 18 Recent trends in spin chemistry research analyzed by year and by country, measured as citations of the landmark review of spin chemistry. Data from ISI Web of Knowledge 2008

The ways in which magnetic fields can affect chemical reactions have long been the subject of investigation, but only recently, with the theoretical insight given by the interpretation of chemically induced magnetic polarization,⁷ has significant progress been made. [34] (R. Lepley and G. L. Closs, 1973)

(U. E. Steiner, T. Ulrich, 1989) states that magnetic fields can alter the rate, yield, or product distribution of chemical reactions. [35,36] (F. Z. Tang, A. Katsuki, Y. Tanimoto, 2006) also state that a wide variety of magnetic field effects (MFEs) are now known; they occur in diverse chemical systems at field strengths ranging from several Tesla, as at the heart of a superconducting magnet [37], down to only $\sim 40 \mu\text{T}$, which is comparable to the field strength of the Earth.[38] In the latter case, this exquisite magnetic sensitivity arises even though the interaction between such a weak magnetic field and the molecules involved has energy much smaller than the average thermal energy $k_{\text{B}}T$.

As we shall see, these phenomena arise through a detailed interplay of diffusion, reaction and quantum mechanical effects on the electron, and nuclear spins of the species involved. Measurement and analysis of MFEs has given rise to information on the reactivity, structure, and motion of these species. Such investigations are central to the field of endeavor known as spin chemistry. This review gives a short

introduction to spin chemistry, in a form accessible to graduate students and scientists new to the field. It summarizes the historical development of spin chemistry, sets out the essential theoretical framework for the analysis of MFEs, and presents representative examples of recent developments together with an assessment of the opportunities and challenges that lie ahead. The Radical Pair Mechanism (RPM) [39], [40], [41] provides the mechanistic basis for the interpretation of most MFEs in chemical systems.

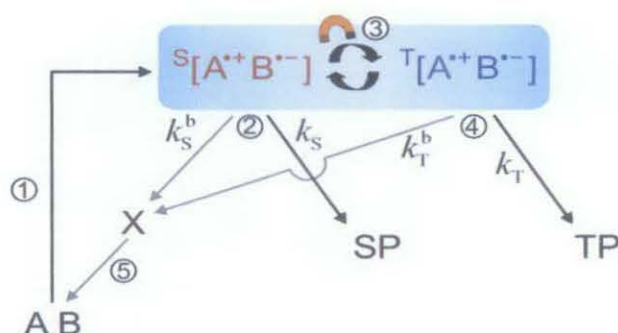


Figure 19 : Radical Pair Mechanism [41]

The essential features, illustrated in Figure 19 are as follows:

- Step 1:
Ground-state precursor species “A B” are excited to produce two radicals whose electron spins are in a well-defined overall spin state, i.e., a spin-correlated radical pair (RP). This excitation is often photochemical, where an incident photon is absorbed leading to the transfer of an electron from A to B, creating radical ions in a ‘singlet’ state. Other possibilities include H atom transfer and thermo-lytic bond cleavage, which both produce uncharged RPs
- Step 2:
The singlet RPs undergoes spin-selective reaction to produce the singlet product (SP) at rate k_s or they react non-selectively to give a back-reaction product X at a rate k_s^b
- Step 3:
Coherent evolution of the RP spin state competes with these reactions, converting a proportion of the singlet (S) RPs back and forth into triplet (T)

RPs. This $S \leftrightarrow T$ interconversion is driven by magnetic interactions in the RP and by any applied magnetic field

- Step 4:

The triplet RPs undergo their own spin-selective reaction to produce the triplet product TP at a rate k_T or again they react nonselectively to give the back-reaction product X, this time at a rate k_T^b which is not normally equal to k_S^b

- Step 5:

In many cases, the nonselective product X (or SP or TP) converts back into the precursor species “A B” which is then free again to begin step 1

The key feature of the RPM is the spin evolution between singlet and triplet states in step 3. Externally applied magnetic fields affect the rate and extent of this spin evolution and hence affect the yields of reaction products SP, TP, and X. Even weak magnetic fields whose interaction energies are far less than the thermal energy $k_B T$ may cause significant changes in the yield of SPs. This does not contradict the laws of thermodynamics because generation of the RP in step 1 requires much more than the thermal energy $k_B T$. The subsequent formation of products SP, TP, and X is determined by competitive kinetics. A helpful analogy is that of a railway train approaching a set of points. To drive the train, much energy is supplied by the locomotive just as in step 1, but the ultimate destination of the train will be determined by a small force used by the signal man to set the points. Even though the magnetic interactions with weak fields in step 3 are tiny, they may cause significant changes in the product yields.

In fields $B_0 < 50$ mT, the singlet–triplet inter-conversion responsible for MFEs is governed primarily by the isotropic electron Zeeman and the hyperfine interactions. This is known as the hyperfine mechanism. At higher fields, the situation is rather different. There, singlet–triplet inter-conversion arises for the most part because of small differences in the g -tensors of the two radicals, in what is known as the Δg -mechanism. Figure 20 summarizes this change in mechanism.

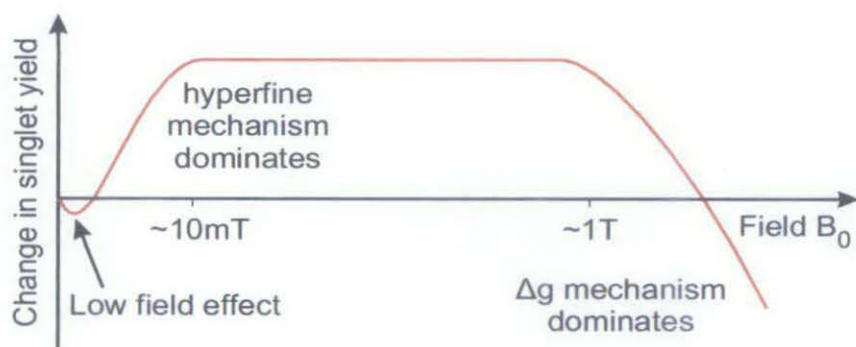


Figure 20 : Typical MFEs in Organic RPs From Zero Field Up to A Few Tesla

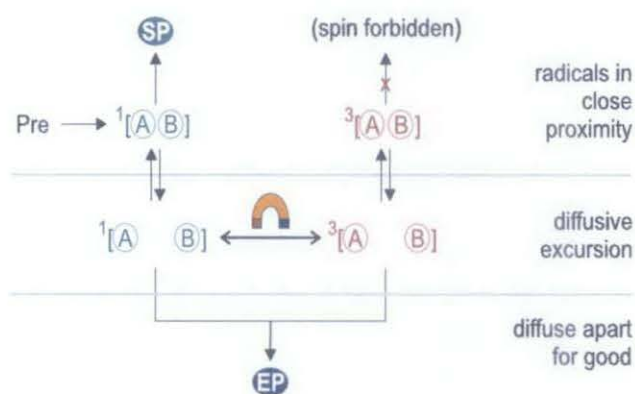


Figure 21 : Reaction-Diffusion in Liquids

Studies of chemical MFEs have provided a good deal of insight into the chemical physics of liquids and solutions. Radical pair mechanisms as outlined in Figure 20 revolve around kinetic competition that determines which products are formed from RP intermediates. In the general scheme above, this competition was governed by first-order rate constants k_s , k_s^b , etc.

In the liquid phase, the magnitude and features of Chemically Induced Dynamic Nuclear Polarization (CIDNP), Chemically Induced Dynamic Electron Spin Polarization Span (CIDEP), and chemical MFEs depend critically on the diffusive motion of the RP involved. The kinetics controlling the reaction of the RPs may be understood more explicitly in terms of the reaction-diffusion form of the RPM shown in Figure 21, the key features of which are as follows:

- The precursor(s) react to form an RP in a well-defined spin state, e.g., the singlet $^S[A^{\cdot} B^{\cdot}]$. The RP is excited by much more than $k_B T$, which ensures that its subsequent fate is controlled kinetically and not by equilibrium thermodynamics
- For ~ 500 ps after this, the radicals are caught in very close proximity by a ‘cage’ of surrounding solvent molecules. They collide frequently with one another during this first encounter. A proportion of the RPs reacts during these frequent collisions to form the SP. This step, known as ‘primary geminate recombination’, is insensitive to magnetic fields [31] because the exchange interaction is strong at short separation which inhibits $S \leftrightarrow T$ inter-conversion. Experimentally, it is often suppressed using modulation and phase-sensitive detection techniques such that it may, to all intents and purposes, be ignored
- Some RPs, however, does not react in these first instants, and separate instead, making a ‘diffusive excursion’ in the surrounding liquid. The exchange interaction between electron spins that was very large when the radicals were in close proximity is now much less significant. Hence, the RP is free to undergo $\leftrightarrow T$ inter-conversion under the influence of molecular hyperfine interactions and, crucially, under the influence of the applied magnetic field
- At the end of a diffusive excursion, some RPs separate for good, whence they react ultimately, e.g., by H atom abstraction from the solvent, to form the ‘escape product’ (EP)
- Other RPs re-encounter one-another, whereupon the radicals are once more held within a solvent cage and undergo frequent collisions, which afford them opportunity to react with one another. Such reactions are known as ‘secondary geminate recombination’
- Whether the radicals react during a re-encounter depends on the spin evolution during the preceding diffusive excursion. For example, in the reaction between pyrene (Py) and *N,N*-dimethylaniline (DMA) shown in Figure 2.4.4.4.4, spin is conserved during the back-electron transfer reaction to form an exciplex. This

means that the radicals may only undergo back-electron transfer during a re-encounter when the RP is in an overall singlet spin state. We refer to such products as the ‘singlet product’ (SP). RPs in a triplet state can do nothing other than to separate once more.

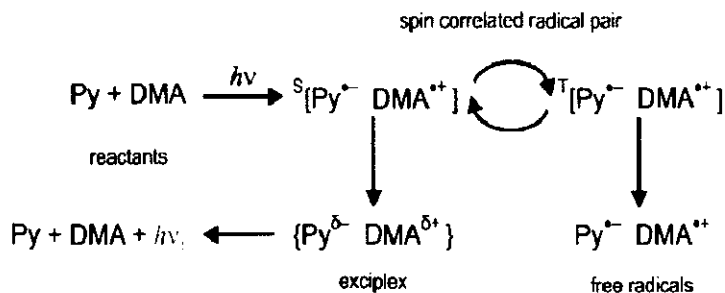


Figure 22 : Regularization Methods Allow Details of the Diffusive Motion of RPs to be recovered From Experimental MFE Data [35]

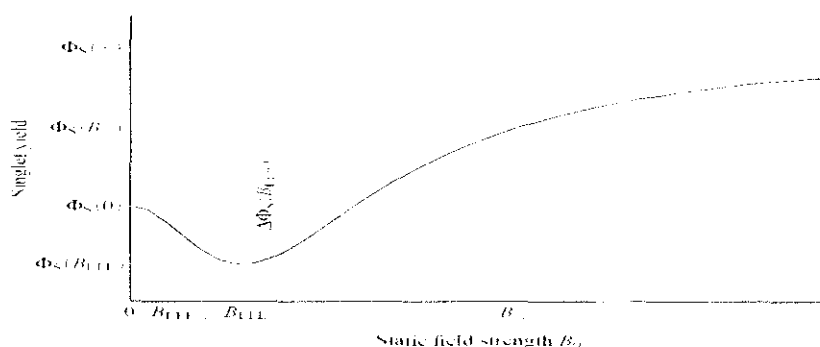
A number of different approaches have been taken to measuring chemical MFEs in the liquid phase. Some of these approaches are presented here, serving as both an introduction to experimental work in the field and an illustration of the reaction-diffusion theory presented above. A multitude of names have been given to these closely related experiments. In these experiments, the RP spins typically evolve under a Hamiltonian. [35]

$$\widehat{H} = \sum_{N=\{A,B\}} \{ -\gamma_c B_0 \cdot \hat{S}^N - \gamma_c B_1(t) \cdot \hat{S}^N + \sum_i a_{Ni} \hat{S}^N \cdot \hat{I}^{Ni} \} - e^{\frac{-t}{T}} J_0 \hat{S}^A \hat{S}^B \quad (21)$$

By using the notation defined above with B_0 denoting the static (time-independent) magnetic field and $B_{0(t)}$ its time-dependent component. Since a typical RP lifetime is of the order of 10 ns – 1 μs, fields with frequency $\nu_{rf} > 1$ MHz could show resonant effects. It transpires that in weak static fields, radiofrequencies (MHz) are most appropriate, whilst microwave frequencies (GHz) are best in strong (>1 T) static fields. Experimental measurements of chemical MFEs customarily record the singlet or triplet product yield as a function of the field strengths B_0 and B_1 , or as a function of the frequency of the time dependent field. Measuring the product yield as

a function of the static field strength B_0 , without RF, generates what is known as a MARY (magnetic field modulation of the reaction yields) 'spectrum' [36].

Examples and references to the literature are given below in connection with Figures 23 and Figure 24.



(a) MARY curve for a one-proton radical pair marked with the principal empirical parameters discussed in the main text.

Figure 23 : Characterizing MARY curves[37]

MFEs on yields and lifetimes of chemical systems are widespread. They may be interpreted convincingly by means of the RPM, giving insights into the kinetics, diffusion, and structure of the radicals involved. When static and RF fields are applied simultaneously, chemical MFEs are closely related to more conventional forms of EPR spectroscopy. [37]

2.4.5 Magneto-Thermodynamic Effect in Chemical Reaction

This subsection is concerned with the magnetic field effects (MFEs) on the chemical equilibrium and related phenomena. (Yamaguchi,1987) showed an indubitable evidence of the MFE on the chemical equilibrium in by applying high magnetic fields to the ferromagnetic metal-hydrogen system caused to dissociate hydrogen from the metal hydride, associated with an increase in the equilibrium hydrogen pressure. This also means that the equilibrium constant is affected by magnetic fields.

Besides the equilibrium constant, a chemical reaction is accompanied by important thermodynamic quantities, such as the heat, the free energy and the entropy of reaction. Let us consider the chemical system in which k kinds of ideal gasses are reacted with each other at the stoichiometric coefficients v_i ($i = 1 \sim k$) under the influence of a magnetic field. Then, the condition of a chemical equilibrium is written by,

$$\sum_{i=1}^k v_i \mu_i = 0 \quad (22)$$

Where the chemical potential of the i -th gas consists of the non-magnetic term $\mu^{(0)}$ and the magnetic term $\mu^{(m)}$ as,

$$\mu_i = \mu_i^{(0)} + \mu_i^{(m)} = \mu_i^* + RT \ln \frac{P_i}{P^*} - \int_0^H \mu_0 m_i dH \quad (23)$$

Where μ_i^* is the standard chemical potential at temperature T and the standard pressure P^* in zero magnetic fields. P_i and m_i are the partial pressure and the molar magnetization for the i -th component. μ_0 is the permeability of a vacuum. The integration must be done with respect to the magnetic field strength H at constant temperature T . The equilibrium constant K_p is derived from equation 22 and equation 23 as,

$$\ln K_p = \sum_{i=1}^k v_i \ln \frac{P_i}{P^*} = -\frac{1}{RT} \sum_{i=1}^k v_i (\mu_i^* + \mu_i^{(m)}) \quad (24)$$

Equation 24 leads to the magnetic field-induced change in the equilibrium constant.

$$\ln K_p^{[H]} - \ln K_p^{[0]} = -\frac{1}{RT} \left(-\sum_{i=1}^k v_i \int_0^H \mu_0 m_i dH \right) = -\frac{1}{RT} g^{(m)} \quad (25)$$

Where $^{[H]}$ and $^{[0]}$ is the equilibrium constant in the magnetic field and in the zero fields respectively. Below similar notations are used for other thermodynamic

quantities. $g^{(m)}$ is the magnetic free energy change per unit reaction. Moreover, the heat of reaction ΔH^0 , the free energy of reaction ΔG^0 and the entropy of reaction ΔS^0 are a function of temperature T and magnetic field strength H , too. In this paper we omit the superscript 0 from the notation for simplification. Using the standard theory of the chemical thermodynamics yields the magnetic field-induced changes in these thermodynamic quantities as

$$\Delta H^{[H]} - \Delta H^{[0]} = g^{(m)} - T \frac{d}{dT} g^{(m)} \quad (26)$$

$$\Delta G^{[H]} - \Delta G^{[0]} = g^{(m)} \quad (27)$$

$$\Delta S^{[H]} - \Delta S^{[0]} = -\frac{d}{dT} g^{(m)} \quad (28)$$

Equations 25 to 28 are the general formulae for the magneto-thermodynamic effects in chemical reactions. This magneto-thermodynamic formulation is applicable to all of the MFEs in chemical reactions. [76]

2.5 Helmholtz Coil

A magnetic field is a pretty awesome thing. As a fundamental force of the universe, they are something without which, planetary orbits, moving electrical charges, or even elementary particles could not exist. It is therefore intrinsic to scientific research that we be able to generate magnetic fields ourselves for the purpose of studying electromagnetism and its fundamental characteristics. One way to do this is with a device known as the Helmholtz Coil.

A Helmholtz coil is a device for producing a region of nearly uniform magnetic field. It consists of two identical circular magnetic coils that are placed symmetrically, one on each side of the experimental area along a common axis, and separated by a distance (h) equal to the radius (R) of the coil. Each coil carries an equal electrical current flowing in the same direction. A number of variations exist,

including use of rectangular coils, and numbers of coils other than two. However, a two-coil Helmholtz pair is the standard model, with coils that are circular and in shape and flat on the sides. In such a device, electric current is passed through the coil for the purpose of creating a very uniform magnetic field. [42] (Matt Williams, 2011)

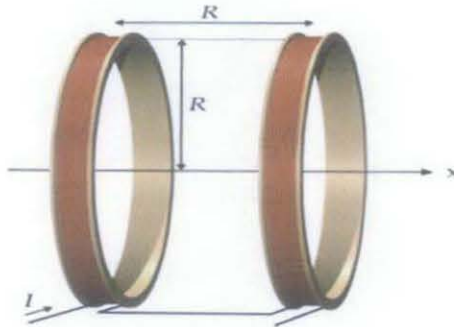


Figure 24 : Helmholtz Coil

Helmholtz coils are used for a variety of purposes. In one instance, they were used in an argon tube experiment to measure the charge to mass ratio ($e: m$) of electrons. In addition, they are often used to measure the strength and fields of permanent magnets. In order to do this, the coil pair is connected to a flux meter, a device which contains measuring coils and electronics that evaluate the change of voltage in the measuring coils to calculate the overall magnetic flux. In some applications, a Helmholtz coil is used to cancel out Earth's magnetic field, producing a region with magnetic field intensity much closer to zero. This can be used to see how electrical charges and magnetic fields operate when not acted on by the gravitational pull of the Earth or other celestial bodies.

A pair of conducting circular coils each having N turns, each carrying a current I , separated by a distance equivalent to the radius of the circular loops, produce a homogeneous magnetic field B in the mid-plane between the two circular coils. [43] (Hermann von Helmholtz, 1821-1894)

$$B = \frac{32\pi NI}{5\sqrt{5}a} \times 10^{-7} \text{ tesla} \quad (29)$$

Where,

a = radius of the coils

a = separation between the coils

$\frac{a}{2}$ = distance to the mid-plane

B = magnetic field at the mid-plane

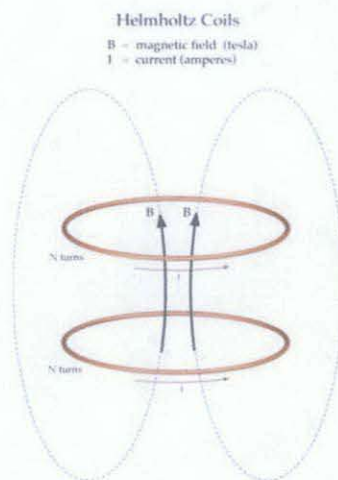


Figure 25 : Magnetic Field Applied by Hemholtz Coil

A magnetic field is created whenever charge is in motion--either moving in space or spinning around it. A charge moving in space is called a "current" (denoted by the symbol I) and is measured in coulombs/sec or amperes.

The strength of magnetic field is measured at a point in space (often called the field point). In the case of the Helmholtz coils, the field points of interest are located in the mid-plane between the two coils. As shown in the equation above, the strength of the magnetic field is dependent upon three quantities:

The current I ,

The number of turns N in each coil, and

The radius a of the coil.

The total current in each coil is NI .

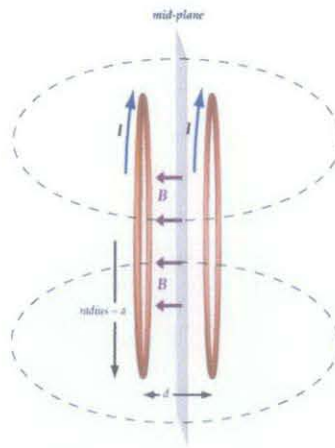


Figure 26 : Magnetic Strength, B

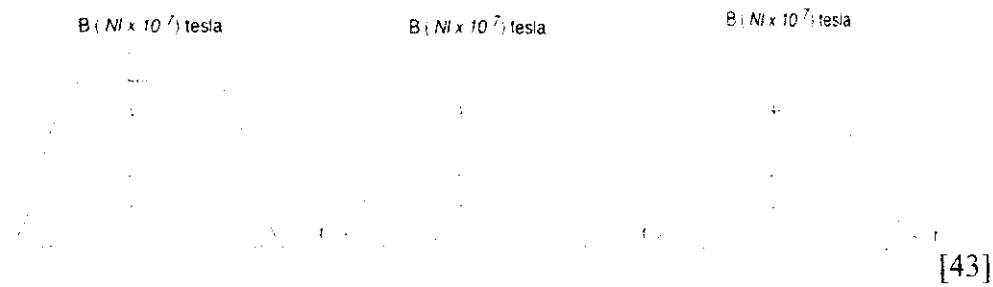
To determine the uniformity of the magnetic field requires more than the above equation and involves some complicated integral calculus. However, we can generate some figures that graphically show how the magnetic field varies on the mid-plane as a function of r (the distance from the axis of symmetry passing between the centers of the two coils) and d the separation between the two coils.

In the figures to the right, we can see how uniform the magnetic field is on the mid-plane when the spacing d is too close, just right, and too far. The figures to the right are calculated for coils with a radius of 20 cm (i.e., $a = 0.20$ m).

The following integral was evaluated to produce the three curves at the right

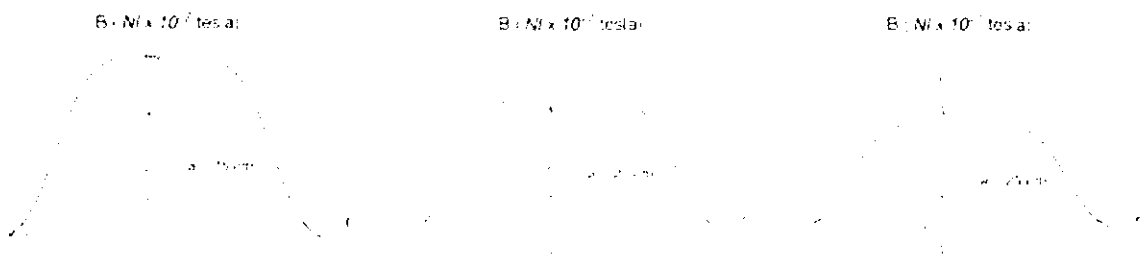
$$B_z(r) = NI \times 10^{-7} \int_0^{2\pi} \frac{2a(a-r\cos(\theta))d\theta}{(a^2+b^2+r^2-2ar\cos(\theta))^{\frac{3}{2}}} \quad (30)$$

Where the factor of "2" in the numerator takes into account the two coils, and $b = d/2$ is the distance from each coil to the mid-plane.



Coil spacing is "too close." Coil spacing is "just right." Coil spacing is "too far."
 $d = a$ $d = 0.8 a$ $d = 1.2 a$

The figures below show the range of uniform magnetic field as a function of the coil radius. [43]



2.6 Atom and Magnetic Field

Electricity and magnetism are two aspects of a single electromagnetic force. Moving electric charges produce magnetic forces, and moving magnets produce electric forces. Electricity is the movement of electrons from one atom to another in a constant flow. At the atomic level, electrons create a magnetic field as they spin about the atom's nucleus. For example, when skin in touch with an object, the brain will tell whether it is soft or hard, rough or smooth. The reality is that the magnetic fields of the electrons in the skin's atoms are actually rubbing against the magnetic fields of the touched object's atoms. These magnetic fields are repelling each other.

Magnetic fields surround everything. Some purported inventions claim to help human bodies realign their magnetic fields for better health. The earth and magnets have strong magnetic fields. The difference between humans, the earth, and a magnet lies in the types of atoms and the molecular structure in which the atoms are arranged. Molecules in human bodies comprised of carbon, oxygen, and hydrogen are very poor at forming magnetic fields. Iron atoms are great at lining up their electrons, in what is called "domains," to form a magnetic field. This is what happens in the earth's core.

Certain elements, when organized in particular lattices, have atomic properties that make their electrons' magnetic fields stronger. Rare elements, such as those in magnetite, provide material for the types of magnets used around us every day. Hard drives, television sets, and stereo speakers all rely on magnets to work. There is a great deal of magnetic activity on the sun. Atoms are stripped of their electrons, which then move around with other electrons at high speeds, creating huge magnetic fields. [44]

2.7 Application of Magnetic Nano-catalyst

Magnetic iron nano-catalysts

Iron oxide nanoparticles make efficient recyclable catalysts for organic reactions. Environmentally friendly, economical and efficient catalysts for carbon-carbon bond forming reactions are desirable for industrial chemists. Magnetically recoverable catalysts are especially attractive due to their ease of separation from the reaction mixture. Iron oxide nanoparticles are efficient magnetic catalysts that can be reused up to twelve times without losing their effectiveness. [45](Chao-Jun Li, 2010)

Iron oxides nanoparticles stick to the stirring bar when the reaction stops. The separation and reuse of the magnetic iron oxide nanoparticles were very simple, effective and economical. In addition, the use of iron oxides as catalysts is also more environmentally friendly and safer than other transition metal catalysts.

The ease of separation of these catalysts helps to avoid difficult and elaborated separation procedures involving filtration and centrifuging materials, equipments and solvents; thereby contributing immensely to the environmentally friendly aspects of the process. [46] (Unni Pillai, 2010)

Yttrium iron garnet (YIG) Nanocatalyst

Yttrium iron garnet (YIG) is a synthetic garnet with chemical composition of $Y_3Fe_2(FeO_4)_3$ or $Y_3Fe_5O_{12}$. It is a ferrimagnetic material with Curie temperature of 550K. In YIG, the five iron (III) ions occupy two octahedral and three tetrahedral sites with the yttrium(III) ions coordinated by eight oxygen ions in an irregular cube. The iron ions in the two coordination sites exhibit different spins, resulting in magnetic behavior.

Besides, YIG has a high Verdet constant which result in the Faraday effect, high Q factor in microwave frequencies, low adsorption of infrared wavelengths up to 600nm and very small linewidth in electron spin resonance.

Hematite Nanocatalyst

The nano iron oxides have been synthesized by almost all the known wet chemical methods which include precipitation at ambient/elevated temperatures, surfactant mediation, emulsion/micro-emulsion, electro-deposition etc. Iron oxides in nano-scale have exhibited great potential for their applications as catalytic materials, wastewater treatment adsorbents, pigments, flocculants, coatings, gas sensors, ion exchangers, magnetic recording devices, magnetic data storage devices, toners and inks for xerography, magnetic resonance imaging, bio-separation and medicine. In

catalysis both iron oxides and hydroxides find application in numerous synthesis processes. Iron oxides are one of the most important transition metal oxides of technological importance. Sixteen pure phases of iron oxides, i.e., oxides, hydroxides or oxy-hydroxides are known to date. These are $\text{Fe}(\text{OH})_3$, $\text{Fe}(\text{OH})_2$, $\text{Fe}_5\text{HO}_8 \cdot 4\text{H}_2\text{O}$, Fe_3O_4 , FeO , five polymorphs of FeOOH and four of Fe_2O_3 . Characteristics of these oxide compounds include mostly the trivalent state of the iron, low solubility and brilliant colors (Cornell and Schwertmann, 1996)

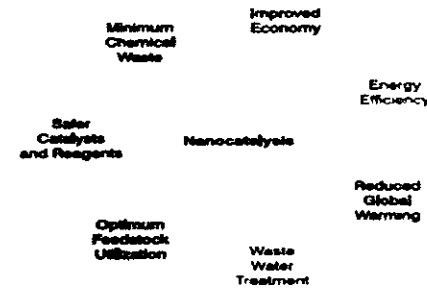
The structure of 'hematite', $\alpha\text{-Fe}_2\text{O}_3$, is isostructural with corundum, $\alpha\text{-Al}_2\text{O}_3$. The structure has also a three-dimensional framework built up with trigonally distorted octahedra FeO_6 , linked to thirteen neighbors by one face, three edges and six vertices. The space group is $R\bar{3}c$ (N $^\circ$ 167, rhombohedral symmetry) and the lattice parameters given in the hexagonal cell are: $a = 5.0346 \text{ \AA}$, $c = 13.752 \text{ \AA}$. The structure is similar to that of corundum, and consists essentially of a dense arrangement of Fe^{3+} ions in octahedral coordination with oxygens in hexagonal closest-packing. The structure can also be described as the stacking of sheets of octahedrally (six-fold) coordinated Fe^{3+} ions between two closed-packed layers of oxygens. Since Fe is in a trivalent state (ferric Fe), each of the oxygens is bonded to only two Fe ions, and therefore, only two out of three available oxygen octahedrons are occupied. This arrangement makes the structure neutral with no charge excess or deficit. The Fe-O sheets are held together by strong covalent bonds. The crystal system of hematite is hexagonal, but crystals appear in a wide variety of forms. The specific surface area ranges from 10 - 90 m^2/g . (Cornell and Schwertmann, 2003)

Moreover, iron oxide-based materials have been found to be good candidates as cheap and efficient catalysts, especially in environmental catalysis. (Miyata, 1978) studied the catalytic activity of several iron oxides and oxide hydroxides of various particle sizes for the reduction of 4-nitrotoluene using hydrazine hydrate as reducing agent, and found $\beta\text{-FeOOH}$ was the most effective catalyst. Nano-particle iron oxide is significantly more effective than conventional micron-sized iron oxide (Walker 1988; Li 2003) for the oxidation of CO and the oxidative pyrolysis of biomass (Li, 2003) or biomass model compounds. (Li, 2004; Shin, 2004)

On the other hand, nanoparticles of magnetic oxides, including most representative ferrites, have been studied for many years for their application as magnetic storage media and ferro-fluids. Over the recent years, gamma iron oxide (γ Fe₂O₃), a ferromagnetic material is widely used as magnetic storage media in audio and video recording (Tsakalakos,2003), magneto-optical devices (Goya, 2003; Kawanishi, 1997), magnetic refrigeration (McMichael,1992) whereas α Fe₂O₃ in nano-size is a potential candidate for photo anode for possible photo-electrochemical cells (Prosini, 2002; Wang, 2004a). Cheng *et al.* (2006) prepared a nano-sized iron oxy-hydroxide (FeOOH) via a hydrolyzing route under mild and facile synthesis condition which delivered a capacity of about 237 mAh/g in the voltage range from 1.5 V to 4.2 V, and showed a very good cycling performance in the voltage range from 1.6 V to 3.3 V with a capacity of 170 mAh/g. A novel "sacrificial template-accelerated hydrolysis" (STAH) approach to the synthesis of iron oxide-based nanotube arrays including hematite octahedral-Fe₂O₃ and magnetite Fe₃O₄ was reported by Liu (2010). By introducing glucose into the precursor solution, they obtained carbon/hematite(C/ α -Fe₂O₃) composite nanotube arrays on large-area flexible alloy substrate, with a large number of pores and uniform carbon distribution at a nanoscale in the nanotube walls. These arrays have been demonstrated as excellent additive-free anode materials for lithium ion batteries in terms of good cycling performance up to 150 times (659 mA h g⁻¹) and outstanding rate capability.

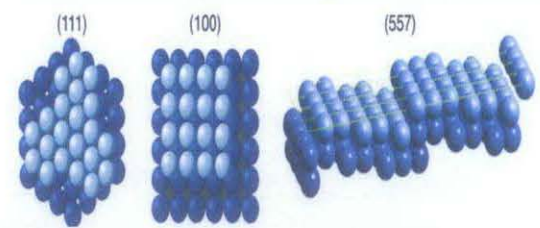
[47]

Table 6 : Literature Review Summary of Application of Nano-catalyst in Chemical Industry

Author	Objective	Description	Advantages	Ref
P. N.Rao, 2010	To produce catalysts with 100% selectivity, extremely high activity, low energy consumption, and long lifetime	<ul style="list-style-type: none"> • This can be achieved only by precisely controlling the size, shape, spatial distribution, surface composition and electronic structure, and thermal and chemical stability of the individual nano-components • Since nanoparticles have a large surface-to-volume ratio compared to bulk materials, they are attractive candidates for use as catalysts • In homogeneous catalysis, transition metal nanoparticles in colloidal solutions are used as catalysts. In this type of catalysis, the colloidal transition metal nanoparticles are finely dispersed in an organic 	 <ul style="list-style-type: none"> • Increased selectivity and activity of catalysts by controlling pore size and particle characteristics • Replacement of precious metal catalysts by catalysts tailored at the nanoscale and use of base metals, thus improving chemical reactivity and reducing process costs • Catalytic membranes by design that can remove unwanted molecules from gases or 	[48]

		or aqueous solution, or a solvent mixture	liquids by controlling the pore size and membrane characteristics	
Adem Yildirim	In designing and synthesizing new solid inorganic catalysts the aims are to maximize surface area, activity, selectivity, longevity, and durability	<ul style="list-style-type: none"> • Nanocatalysis research can be explained as the preparation of heterogeneous catalysts in the nanometer length scale • They are very promising and it can be expected that use of nanocatalysts can decrease the energy usage in the chemical processes results in a greener chemical industry • Also they can be used for water and air cleaning processes and new generation fuel cells • However, these new features come with new problems like, thermal stability and separation after reaction completed 	<ul style="list-style-type: none"> • Size Effects <ul style="list-style-type: none"> - The initial incentive to reduce the size of the particles of active components was to maximize the surface area exposed to the reactants, and thus minimize the specific cost per function • Shape Effect <ul style="list-style-type: none"> - The shape of the nanoparticle determines surface atomic arrangement and coordination - For example, studies with single-crystal surfaces of bulk Pt have shown that high-index planes generally exhibit much higher catalytic activity than that of the most common stable planes, such as {111}, {100}, and even {110} 	[49]

		<ul style="list-style-type: none"> Parameters like surface area, activity, selectivity, longevity, and durability must be well characterized 	<ul style="list-style-type: none"> High-index planes like; $\{210\}$, $\{410\}$ and $\{557\}$ have a high density of atomic steps, ledges, and kinks, which usually serve as active sites for breaking chemical bonds 	
<p>J.Rolnitzky, 2005</p>	<p>The general purpose of catalysts is to increase the speed of a given reaction. This is achieved through kinetic means and does not directly affect the thermodynamic properties of a</p>	<ul style="list-style-type: none"> Smaller objects have more surface area with respect to their volume. This has important implications for chemical reactions. High surface area-to-volume ratios are favorable for chemical reactions Introducing a catalyst increases the speed of a reaction in one of three ways; it can lower the activation energy for the reaction, act as a 	<ul style="list-style-type: none"> Nano-materials are more effective than conventional catalysts for two reasons <ul style="list-style-type: none"> First, their extremely small size (typically 10-80 nanometers) yields a tremendous surface area-to-volume ratio Also, when materials are fabricated on the nanoscale, they achieve properties not found within their macroscopic counterparts. Both of these reasons account for the versatility and 	<p>[50]</p>



	chemical system	facilitator and bring the reactive species together more effectively, or create a higher yield of one species when two or more products are formed	effectiveness of nanocatalysts	
--	-----------------	--	--------------------------------	--

2.8 Catalytic Reaction

Activation of catalyst is an initial process that has to be performed before the reaction takes place. It involves the reduction from the metal oxide to the metallic state in hydrogen as reducing gas. The purpose of reduction is to eliminate oxygen to allow the electron pairing or sharing between the reactant atoms and partially filled d-orbital of a reduced metal. The overall chemical reaction is as follows [51]:



The mechanism of reduction involves two main processes which occur separately. The first process is the generation of reducing electron via reaction of hydrogen. And the process continued by the metallic forming. The mechanism is illustrated as below:



2.8.1 Catalyst and Magnetism

Catalysts have been characterized through their magnetic properties for many years. Bulk phases, such as metals, oxides, carbides, etc., are easily identified by magnetic transitions and moments. Unique magnetic contributions to catalysis occur in catalyst dispersions and adsorption. Catalysts are prepared as small crystallites upon the surface of a refractory support. These crystallites are in the diameter range of 10 to 200 Å, which means they are super-paramagnetic for ferromagnetic metals and super-antiferromagnetic for antiferromagnetic oxides. Magnetization measurements lead to crystallite size distributions of dispersed nickel and these have been useful in the investigation of preparation methods, crystallite size effects in adsorption and catalysis and sintering phenomena. Similar results are possible for supported oxides, such as NiO, Fe₂O₃, etc., but reported applications are not

extensive. Adsorption of gases on ferro- and paramagnetic catalysts may result in a transfer of electrons, detectable through magnetic changes. This effect has been applied to adsorption intermediates. Current trends in catalysis indicate the importance of molecular clusters of atoms, which will be a promising application for magnetism, both experimental and theoretical. [52]

2.8.1 Adsorption Process

Adsorption process in ammonia synthesis is an essential process where the reactant molecules in this case the hydrogen and nitrogen gasses adhere to the surface of the metal catalyst. It is categorized into two parts which are physical (physisorption) and chemical (chemisorption). When these reactant gases are flowed in the reaction medium, they will be firstly adsorbed to the metal surfaces by physisorption. At this stage, it involves a Van der Waals interaction between the reactants and metal surfaces.

The enthalpy change due to adsorption (ΔH_{ads}) is 5–50 kJ/mole [53]. This enthalpy change is insufficient for the bond breaking to occur. Hence physisorbed molecules are retained. Multilayer adsorption would then occur. Multilayer adsorption is a phenomenon where the adsorption surface allows more than one layer of molecules. It should be noted that not all adsorbed molecules are in direct contact with the surface of the metal. Because of this, the chemisorption is performed to initiate the dissociation of molecules so that the next process can be completed.

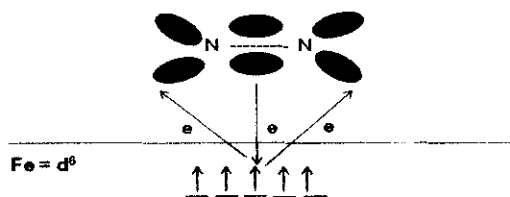


Figure 27 :Mechanism of chemisorption on the iron metal surface

Figure 27 reveals the chemisorption mechanism on the iron metal surface [53, 54]. Chemical adsorption is a process of sharing or exchanging electrons between the reactants and the partially occupied d-orbital of iron forming chemical bond. The chemisorption enthalpy is 50–500 kJ/mole which is greater than for physisorption [54].

Theoretically when the nitrogen molecules are chemically adsorb, the triple bond which ties two nitrogen atoms together is favored to donate their electron to the partially occupied d-orbital of iron metal. This is usually referred as sigma(s) donation which forms a strong chemical bond which resulting in shorter distance between the adsorb nitrogen molecules and iron metal surfaces. Iron metal has four unpaired electron (d^6) in d-orbital and needs four additional electrons to be stabilized. Because of this, the excess electron will be donated back to the empty pi (p^*) orbital's of nitrogen molecules. This process is known as p-back donation. In consequence, the N-N bond is lengthened and weakens. Thus, the nitrogen molecules will be torn apart or rather separated and fragmented on the iron metal surface to form monolayer adsorption.

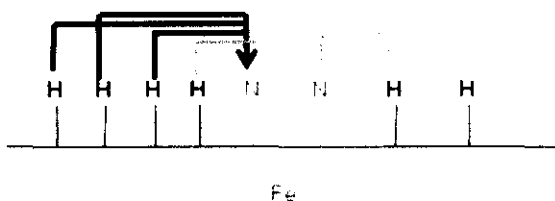


Figure 28 : Mechanism of migration on the iron metal surface

At this stage, all the adsorbed atoms are in contact with the surface layer of the adsorbent [53, 54]. Figure 28 shows the mechanism of migration process occurs on the iron metal surfaces. The migration process involves the movement of chemisorbed single atoms and reacts among each other's to form the product in this case ammonia. It happens because the bonding between chemisorbed molecules and

the iron metal surfaces provide thermodynamic driving force for the release of atoms so that the migration can be accomplished [51].

2.8.2 Desorption

Figure 29 shows how the mechanism of desorption process occurs on the iron metal surfaces.

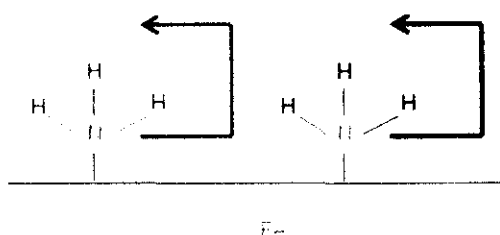


Figure 29 : Mechanism of desorption on the iron metal surface

When the product is formed, the intermediate strength of surface bonds allow desorption of products (NH_3). It leaves free active sites for the incoming hydrogen and nitrogen reactants molecules to be adsorbed and react on the iron metal surfaces. Using nanosize catalyst is attractive due to its high surface area leading to its active site for physi- and chemi-sorption process.

Understanding of adsorption and desorption process is utmost important for catalytic reaction from the viewpoint of fundamental science in the ammonia production. It should be noted that the first commercial ammonia plant was built in Oppau, Germany and has the production capacity of 30 tons/day [55]. This plant was set up by a German chemical giant, Badische Anilin und Soda Fabrik (BASF).

2.9 Micro-Reactor

The micro-reactor is designed for ammonia synthesis with electromagnetic (EM) induction method. Hydrogen and nitrogen gas were mixed and flowed (1.2bar) into the inlet with 0.2g nano-catalyst. The reaction was done below ambient temperature that is (0°C to 7°C). The reactor was placed in a Helmholtz Coils to induced strong EM field. The percentage of ammonia yield will be calculated based on Kjeldahl's method.

The advantage of micro-reactor is it has higher surface reacted area to volume ratio. Due to small volume, fast changes of operating conditions can be performed with minimal time demand to reach equilibrium state. As a result, the capability to test a number of catalytic reactions in separate reaction chambers without any interference by flow mixing would guarantee high accuracy and reliability of the final results.

The silicon or glass micro-reactor was able to handle high pressure and provide optical excess to the reaction channel for flow investigation. The design was able to produce ammonia with conversion as high as 20% with the temperature difference between different reaction channels. On the other hand, the most advanced solid catalyst interaction applied for this system is fix-bed reactor principle.

The technology of micro-reactor lead to an enhanced mass and energy transport. An accurate control of process parameters like pressure, temperature, and flow rate and residence time can be easily controlled. The other advantages of micro-reactor is yield improvement of 10 to 25 percent, energy cost saving, reduced laboratory and investment cost. However, the disadvantage of the micro-reactor is low melting point that is 660°C. [56]

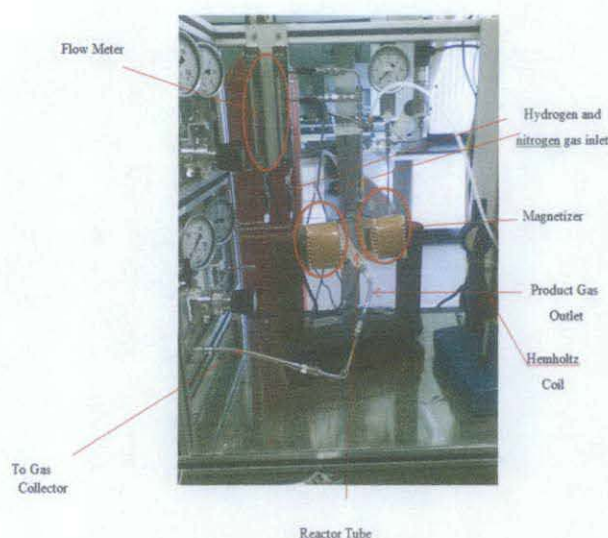


Figure 30 : Ammonia Micro-Reactor

2.10 Kjeldahl Method

Ammonia gas is passed into a known volume of standard acid solution where it reacts with the acid to form the ammonium salt. The unconsumed acid is then titrated against a standard solution of alkali. By this method, volume of acid neutralized by ammonia gas can be calculated. [57]

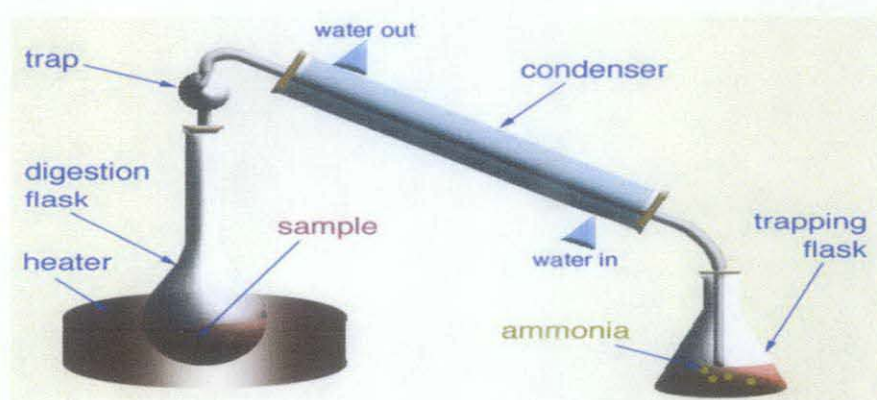


Figure 31 : Estimation of Nitrogen by Kjeldahl Method

The Kjeldahl method consists of three steps, which have to be carefully carried out in sequence:

- The sample is first digested in strong sulfuric acid in the presence of a

catalyst, which helps in the conversion of the amine nitrogen to ammonium ions

- The ammonium ions are then converted into ammonia gas, heated and distilled. The ammonia gas is led into a trapping solution where it dissolves and becomes an ammonium ion once again
- Finally the amount of the ammonia that has been trapped is determined by titration with a standard solution, and a calculation made

Step One: Digestion of the Sample

The purpose of this step is to break down the bonds that hold the polypeptides together, and convert them to simpler chemicals such as water, carbon dioxide and ammonia. Such reactions can be considerably speeded up by the presence of a catalyst and by a neutral substance, such as potassium sulfate (K_2SO_4), which raises the boiling point of the digesting acid and thus the temperature of the reaction.

Step Two: Distillation

The purpose of the next step, distillation, is to separate the ammonia (that is, the nitrogen) from the digestion mixture. This is done by:

- Raise the pH of the mixture using sodium hydroxide (45% NaOH solution). This has the effect of changing the ammonium (NH_4^+) ions (which are dissolved in the liquid) to ammonia (NH_3), which is a gas
- Separate the nitrogen away from the digestion mixture by distilling the ammonia (converting it to a volatile gas, by raising the temperature to boiling point) and then trapping the distilled vapors in a special trapping solution of about 15 ml HCl (hydrochloric acid) in 70 ml of water
- Remove the trapping flask and rinsing the condenser with water so as to make sure that all the ammonia has been dissolved

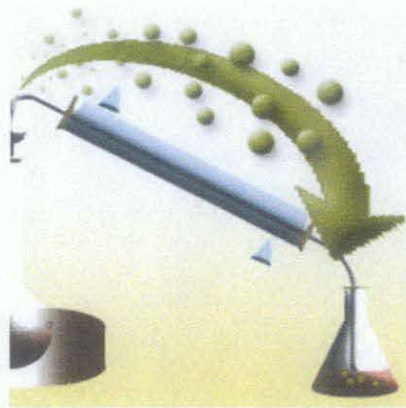


Figure 32 : Distillation

Step Three: Titration

As the ammonia dissolves in the acid trapping solution, it neutralizes some of the HCl it finds there. What acid is left can then be "back titrated", that is titrated with a standard, known solution of base (usually NaOH). In this way the amount of ammonia distilled off from the digestive solution can be calculated, and hence the amount of nitrogen in the protein determined.

The quantities of acid, and hence ammonia is determined by:

- i. Adding an indicator dye to the acid/ammonia trapping solution. This dye should turn a strong color, indicating that a significant amount of the original trapping acid is still present
- ii. Putting a standard solution of NaOH (sodium hydroxide) into the buret (a long tube with a tap at the end), and slowly, slowly adding small amounts of the sodium hydroxide solution to the acid solution with the dye
- iii. Watching for the point at which the dye turns orange, indicating that the "endpoint" has been reached and that now all the acid has been neutralized by the base
- iv. Recording the volume of the neutralizing base (sodium hydroxide solution) that was necessary to reach the endpoint
- v. Performing a calculation to find the amount of ammonia, and thus nitrogen, that came from the original sample



Figure 33 : Titration

Step 4: Calculations

One mole of ammonia coming from the digestion mixture (and hence from the original protein) will neutralize exactly one mole of the acid in the trapping flask. To find the number of moles of ammonia that have been produced and then trapped in sample(s) is done by:

- Calculating the number of moles of acid in the trapping flask originally (before any ammonia was trapped) by multiplying the molarity of the acid solution by the volume of the trapping solution

$$\text{moles of acid} = \text{molarity of acid} \times \text{volume used in flask} \quad (\text{moles}A = M \times V)$$

- Calculating the number of moles of base (NaOH) that were added from the buret to neutralize the remaining acid (that NOT neutralized by the ammonia)

$$\text{moles of base} = \text{molarity of base} \times \text{volume added from buret} \quad (\text{moles}B = M \times V)$$

- Subtracting the "moles of base" added from the "moles of acid" present at the beginning, to get the number of "moles of ammonia" come from the protein
- The number of "moles of ammonia" equal to the number of "moles of nitrogen"

- To calculate the number of grams of nitrogen in the original sample of protein, multiply the "moles of nitrogen" by the atomic mass of nitrogen (mass of atoms of nitrogen)

$$\text{gms nitrogen} = \text{moles nitrogen} \times \text{atomic mass} \quad (\text{gN} = \text{molesN} \times 14.0067) \quad (34)$$

- The percentage of nitrogen found in the original sample can now be calculated by

$$\% \text{nitrogen} = (\text{gms nitrogen} / \text{gms sample}) \times 100$$

$$\% \text{N} = (\text{gN} / \text{gS}) \times 100 \quad [58]$$

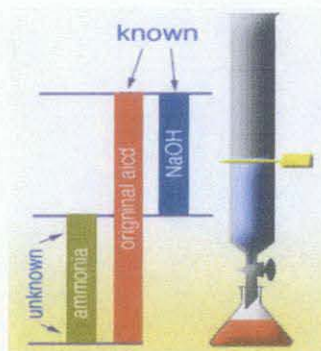


Figure 34 :Calculation

Table 7 : Literature Review Summary of Kjeldahl's Method

Author	Description	Method	Ref
Johan Gustav Christoffer Thorsager Kjeldahl, 1849–1900	Determine the amount of nitrogen in certain organic compounds using a laboratory technique	<ul style="list-style-type: none"> • The method consists of heating a substance with sulfuric acid, which decomposes the organic substance by oxidation to liberate the reduced nitrogen as ammonium sulfate • Chemical decomposition of the sample is complete when the medium has become clear and colorless • The solution is then distilled with sodium hydroxide (added in small quantities) which converts the ammonium salt to ammonia. The amount of ammonia present (hence the amount of nitrogen present in the sample) is determined by back titration • The end of the condenser is dipped into a solution of boric acid. The ammonia reacts with the acid and the remainder of the acid is then titrated with a sodium carbonate solution with a methyl orange pH indicator • Degradation: $\text{Sample} + \text{H}_2\text{SO}_4 \rightarrow (\text{NH}_4)_2\text{SO}_4(\text{aq}) + \text{CO}_2(\text{g}) + \text{SO}_2(\text{g}) +$ 	[59]

		<p>H₂O(g)</p> <ul style="list-style-type: none"> • Liberation of ammonia: $(\text{NH}_4)_2\text{SO}_4(\text{aq}) + 2\text{NaOH} \rightarrow \text{Na}_2\text{SO}_4(\text{aq}) + 2\text{H}_2\text{O}(\text{l}) + 2\text{NH}_3(\text{g})$ • Capture of ammonia: $\text{B}(\text{OH})_3 + \text{H}_2\text{O} + \text{NH}_3 \rightarrow \text{NH}_4^+ + \text{B}(\text{OH})_4^-$ • Back-titration: $\text{B}(\text{OH})_3 + \text{H}_2\text{O} + \text{Na}_2\text{CO}_3 \rightarrow \text{NaHCO}_3(\text{aq}) + \text{NaB}(\text{OH})_4(\text{aq}) + \text{CO}_2(\text{g}) + \text{H}_2\text{O}$ 	
S. K. Kundra, Ekta, 2004	Determine ammonia and organic nitrogen	<ul style="list-style-type: none"> • Ammonia gas is passed into a known volume of standard acid solution where it reacts with the acid to form the ammonium salt • The unconsumed acid is then titrated against a standard solution of alkali • By this method, volume of acid neutralized by ammonia gas can be calculated 	[60]
Professor John Blamire, 2003	Determine the amount of nitrogen in mixtures of substances containing	<ul style="list-style-type: none"> • The Kjeldahl method consists of three steps, which have to be carefully carried out in sequence: -The sample is first digested in strong sulfuric acid in the 	[58]

	ammonium salts, nitrate, or organic nitrogen compounds	<p>presence of a catalyst, which helps in the conversion of the amine nitrogen to ammonium ions</p> <ul style="list-style-type: none">- The ammonium ions are then converted into ammonia gas, heated and distilled. The ammonia gas is led into a trapping solution where it dissolves and becomes an ammonium ion once again- Finally the amount of the ammonia that has been trapped is determined by titration with a standard solution, and a calculation made	
--	--	--	--

2.11 Temperature Programmed Reduction (TPR)

Temperature Programmed Reduction (TPR) was used to estimate the temperatures required to reduce a metal oxide to a metallic state. Additional information that can also be evaluated from the TPR profiles is metal-support interaction, number of active sites and dispersion. The typical reducing agents employed are hydrogen, H_2 and carbon monoxide, CO gases.

TPR studies were conducted using a Thermo Finnigan TPDRO 1100 instrument equipped with a TCD detector. TPR process consists of two stages namely a pre-treatment step and the analysis step. About 0.12 g of catalyst was weighed then placed in between two layers of glass wool in the quartz sample cell. The quartz cell was then placed in the holder of the electrical furnace. The catalyst was pre-treated in a stream of nitrogen, N_2 at a flow rate of 20 cc/min and heating rate of $40^\circ C/min$. The temperature was set to $200^\circ C$ and held at $200^\circ C$ for 10 minutes. The sample was analyzed in a stream of 5% H_2-N_2 gas at heating rate of $10^\circ C/min$. TPR profiles were obtained from room temperature until $800^\circ C$. The sample was held at $800^\circ C$ for 10 min. This analysis gas passed through a thermal conductivity detector (TCD) which detected the change in hydrogen concentration in the gas stream. Distinct reducible species in the catalyst were shown as peaks in the TPR spectra.



Figure 35 : Temperature Program Reduction Equipment

CHAPTER 3

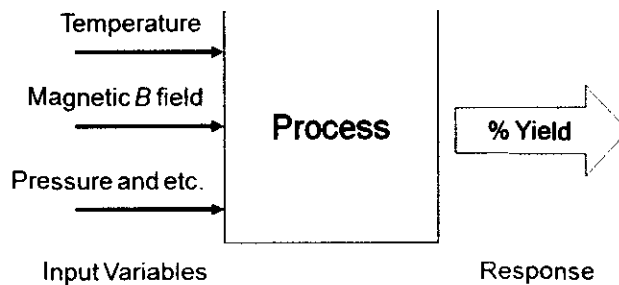
METHODOLOGY

3.1 Design of Experiments

1. Effects of the changing the variable factors on the process response is evaluated.

Advantages:

- We design/plan the experiments
- Multiple factors are varied at the same time
- Interaction between factors can be studied



2. Design of experiment in this project involved four phases that are planning, screening, optimization and verifications.

- Phase 1: Planning
 - Plan and design for the experiment
 - Select the factors and levels (high and low levels) - Temperature, pressure, magnetic field strength, catalysts and etc.
- Phase 2: Screening
 - Reduce the number of variables by identifying the key variables so that subsequent control or optimization can be effectively carried out
 - Hypothesis testing to screen out the insignificant factors
- Phase 3: Optimization

- Create 2-level full factorial designs.
- Number of runs = $(2)^{\text{factors}}$
- 2 factors (temperature and magnetic B field)
- 2 levels for each factor (high and low)
- Number of runs = $2^2 = 4$ runs
- Temperature = 0°C to 25°C
- Magnetic B field = 0.01 Tesla to 0.02 Tesla
- Then, the main effects and interaction effects that cause by temperature and magnetic B field can be evaluated

		Factor B	
		Low	High
Factor A	Low	A_1B_1	A_1B_2
	High	A_2B_1	A_2B_2

Where,

Factor A = Temperature

Factor B = Magnetic B field

- Phase 4: Verification
 - Confirmations run before full implementation.
 - Obtaining the confidence interval for the mean response
3. Few type of experiments that were done:
- Experiment to find the trend of the optimum catalytic induction at 25°C
 - Synthesis of ammonia at different conditions that are with magnetic induction and without magnetic induction at 0°C
 - Synthesis of ammonia by using different type of catalysts that are Hematite (Fe_2O_3), Magnetite (Fe_3O_4), Manganese Zinc Ferrite ($\text{Mn}_{0.8}\text{Zn}_{0.2}\text{Fe}_2\text{O}_4$), YIG ($\text{Y}_3\text{Fe}_5\text{O}_{12}$) and Manganese Oxide (MnO) at 0°C
 - Synthesis of ammonia at different temperature that is 0°C and 25°C
 - Synthesis of ammonia at different temperature of inlet gas
 - Synthesis of ammonia at different magnetic strength

3.2 Elements Determination

The catalysts that have been used in this experiment are Hematite (Fe_2O_3), Magnetite (Fe_3O_4), Manganese Zinc Ferrite ($\text{Mn}_{0.8}\text{Zn}_{0.2}\text{Fe}_2\text{O}_4$), YIG ($\text{Y}_3\text{Fe}_5\text{O}_{12}$) and last but not least, Manganese Oxide (MnO).

3.3 Sample Preparation

3.3.1 Experiment 1: Find the Trend of the Optimum Catalytic Induction

Loading the Catalyst

1. The glass wool is insulated with ice
2. Hematite catalyst is loaded between two layers of glass wool inside the tubular tube
3. The screws of the tube holder pair ring is loosen. Then, the tubular reactor system is placed into the rings and the screws tighten up
4. A magnet block consisting of north and south poles is placed. The location of the magnetic block and chamber is then adjusted so that both of them are in parallel position
5. Two ends of the loaded tubular tube with inlet and out let gas tubes are connected. Then, the screws is tighten

Starting the Reactor

6. The regulator terminals of reactant gases (H_2 and N_2) to the gas ports of micro reactor are connected. The control valves of gas tanks as well needle valves of regulator are opened
7. The needle valves are opened to flow the H_2 and N_2 into the system
8. The control valves (H_2 and N_2) are adjusted until the pressure gauge ($\text{H}_2:\text{N}_2$) indicators reach 1.2 barg
9. The needle valves of flow meter are opened. After that, the flow rate of the feed gas (H_2 and N_2) is set according to the desired ratio (3:1 ratio) using fine controller. The reactant gas is now flowed into the tubular reactor system
10. The magnetizer is turned on

11. The needle valve of gas outlet is turned to “outlet” selection to bubble the outlet gas into hydrochloric acid

Sample Testing

12. The reacted ammonia will be flowed into a beaker containing HCl (25ml)
13. The product in the HCl beaker will be collected every 8 minutes
14. Five drops of Phenolphthalein is added into the beaker
15. Drop 1 μ m of sodium hydroxide (NaOH) continuously until the liquid turned purple (mixture is neutral)
16. Step 13 is repeated until 1 hour
17. The trend of the yield every 8 minutes is evaluated

3.3.2 Experiment 2: Synthesis of Ammonia at Different Magnetic Conditions

Loading the Catalyst

1. The glass wool is insulated with ice to set up the system at 0°C
2. YIG/ Hematite catalyst is loaded between two layers of glass wool inside the tubular tube
3. The screws of the tube holder pair ring is loosen. Then, the tubular reactor system is placed into the rings and the screws tighten up
4. A magnet block consisting of north and south poles is placed. The location of the magnetic block and chamber is then adjusted so that both of them are in parallel position
5. Two ends of the loaded tubular tube with inlet and out let gas tubes are connected. Then, the screws is tighten

Starting the Reactor

6. The regulator terminals of reactant gases (H₂ and N₂) to the gas ports of micro reactor are connected. The control valves of gas tanks as well needle valves of regulator are opened
7. The needle valves are opened to flow the H₂ and N₂ into the system
8. The control valves (H₂ and N₂) are adjusted until the pressure gauge (H₂:N₂) indicators reach 1.2 barg

9. The needle valves of flow meter are opened. After that, the flow rate of the feed gas (H_2 and N_2) is set according to the desired ratio (3:1 ratio) using fine controller. The reactant gas is now flowed into the tubular reactor system
10. The magnetizer is turned on at 0.1T
11. The needle valve of gas outlet is turned to “outlet” selection to bubble the outlet gas into hydrochloric acid

Sample Testing

12. The reacted ammonia will be flowed into a beaker containing HCl (25ml)
13. The product in the HCl beaker will be collected
14. Five drops of Penalptalin is added into the beaker
15. Drop $1\mu\text{m}$ of sodium hydroxide (NaOH) continuously until the liquid turned purple (mixture is neutral)
16. Step Step 6 to 10 is repeated but the magnetizer is turned off
17. The trend of the product yield by using different magnetic condition is evaluated

3.3.3 Experiment 3: Synthesis of Ammonia Using Different Type of Catalysts

Loading the Catalyst

1. The glass wool is insulated with ice to set up the system at 0°C
2. Hematite (Fe_2O_3) catalyst is loaded between two layers of glass wool inside the tubular tube
3. The screws of the tube holder pair ring is loosen. Then, the tubular reactor system is placed into the rings and the screws tighten up
4. A magnet block consisting of north and south poles is placed. The location of the magnetic block and chamber is then adjusted so that both of them are in parallel position
5. Two ends of the loaded tubular tube with inlet and out let gas tubes are connected. Then, the screws is tighten

Starting the Reactor

6. The regulator terminals of reactant gases (H_2 and N_2) to the gas ports of micro reactor are connected. The control valves of gas tanks as well needle valves of regulator are opened

7. The needle valves are opened to flow the H₂ and N₂ into the system
8. The control valves (H₂ and N₂) are adjusted until the pressure gauge (H₂:N₂) indicators reach 1.2 barg
9. The needle valves of flow meter are opened. After that, the flow rate of the feed gas (H₂ and N₂) is set according to the desired ratio (3:1 ratio) using fine controller. The reactant gas is now flowed into the tubular reactor system
10. The magnetizer is turned on
11. The needle valve of gas outlet is turned to “outlet” selection to bubble the outlet gas into hydrochloric acid

Sample Testing

12. The reacted ammonia will be flowed into a beaker containing HCl (25ml)
13. The product in the HCl beaker will be collected
14. Five drops of Penaltalin is added into the beaker
15. Drop 1µm of sodium hydroxide (NaOH) continuously until the liquid turned purple (mixture is neutral)
16. Step 1 is repeated by using Magnetite (Fe₃O₄), Manganese Zinc Ferrite (Mn_{0.8}Zn_{0.2}Fe₂O₄), YIG (Y₃Fe₅O₁₂) and Manganese Oxide (MnO) at 0°C
17. The trend of the product yield by using different catalyst is evaluated

3.3.4 Experiment 4: Synthesis of Ammonia at Different System’s Temperature

Loading the Catalyst

1. The glass wool is insulated with ice to set up the system at 0°C
2. YIG catalyst is loaded between two layers of glass wool inside the tubular tube
3. The screws of the tube holder pair ring is loosen. Then, the tubular reactor system is placed into the rings and the screws tighten up
4. A magnet block consisting of north and south poles is placed. The location of the magnetic block and chamber is then adjusted so that both of them are in parallel position

5. Two ends of the loaded tubular tube with inlet and outlet gas tubes are connected. Then, the screws are tightened

Starting the Reactor

6. The regulator terminals of reactant gases (H_2 and N_2) to the gas ports of micro reactor are connected. The control valves of gas tanks as well as needle valves of regulator are opened
7. The needle valves are opened to flow the H_2 and N_2 into the system
8. The control valves (H_2 and N_2) are adjusted until the pressure gauge ($H_2:N_2$) indicators reach 1.2 barg
9. The needle valves of flow meter are opened. After that, the flow rate of the feed gas (H_2 and N_2) is set according to the desired ratio (3:1 ratio) using fine controller. The reactant gas is now flowed into the tubular reactor system
10. The main control panel switch is switched on and the temperature from is set 0° to a desired value using temperature controller
11. The magnetizer is turned on
12. The needle valve of gas outlet is turned to "outlet" selection to bubble the outlet gas into hydrochloric acid

Sample Testing

13. The reacted ammonia will be flowed into a beaker containing HCl (25ml)
14. The product in the HCl beaker will be collected
15. Five drops of Phenolphthalein is added into the beaker
16. Drop $1\mu\text{m}$ of sodium hydroxide (NaOH) continuously until the liquid turned purple (mixture is neutral)
17. Step 1 is repeated at temperature of 25°C
18. The trend of the product yield at different temperature is evaluated

3.3.5 Experiment 5: Synthesis of Ammonia at Different Temperature of Inlet Gas

Loading the Catalyst

1. MnO catalyst is loaded between two layers of glass wool inside the tubular tube

2. The screws of the tube holder pair ring is loosen. Then, the tubular reactor system is placed into the rings and the screws tighten up
3. A magnet block consisting of north and south poles is placed. The location of the magnetic block and chamber is then adjusted so that both of them are in parallel position
4. Two ends of the loaded tubular tube with inlet and out let gas tubes are connected. Then, the screws is tighten

Starting the Reactor

5. The regulator terminals of reactant gases (H_2 and N_2) to the gas ports of micro reactor are connected. The control valves of gas tanks as well needle valves of regulator are opened
6. The needle valves are opened to flow the H_2 and N_2 into the system at $25^\circ C$
7. The control valves (H_2 and N_2) are adjusted until the pressure gauge ($H_2:N_2$) indicators reach 1.2 barg
8. The needle valves of flow meter are opened. After that, the flow rate of the feed gas (H_2 and N_2) is set according to the desired ratio (3:1 ratio) using fine controller. The reactant gas is now flowed into the tubular reactor system
9. The magnetizer is turned on at 0.1T
10. The needle valve of gas outlet is turned to "outlet" selection to bubble the outlet gas into hydrochloric acid

Sample Testing

11. The reacted ammonia will be flowed into a beaker containing HCl (25ml)
12. The product in the HCl beaker will be collected
13. Five drops of Penalptalin is added into the beaker
14. Drop $1\mu m$ of sodium hydroxide (NaOH) continuously until the liquid turned purple (mixture is neutral)
15. Step 5 to 9 is repeated but the H_2 and N_2 gas is heated to $100^\circ C$ before enter the system
16. The trend of the product yield by using different inlet gas temperature is evaluated

3.3.6 Experiment 6: Synthesis of Ammonia at Different TPR Condition

Loading the Catalyst

1. Unreduced catalyst is loaded between two layers of glass wool inside the tubular tube
2. The screws of the tube holder pair ring is loosen. Then, the tubular reactor system is placed into the rings and the screws tighten up
3. A magnet block consisting of north and south poles is placed. The location of the magnetic block and chamber is then adjusted so that both of them are in parallel position
4. Two ends of the loaded tubular tube with inlet and out let gas tubes are connected. Then, the screws is tighten

Starting the Reactor

5. The regulator terminals of reactant gases (H_2 and N_2) to the gas ports of micro reactor are connected. The control valves of gas tanks as well needle valves of regulator are opened
6. The needle valves are opened to flow the H_2 and N_2 into the system
7. The control valves (H_2 and N_2) are adjusted until the pressure gauge ($H_2:N_2$) indicators reach 1.2 barg
8. The needle valves of flow meter are opened. After that, the flow rate of the feed gas (H_2 and N_2) is set according to the desired ratio (3:1 ratio) using fine controller. The reactant gas is now flowed into the tubular reactor system
9. The magnetizer is turned on at magnetic strength is set at 0.1 Tesla
10. The needle valve of gas outlet is turned to "outlet" selection to bubble the outlet gas into hydrochloric acid

Sample Testing

11. The reacted ammonia will be flowed into a beaker containing HCl (25ml)
12. The product in the HCl beaker will be collected
13. Five drops of Phenolphthalein is added into the beaker
14. Drop $1\mu\text{m}$ of sodium hydroxide (NaOH) continuously until the liquid turned purple (mixture is neutral)
15. Step 1 to 14 is repeated by using Reduced Catalyst
16. The trend of the product yield by using different TPR condition is analyzed

3.3.7 Experiment 7: Synthesis of Ammonia at Different Magnetic Strength

Loading the Catalyst

1. Catalyst is loaded between two layers of glass wool inside the tubular tube
2. The screws of the tube holder pair ring is loosen. Then, the tubular reactor system is placed into the rings and the screws tighten up
3. A magnet block consisting of north and south poles is placed. The location of the magnetic block and chamber is then adjusted so that both of them are in parallel position
4. Two ends of the loaded tubular tube with inlet and out let gas tubes are connected. Then, the screws is tighten

Starting the Reactor

5. The regulator terminals of reactant gases (H_2 and N_2) to the gas ports of micro reactor are connected. The control valves of gas tanks as well needle valves of regulator are opened
6. The needle valves are opened to flow the H_2 and N_2 into the system
7. The control valves (H_2 and N_2) are adjusted until the pressure gauge ($H_2:N_2$) indicators reach 1.2 barg
8. The needle valves of flow meter are opened. After that, the flow rate of the feed gas (H_2 and N_2) is set according to the desired ratio (3:1 ratio) using fine controller. The reactant gas is now flowed into the tubular reactor system
9. The magnetizer is turned on at magnetic strength is set at 0.1 Tesla and no Hemholtz coil
10. The needle valve of gas outlet is turned to "outlet" selection to bubble the outlet gas into hydrochloric acid

Sample Testing

11. The reacted ammonia will be flowed into a beaker containing HCl (25ml)
12. The product in the HCl beaker will be collected
13. Five drops of Penalptalin is added into the beaker
14. Drop 1 μ m of sodium hydroxide (NaOH) continuously until the liquid turned purple (mixture is neutral)
15. Step 1 to 9 is repeated but the magnetizer is set up at 0.2 Tesla and Hemholtz Coil is set up at 20 Ampere before enter the system

16. The trend of the product yield by using different inlet gas temperature is evaluate

3.3.8 Experiment 8: Synthesis of Ammonia with Different Magnetic Strength Using Helmholtz Coil

Loading the Catalyst

1. MnO catalyst is loaded between two layers of glass wool inside the tubular tube
2. The screws of the tube holder pair ring is loosen. Then, the tubular reactor system is placed into the rings and the screws tighten up
3. A magnet block consisting of north and south poles is placed. The location of the magnetic block and chamber is then adjusted so that both of them are in parallel position
4. Two ends of the loaded tubular tube with inlet and out let gas tubes are connected. Then, the screws is tighten

Starting the Reactor

5. The regulator terminals of reactant gases (H_2 and N_2) to the gas ports of micro reactor are connected. The control valves of gas tanks as well needle valves of regulator are opened
6. The needle valves are opened to flow the H_2 and N_2 into the system
7. The control valves (H_2 and N_2) are adjusted until the pressure gauge ($H_2:N_2$) indicators reach 1.2 barg
8. The needle valves of flow meter are opened. After that, the flow rate of the feed gas (H_2 and N_2) is set according to the desired ratio (3:1 ratio) using fine controller. The reactant gas is now flowed into the tubular reactor system
9. The magnetizer is turned on at magnetic strength is set at 0.1 Tesla and no Hemholtz coil
10. The needle valve of gas outlet is turned to "outlet" selection to bubble the outlet gas into hydrochloric acid

Sample Testing

11. The reacted ammonia will be flowed into a beaker containing HCl (25ml)
12. The product in the HCl beaker will be collected
13. Five drops of Penaltalin is added into the beaker
14. Drop 1 μ m of sodium hydroxide (NaOH) continuously until the liquid turned purple (mixture is neutral)

CHAPTER 4

RESULT AND DISCUSSION

4.1 Data Gathering & Analysis

The reduction of various iron oxides in hydrogen and carbon monoxide atmospheres has been investigated by temperature programmed reduction (TPR_{H2}) and conventional and “in situ” XRD methods. Five different compounds of were characterized: hematite α -Fe₂O₃, magnetite Fe₃O₄, manganese oxide MnO, and Manganese Zinc Ferrite MnZnFe₂O₄, YIG Y₃Fe₅O₁₂. The reduction process takes place after accompanying dehydration up to 1000 °C.

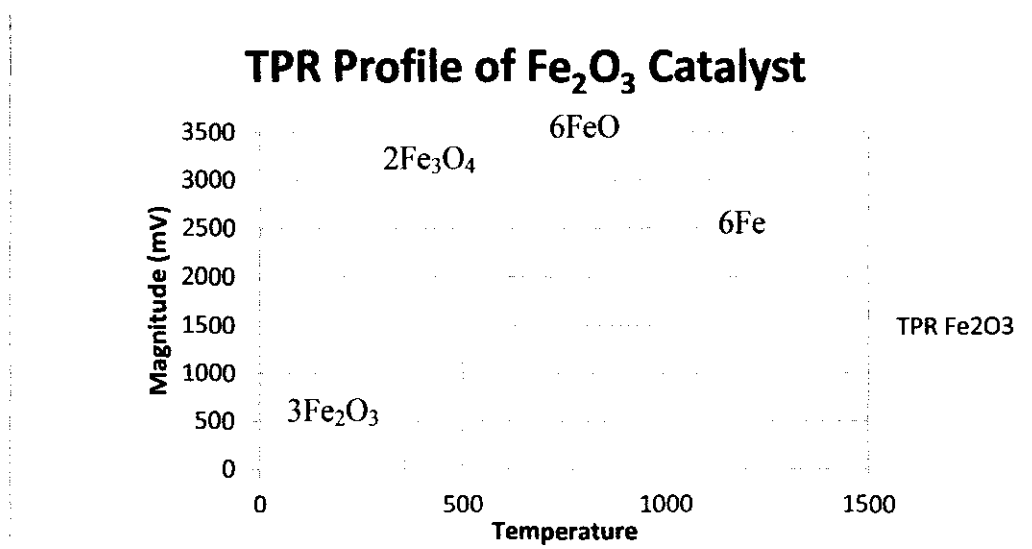


Figure 36 : TPR Profile of Fe₂O₃ (Hematite) Nanocatalyst

The reduction mechanisms suggested in Figure 36 are, [61]

Table 8 : Reduction Mechanism of Fe₂O₃ (Hematite) Nanocatalyst

Reaction	Temperature(°C)
$3\text{Fe}_2\text{O}_3 \rightarrow 2\text{Fe}_3\text{O}_4$	250-570
$2\text{Fe}_3\text{O}_4$	570
$2\text{Fe}_3\text{O}_4 \rightarrow 6\text{FeO}$	570-795

6FeO	795
6FeO → 6Fe	795-1025
6Fe	1025

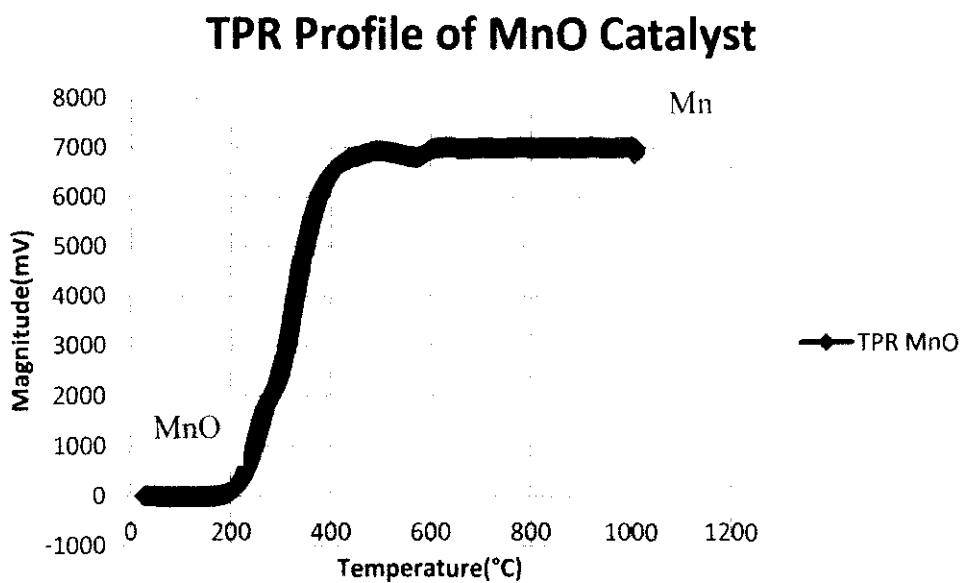


Figure 37 : TPR Profile of MnO (Manganese Oxide) Nanocatalyst

The reduction mechanisms suggested in Figure 37 are, [62]

Table 9 : Reduction Mechanism of MnO (Manganese Oxide) Nanocatalyst

Reaction	Temperature(°C)
$\text{MnO} + \text{H}_2 \rightarrow \text{Mn}$	200-475
Mn	475-1000

TPR Profile of $Mn_{0.8}Zn_{0.2}Fe_2O_4$ Catalyst

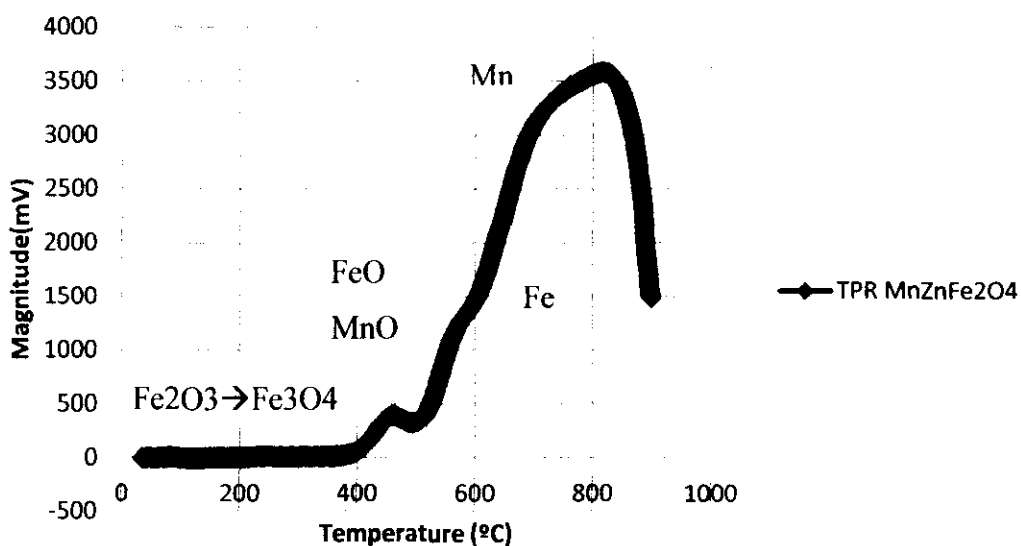


Figure 38 : TPR Profile of $Mn_{0.8}Zn_{0.2}Fe_2O_4$ (Manganese Zinc Ferrite) Nanocatalyst

The reduction mechanisms in Figure 38 suggested are, [63], [64], [65], [66], [67]

Table 9: Reduction Mechanism of $Mn_{0.8}Zn_{0.2}Fe_2O_4$ (Manganese Zinc Ferrite) Nanocatalyst

Reaction	Temperature(°C)
$Fe_3O_4 \rightarrow Fe_2O_3$	273-350
MnZnO	463
$Fe_3O_4 \rightarrow FeO$	540
$FeO \rightarrow Fe$	650
$MnZnO \rightarrow MnZn$	736

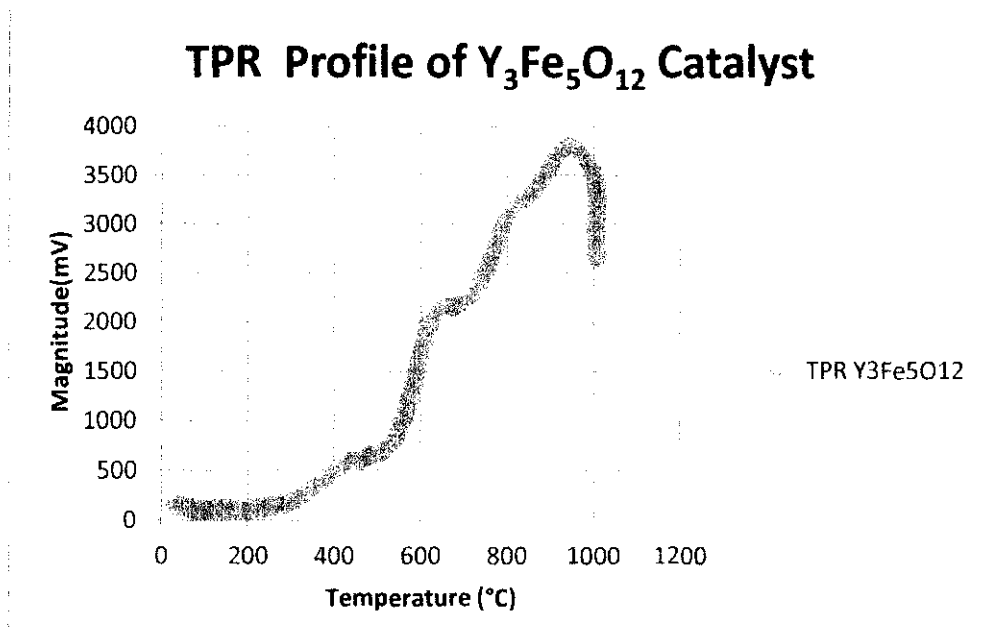


Figure 39 : TPR Profile of $Y_3Fe_5O_{12}$ (YIG) Nanocatalyst

The reduction mechanisms suggested in Figure 39 are, [65]

Table 10: Reduction Mechanism of of $Y_3Fe_5O_{12}$ (YIG) Nanocatalyst

Reaction	Temperature(°C)
$Y_3Fe_5O_{12} \rightarrow FeO+YO_2+O_2$	273-350
$FeO \rightarrow Fe$	795
$YO_2 \rightarrow Y_3$	960

4.2 Results and Discussion

Experiment 1: Find the Trend of the Optimum Catalytic Induction

The synthesis of ammonia was conducted at temperature of 25°C using $Y_3Fe_5O_{12}$ (YIG) nanocatalyst. The reactant gases were reacted with $Y_3Fe_5O_{12}$ (YIG) nanocatalyst with magnetic induction method (MIM) applied of 0.1 Tesla. Then, the product of ammonia is collected for every 8 minutes until 10 readings were measured and yield is measured using Kjeldahl's Method.

Time (mins)	$HCl_{\text{excess}}=NaOH$	$HCl_{\text{reacted}}=NH_3$	Mole fraction NH_3
8	$=1.248 \times 10^{-6}$ mole	$=(2.5 \times 10^{-5} \text{mole}) - (1.248 \times 10^{-6} \text{mole})$ $=2.3752 \times 10^{-5}$ mole	$NH_3 = 2.3752 \times 10^{-5}$ mole Yield = 890.7 $\mu\text{mol/h.g-cat}$
16	$=1.056 \times 10^{-6}$ mole	$=(2.5 \times 10^{-5} \text{mole}) - (1.056 \times 10^{-6} \text{mole})$ $=2.3944 \times 10^{-5}$ mole	$NH_3 = 2.3944 \times 10^{-5}$ mole Yield = 897.9 $\mu\text{mol/h.g-cat}$
24	$=1.056 \times 10^{-6}$ mole	$=(2.5 \times 10^{-5} \text{mole}) - (1.056 \times 10^{-6} \text{mole})$ $=2.3944 \times 10^{-5}$ mole	$NH_3 = 2.3944 \times 10^{-5}$ mole Yield = 897.9 $\mu\text{mol/h.g-cat}$
32	$=1.056 \times 10^{-6}$ mole	$=(2.5 \times 10^{-5} \text{mole}) - (1.056 \times 10^{-6} \text{mole})$ $=2.3944 \times 10^{-5}$ mole	$NH_3 = 2.3944 \times 10^{-5}$ mole Yield = 897.9 $\mu\text{mol/h.g-cat}$
40	$=0.96 \times 10^{-6}$ mole	$=(2.5 \times 10^{-5} \text{mole}) - (0.96 \times 10^{-6} \text{mole})$ $=2.404 \times 10^{-5}$ mole	$NH_3 = 2.404 \times 10^{-5}$ mole Yield: 901.5 $\mu\text{mol/h.g-cat}$
48	$=1.224 \times 10^{-6}$ mole	$=(2.5 \times 10^{-5} \text{mole}) - (1.224 \times 10^{-6} \text{mole})$ $=2.3776 \times 10^{-5}$ mole	$NH_3 = 2.3776 \times 10^{-5}$ mole Yield: 891.6 $\mu\text{mol/h.g-cat}$
56	$=1.224 \times 10^{-6}$ mole	$=(2.5 \times 10^{-5} \text{mole}) - (1.224 \times 10^{-6} \text{mole})$ $=2.3776 \times 10^{-5}$ mole	$NH_3 = 2.3776 \times 10^{-5}$ mole Yield: 891.6 $\mu\text{mol/h.g-cat}$

64	$=1.224 \times 10^{-6}$ mole	$=(2.5 \times 10^{-5}\text{mole})-$ $(1.224 \times 10^{-6}\text{mole})$ $=2.3776 \times 10^{-5}$ mole	$\text{NH}_3 = 2.3776 \times 10^{-5}$ mole Yield: 891.6 $\mu\text{mol/h.g-cat}$
72	$=1.224 \times 10^{-6}$ mole	$=(2.5 \times 10^{-5}\text{mole})-$ $(1.224 \times 10^{-6}\text{mole})$ $=2.3776 \times 10^{-5}$ mole	$\text{NH}_3 = 2.3776 \times 10^{-5}$ mole Yield: 891.6 $\mu\text{mol/h.g-cat}$
80	$=1.224 \times 10^{-6}$ mole	$=(2.5 \times 10^{-5}\text{mole})-$ $(1.224 \times 10^{-6}\text{mole})$ $=2.3776 \times 10^{-5}$ mole	$\text{NH}_3 = 2.3776 \times 10^{-5}$ mole Yield: 891.6 $\mu\text{mol/h.g-cat}$

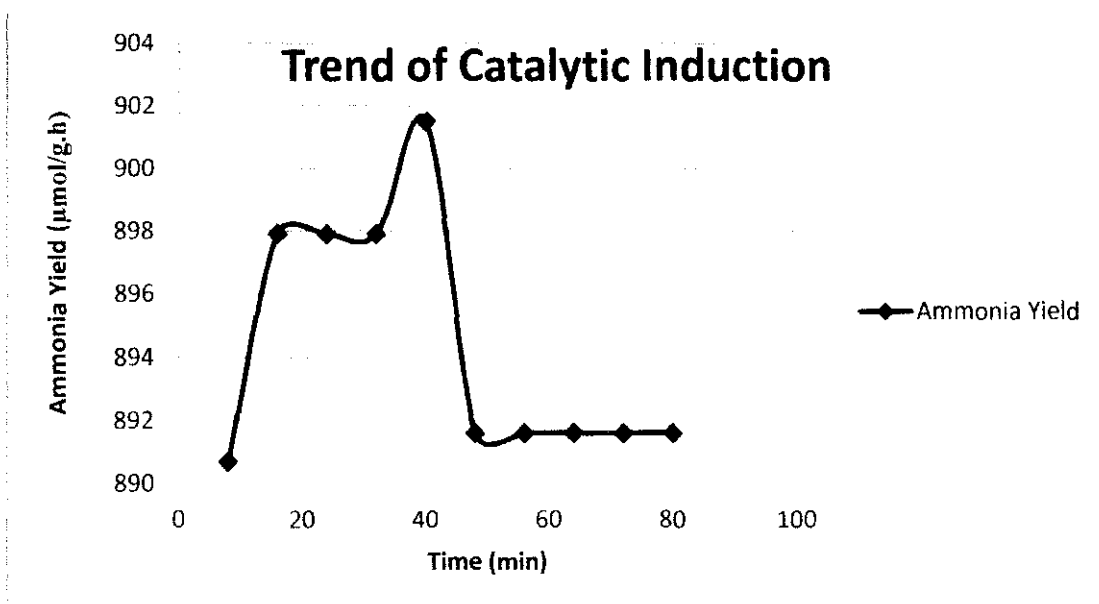


Figure 40 : Trend of Catalytic Induction

Figure 40 shows that the optimum magnetic induction of ammonia synthesis is at 32 minutes (897.9 $\mu\text{mol/h.g-cat}$ NH_3 yield) after the reactor started. It is observed that after 32 minutes, the electron spin achieves the relaxation time. When nonzero spin particle is placed in a magnetic field, the initial random orientation of particle's spin will change due to the spin magnetic spin interaction. As result of the electronic spin-magnetic field interaction, part of the electronic spins will end parallel to the applied magnetic field. However, such a process does not occur instantaneously, and its time dependence defines the characteristic spin relaxation times. How fast or how slow this process happen will depend on the particular mechanism which produces the spin alignment. Some of the possible spin alignment

mechanisms are due to interaction of electronic spins with phonons, other electron spins and nucleus. All these mechanism will be characterized by a spin relaxation time. However, the spin alignment will be finalized in a timescale of the order of shorter spin relaxation time. [68]

Experiment 2: Synthesis of Ammonia at Different Magnetic Conditions

The synthesis of ammonia were conducted at temperature of 0°C using $Y_3Fe_5O_{12}$ (YIG) and Fe_2O_3 (Hematite) nanocatalyst. Firstly, the reactant gases were reacted with $Y_3Fe_5O_{12}$ (YIG) nanocatalyst with magnetic induction method (MIM) applied of 0.1 Tesla for duration of 30 minutes. The experiment repeated by reacting the reactant gases with YIG nanocatalyst without application of MIM. The whole experiment then is repeated by using Fe_2O_3 (Hematite) nanocatalyst.

Type of Catalyst	MIM	$HCl_{\text{excess}}=NaOH$	$HCl_{\text{reacted}}=NH_3$	Mole fraction NH_3
$Y_3Fe_5O_{12}$ (YIG)	0.1T	$=0.744 \times 10^{-6}$ mole	$=(2.5 \times 10^{-5}\text{mole})-$ $(0.744 \times 10^{-6}\text{mole})$ $=2.4256 \times 10^{-5}$ mole	$NH_3 = 2.19 \times 10^{-5}$ mole Yield=242.56μmol/h.g-cat
$Y_3Fe_5O_{12}$ (YIG)	0T	$=1.248 \times 10^{-6}$ mole	$=(2.5 \times 10^{-5}\text{mole})-$ $(1.248 \times 10^{-6}\text{mole})$ $=2.3752 \times 10^{-5}$ mole	$NH_3 = 1.98 \times 10^{-5}$ mole Yield=10 μmol /h.g-cat
Hematite (Fe_2O_3)	0.1T	$=0.84 \times 10^{-6}$ mole	$=(2.5 \times 10^{-5}\text{mole})-$ $(0.84 \times 10^{-6}\text{mole})$ $=2.416 \times 10^{-5}$ mole	$NH_3 = 2.15 \times 10^{-5}$ mole Yield=241.6 μmol/h.g-cat
Hematite (Fe_2O_3)	0T	$=1.272 \times 10^{-6}$ mole	$=(2.5 \times 10^{-5}\text{mole})-$ $(1.272 \times 10^{-6}\text{mole})$ $=2.3728 \times 10^{-5}$ mole	$NH_3 = 1.97 \times 10^{-5}$ mole Yield=7μmol/h.g-cat

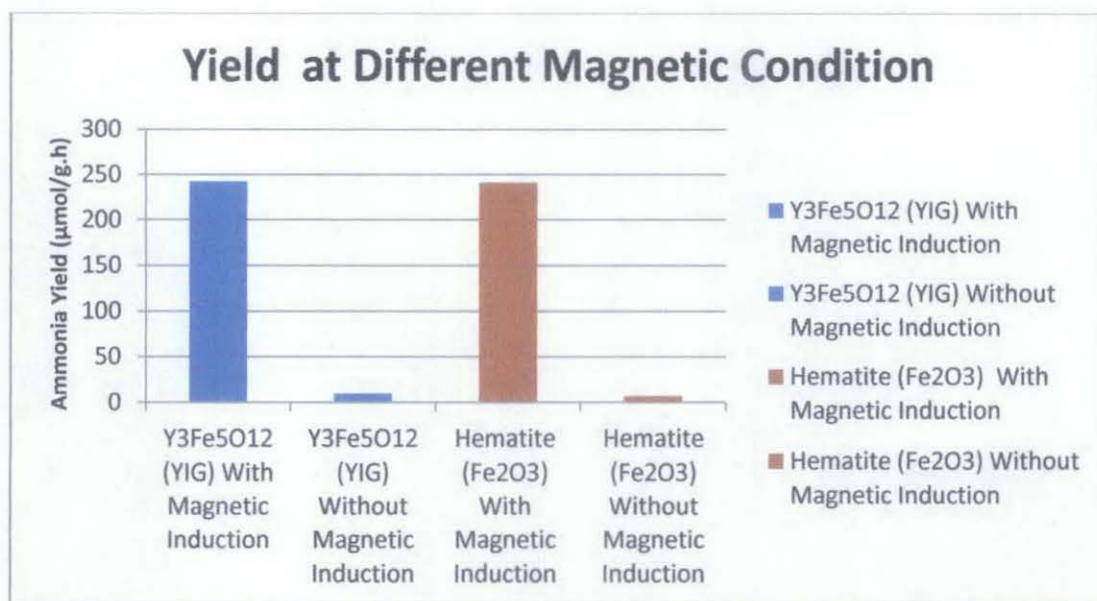


Figure 41 : Yield of Ammonia at Different Magnetic Induction Condition

Figure 41 show that the yield for ammonia synthesis by using $Y_3Fe_5O_{12}$ (YIG) nanocatalyst with MIM is $242.56\mu\text{mole/h.g-cat}$ while $10\mu\text{mole/h.g-cat}$ without MIM. On the other hand, the yield for ammonia synthesis by using Fe_2O_3 (Hematite) nanocatalyst with MIM is $241.6\mu\text{mole/h.g-cat}$ while $7\mu\text{mole/h.g-cat}$ without MIM. The result clearly show that there are huge different between reaction with and without MIM as the percentage different is 95.88% and 97.10% for YIG and Hematite nanocatalyst respectively. The reaction with magnetic induction is much higher than reaction without magnetic induction since the presence of magnetic induction force the electron spin to align while without magnetic induction, the electron spin is random and the reaction will be hard to occur. Magnetic fields can alter the rate, yield, or product distribution of chemical reactions. [74]

Experiment 3: Synthesis of Ammonia at Different System Temperature

The synthesis of ammonia was conducted at temperature of 25°C using $Y_3Fe_5O_{12}$ (YIG) nanocatalyst with magnetic induction of 0.1Tesla. Next, the experiment was repeated at temperature of 0°C and the result is shown below.

Catalyst	T (°C)	HCl _{excess} =NaOH	HCl _{reacted} =NH ₃	Mole fraction NH ₃
YIG	25	=0.096 x 10 ⁻⁶ mole	=(2.5 x 10 ⁻⁵ mol e)-(0.96 x 10 ⁻⁶ mole) =2.404 x 10 ⁻⁵ mole	NH ₃ =2.404 x 10 ⁻⁵ mole Yield=240.4μmol/h.g-cat
YIG	0	=0.744 x 10 ⁻⁶ mole	=(2.5 x 10 ⁻⁵ mole)-(0.744 x 10 ⁻⁶ mole) =2.4256 x 10 ⁻⁵ mole	NH ₃ = 2.4256 x 10 ⁻⁵ mole Yield=242.56μmol/h.g-cat

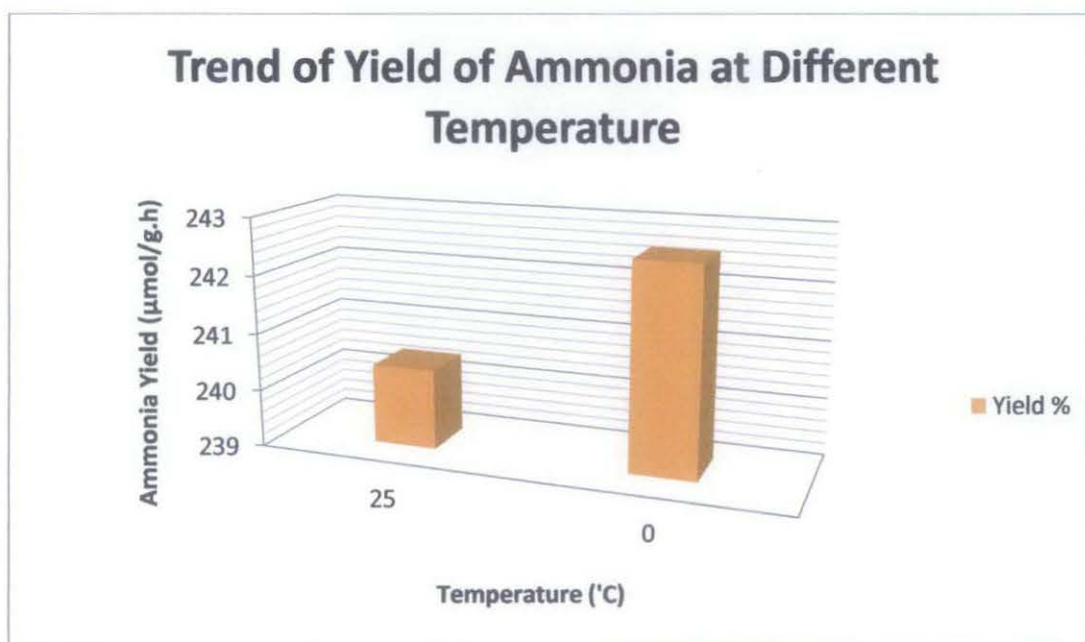


Figure 42 : Trend of Ammonia at Different System Temperature

From Figure 42, it shows that the yield percentage of ammonia is 0.90% higher at 0°C temperature (242.56μmole/h.g-cat) compared than yield at 25°C temperature (240.4μmole/h.g-cat). It approve that the influence of temperature on magnetic material can be determined in the magnetic properties of dose materials. Rising the temperature of a solid will result in the increase of the thermal vibrations of atoms results the atomic magnetic moments free to rotate. This phenomenon the

atoms tend to randomize the directions of any moments that may be aligned. With increasing temperature, the saturation magnetization diminishes gradually and abruptly drops to zero at Curie temperature (T) of YIG which is at 550K. Hence, the lower the temperature is, the higher the alignment of the electron spin in the atom.

Experiment 4: Synthesis of Ammonia Using Different Type of Catalysts

This part is about synthesis of ammonia using different type of nanocatalysts which are $Y_3Fe_5O_{12}$ (YIG), $Mn_{0.8}Zn_{0.2}Fe_2O_4$ (Manganese Zinc Ferrite), Fe_2O_3 (Hematite), MnO (Manganese Oxide) and last but not least is Fe_3O_4 (Magnetite). The syntheses were done at temperature of $0^\circ C$ with magnetic induction method of 0.1 Tesla.

Type of Catalyst	$HCl_{\text{excess}}=NaOH$	$HCl_{\text{reacted}}=NH_3$	Mole fraction NH_3
$Y_3Fe_5O_{12}$ (YIG)	= 0.744×10^{-6} mole	=(2.5×10^{-5} mole)- (0.744×10^{-6} mole) = 2.4256×10^{-5} mole	$NH_3=2.4256 \times 10^{-5}$ mole Yield=242.56μmol/h.g-cat
Manganese Zinc Ferrite ($MnZnFe_2O_4$)	= 1.152×10^{-6} mole	=(2.5×10^{-5} mole)- (1.152×10^{-6} mole) = 2.3848×10^{-5} mole	$NH_3=2.3848 \times 10^{-5}$ mole Yield=238.48μmol/h.g-cat
Hematite (Fe_2O_3)	= 0.84×10^{-6} mole	=(2.5×10^{-5} mole)- (0.84×10^{-6} mole) = 2.416×10^{-5} mole	$NH_3=2.416 \times 10^{-5}$ mole Yield=241.6μmol/h.g-cat
Manganese Oxide (MnO)	= 1.08×10^{-6} mole	=(2.5×10^{-5} mole)- (1.08×10^{-6} mole) = 2.392×10^{-5} mole	$NH_3=2.392 \times 10^{-5}$ mole Yield=239.2μmol/h.g-cat
Magnetite (Fe_3O_4)	= 1.488×10^{-6} mole	=(2.5×10^{-5} mole)- (1.488×10^{-6} mole) = 2.3512×10^{-5} mole	$NH_3=2.3512 \times 10^{-5}$ mole Yield=235.12μmol/h.g-cat

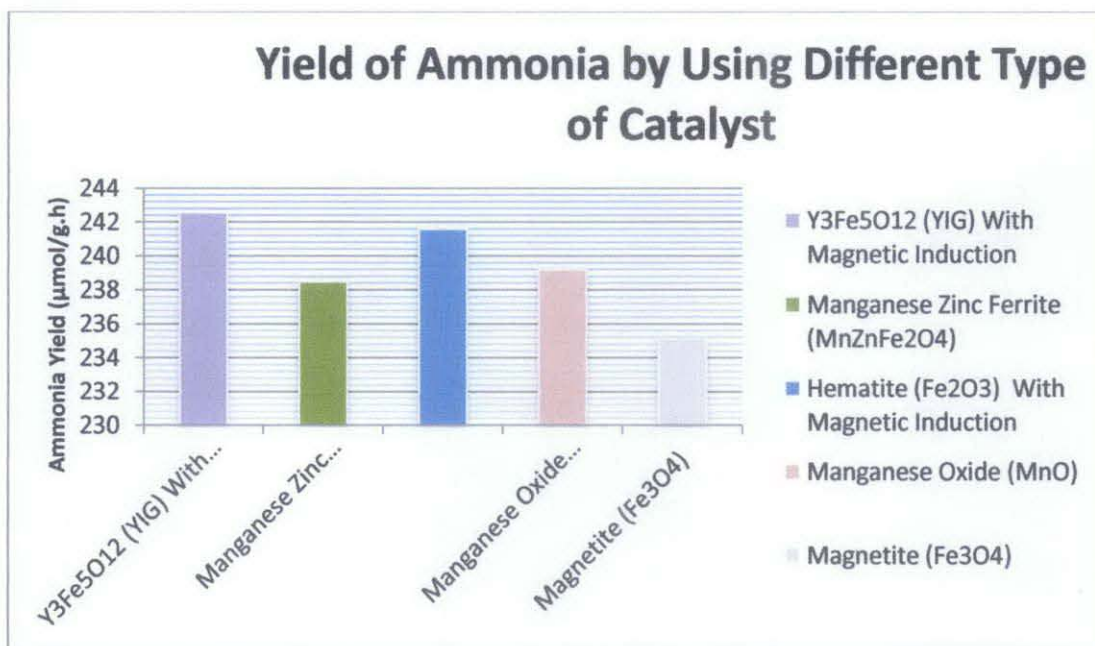


Figure 43 : Yield of Ammonia by Using Different Type of Catalyst

Figure 43 shows that the yield for ammonia synthesis by using Y₃Fe₅O₁₂ (YIG) is the highest (242.56 $\mu\text{mol/g-cat.h}$) followed by Hematite (Fe₂O₃) which is 241.656 $\mu\text{mol/g.h}$, Manganese Oxide (MnO) which is 239.256 $\mu\text{mol/g.h}$, Manganese Zinc Ferrite (MnZnFe₂O₄) which is 238.4856 $\mu\text{mole/h.g-cat}$ and last but not least is Magnetite (Fe₃O₄) which is 235.1256 $\mu\text{mol/g.h}$. The iron ions in the two coordination sites of Yttrium iron garnet (YIG) exhibit different spins which resulting in magnetic behavior. YIG gas high Faraday Effect, high Q factor in microwave frequencies and very small linewidth in electron spin resonance. Yttrium iron garnet (YIG) powders with particle sizes of 9 and 14 nm exhibited super-paramagnetism. The blocking temperature (T_B) decreased with decreasing particle size, whereas the anisotropy constant (K) increased. The saturation magnetization (M_s) decreased with decreasing particle size. These variations are attributed to large surface-to-volume ratios in nanoparticles where the surface moments are predominant. [69] YIG exhibit excellent features of the ferrite/polymer composites, such as sharply reduced dielectric loss compared to in the bulk ferrites, while uninfluenced microwave absorption properties owing to the domination of natural ferromagnetic resonance absorption in the loss mechanism of the ferrite absorber materials, [70] make them quite attractive for applications not only as inductive and capacitive materials but also as microwave absorber materials. [71]

On the other hand, Fe_3O_4 exhibits super para-magnetism which might be more applicable in industry while $\alpha\text{-Fe}_2\text{O}_3$ nanoparticle has correspondingly the similar catalytic performance as Fe_3O_4 while it has no magnetic property which makes it less applicable in industrial production as shown in Table 11 below. [72]

Table 10 : Preparation of 5-substituted 1H-tetrazoles with various catalysts [72]

Catalyst	BET surface area/($\text{m}^2\cdot\text{g}^{-1}$)	Yield/% [61]
Fe_3O_4	63.5	37.9
$\alpha\text{-Fe}_2\text{O}_3$	87.2	49.1

Iron oxide-based materials have been found to be good candidates as cheap and efficient catalysts (Miyata, 1978) studied the catalytic activity of several iron oxides and oxide hydroxides of various particle sizes for the reduction of 4-nitrotoluene using hydrazine hydrate as reducing agent, and found $\beta\text{-FeOOH}$ was the most effective catalyst. Nano-particle iron oxide is significantly more effective than conventional micron-sized iron oxide (Walker, 1988; Li, 2003) for the oxidation of CO and the oxidative pyrolysis of biomass (Li, 2003) or biomass model compounds (Li, 2004; Shin, 2004). Hematite($\text{C}/\alpha\text{-Fe}_2\text{O}_3$) composite nanotube arrays on large-area flexible alloy substrate, with a large number of pores and uniform carbon distribution at a nano-scale in the nanotube walls. These arrays have been demonstrated as excellent additive-free anode materials for lithium ion batteries in terms of good cycling performance up to 150 times (659 mA h g^{-1}) and outstanding rate capability. [73]

Experiment 5: Synthesis of Ammonia at Different Temperature of Inlet Gas

The synthesis of ammonia is done at 0.1 Tesla at 0°C system temperature using YIG nanocatalyst. In this experiment, the reactant gases inlet stream was heated until 100°C in order to ease the hydrogen bond breakage. The different of ammonia yield between inlet gases at room temperature and inlet gases heated is then observed.

Type of Catalyst	Inlet Gas T (°C)	HCl _{excess} =NaOH	HCl _{reacted} =NH ₃	Mole fraction NH ₃
Y ₃ Fe ₅ O ₁₂ (YIG) at 0°C	25°C	=0.96 x 10 ⁻⁶ mole	=(2.5 x 10 ⁻⁵ mole)- (0.96 x 10 ⁻⁶ mole) =2.404 x 10 ⁻⁵ mole	NH ₃ = 2.404x 10 ⁻⁵ mole Yield=240.4μmol/h.g-cat
Y ₃ Fe ₅ O ₁₂ (YIG) at 0°C	100°C	=0.96 x 10 ⁻⁶ mole	=(2.5 x 10 ⁻⁵ mole)- (0.96 x 10 ⁻⁶ mole) =2.404 x 10 ⁻⁵ mole	NH ₃ = 2.404x 10 ⁻⁵ mole Yield=240.4μmol/h.g-cat

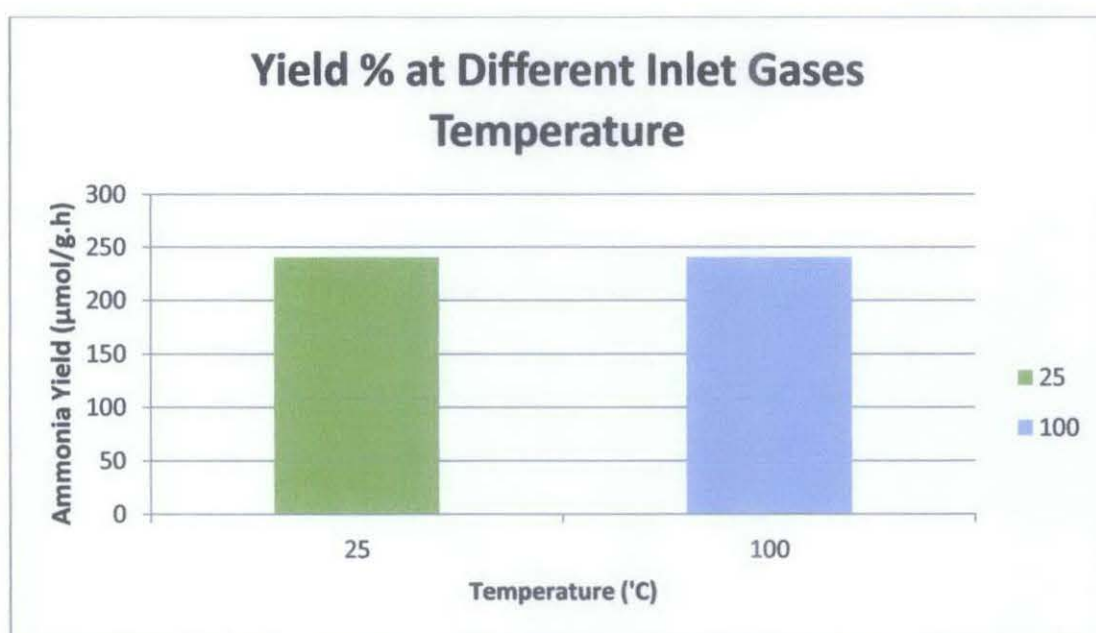


Figure 44 : Yield of Ammonia at Different Temperature of Inlet Gas

The purpose of heating the inlet gases before enter the reactor is to break the hydrogen bondage so that the adsorption process easier to occur. However, based on calculation, the temperature required to break the hydrogen bondage in this system is very huge that is $\Delta T = 14829.49$ °C.

A simple method to calculate the enthalpy change of a reaction is to measure the temperature change caused by the reaction. ΔT depends on:

- ΔH , the enthalpy of the reaction.
- m , the mass of the sample which changes temperature.
- c_p , the heat capacity of the substance which changes temperature.

The heat capacity measures how much energy is required to change the temperature of 1 g of the substance by 1 °C.

$$\Delta H = mc_p \Delta T$$

This will give the energy released during the reaction i.e. kJ. To calculate the *molar* enthalpy change, kJ mol⁻¹, we have to divide by the number of moles used in the reaction.

H-H bond is broken at enthalpy of = 436kJ/mol

$$\Delta H = m c_p \Delta T$$

$$436 \text{ kJ/mol} = (0.00026964 \text{ kg} \times 14.32 \text{ kJ/kg.K} \times \Delta T) / 0.13375 \text{ mol H}_2$$

$$\Delta T = 15102.64 \text{ K}$$

$$\Delta T = 14829.49 \text{ }^\circ\text{C}$$

Figure 44 shows that there are no different in yield percentage between two situations when inlet gas at room temperature (25°C) and when the gases were heated to 100°C.

Experiment 6: Synthesis of Ammonia at Different TPR Condition

The ammonia synthesis is done at 0.1 Tesla at 0°C temperature using Manganese Oxide (MnO) nanocatalyst. Firstly, the reaction is done by using reduced nanocatalyst and the experiment is repeated by using unreduced nanocatalyst to observe the different between ammonia yield between reduced and unreduced nanocatalysts. Next, the experiment is repeated by using Hematite nanocatalyst.

Type of Catalyst	Condition	HCl _{excess} =NaOH	HCl _{reacted} =NH ₃	Mole fraction NH ₃
Manganese Oxide (MnO)	With TPR	=1.1 x 10 ⁻⁶ mole	=(2.5 x 10 ⁻⁵ mole)-(1.1 x 10 ⁻⁶ mole) =2.392 x 10 ⁻⁵ mole	NH ₃ = 2.05 x 10 ⁻⁵ mole Yield=239.2µmol/h.g-cat

Manganese Oxide (MnO)	Without TPR	$=6.24 \times 10^{-7}$ mole	$= (2.5 \times 10^{-5} \text{ mole}) - (0.4 \times 10^{-6} \text{ mole})$ $= 2.44 \times 10^{-5}$ mole	$\text{NH}_3 = 2.46 \times 10^{-5}$ mole Yield = 243.76 $\mu\text{mol/h.g-cat}$
Hematite (Fe₂O₃)	With TPR	$= 0.84 \times 10^{-6}$ mole	$= (2.5 \times 10^{-5} \text{ mole}) - (0.84 \times 10^{-6} \text{ mole})$ $= 2.416 \times 10^{-5}$ mole	$\text{NH}_3 = 2.15 \times 10^{-5}$ mole Yield = 241.6 $\mu\text{mol/h.g-cat}$
Hematite (Fe₂O₃)	Without TPR	$= 0.48 \times 10^{-6}$ mole	$= (2.5 \times 10^{-5} \text{ mole}) - (0.48 \times 10^{-6} \text{ mole})$ $= 2.452 \times 10^{-5}$ mole	$\text{NH}_3 = 2.452 \times 10^{-5}$ mole Yield = 245.2 $\mu\text{mol/h.g-cat}$

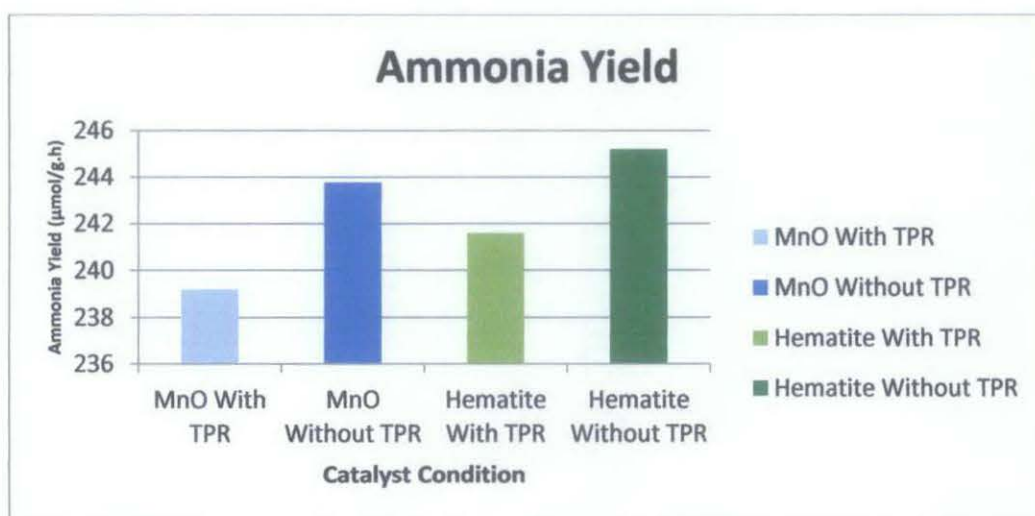


Figure 45 : Ammonia Synthesis at Different TPR Condition

The function of Temperature Programmed Reduction is to reduce the oxidized catalyst to metallic state. Catalyst with TPR means catalyst is in metallic state while Catalyst without TPR is catalyst that contains oxygen. Figure 45 shows that the ammonia yield is 1.87% higher by using unreduced manganese oxide nanocatalyst ($243.76 \mu\text{mole/h/g-cat}$) and 1.45% higher using unreduced hematite nanocatalyst since oxygen is paramagnetic. Oxygen is attracted by the magnetic field but does not

remain magnetic once it leaves the field. The reason that it is paramagnetic is because the oxygen molecule has two unpaired electrons. Electrons not only go around the atom in their orbitals, they also spin, which creates a magnetic field. Unpaired electrons spin in the same direction as each other, which increases the magnetic field effect. When the electron in an orbital become paired with another electron in that orbital, the new electron spins in the opposite direction and this cancels the effect of the first electron. Note that according to Valence Shell Electron Pair Repulsion theory (VSEPR), O₂ has no unpaired electrons but according to Molecular Orbital (MO) theory it does have unpaired electrons. [75]

Experiment 7: Synthesis of Ammonia at Different Magnetic Strength

In this experiment, two type of experiment were done by using permanent magnet (MIM) and soft magnet (Hemholtz Coil). For experiment 7, the ammonia synthesis was done by using Fe₂O₃ (Hematite) nanocatalyst at 0°C temperature with magnetic induction strength of 0.1Tesla. Then the experiment was repeated by using magnetic induction strength of 0.2Tesla.

Type of Catalyst	Magnetic Strength	HCl _{excess} =NaOH	HCl _{reacted} =NH ₃	Mole fraction NH ₃
Y₃Fe₅O₁₂ (YIG)	0.1 Tesla	=0.74 x 10 ⁻⁶ mole	=(2.5 x 10 ⁻⁵ mole)-(0.74 x 10 ⁻⁶ mole) =2.4256 x 10 ⁻⁵ mole	NH ₃ =2.4256 x 10 ⁻⁵ mole Yield=242.56μmol/h.g -cat
Y₃Fe₅O₁₂ (YIG)	0.2 Tesla	=0.096 x 10 ⁻⁶ mole	=(2.5 x 10 ⁻⁵ mole)-(0.096 x 10 ⁻⁶ mole) =2.4904x 10 ⁻⁵ mole	NH ₃ =2.4904x 10 ⁻⁵ mole Yield=249.04μmol/h.g -cat

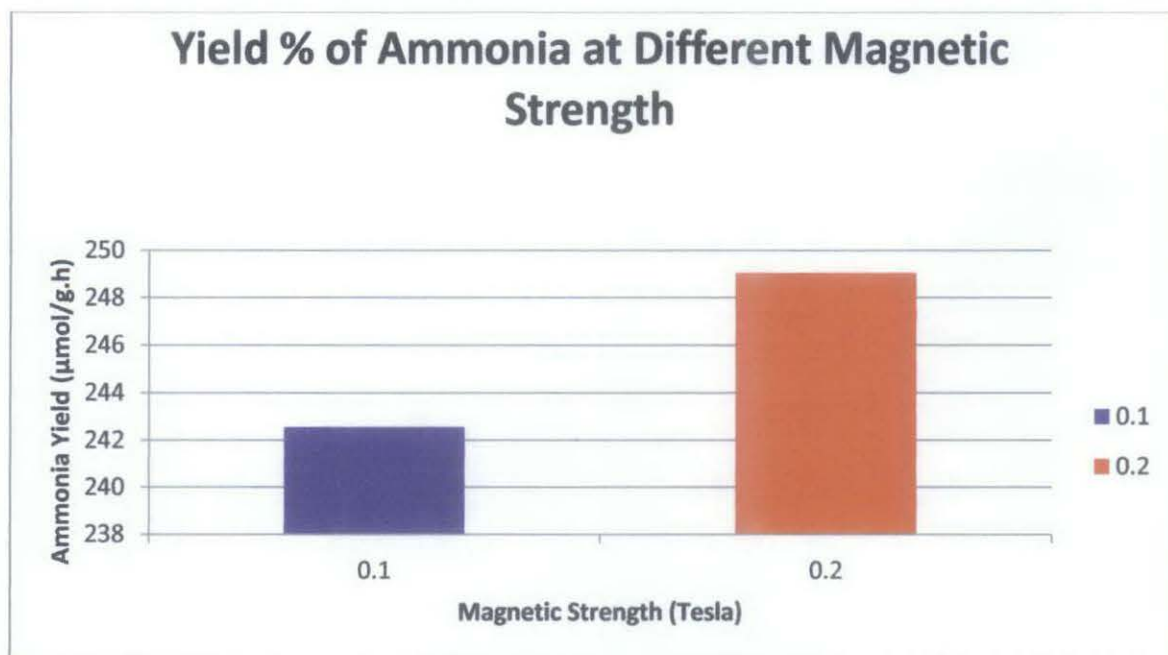


Figure 46 : Yield of Ammonia at Different Magnetic Strength

Figure 46 shows that ammonia synthesis at 0.2Tesla (249.04 μmol/g.h) is 3% higher than ammonia synthesis at 0.1Tesla (242.56μmol/g.h). As shown in the graph, the yield percentage increases significantly when the magnetic strength was increased. It approve that magnetic field can enhance the catalytic induction and enhance the yield of reaction.

Experiment 8: Synthesis of Ammonia at Different Magnetic Strength by Adding Hemholtz Coil

For experiment 8, Helmholtz Coil was added at the inlet of reactant gases stream in order to ease the hydrogen molecules to break the bond before attached to the catalyst. The reaction was done at 25°C temperature using MnO nanocatalyst.

No. of Hemholtz Coil	Magnetic Field	HCl _{excess} =NaOH	HCl _{reacted} =NH ₃	Mole fraction NH ₃
0	1	=0.9 x 10 ⁻⁶ mole	=(2.5 x 10 ⁻⁵ mole)-(0.9 x 10 ⁻⁶ mole) =2.41 x 10 ⁻⁵ mole	NH ₃ = 2.41 x 10 ⁻⁵ mole Yield=241.12μmol/h. g-cat

1	1.0015345 49	= 0.8×10^{-6} mole	= $(2.5 \times 10^{-5} \text{mole}) - (0.8 \times 10^{-6} \text{mole})$ = 2.42×10^{-5} mole	$\text{NH}_3 = 2.42 \times 10^{-5}$ mole Yield=241.6μmol/h.g -cat
6	1.0019181 86	= 0.5×10^{-6} mole	= $(2.5 \times 10^{-5} \text{mole}) - (0.5 \times 10^{-6} \text{mole})$ = 2.45×10^{-5} mole	$\text{NH}_3 = 2.45 \times 10^{-5}$ mole Yield=244.72μmol/h.g-cat

Yield of Ammonia by Adding of Hemholtz Coil

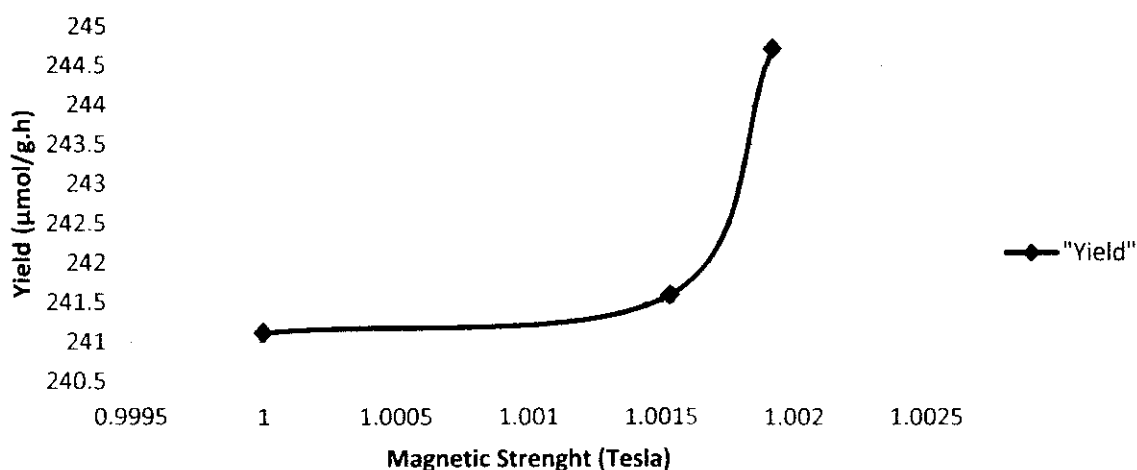


Figure 47 : Synthesis of Ammonia at Different Magnetic Field Adding Helmholtz Coils

Figure 47 shows that as the ammonia yield without addition of Helmholtz Coil is $241.12 \mu\text{mole/h.g-cat}$ while yield increase significantly after addition of a pair of Helmholtz Coil ($241.6 \mu\text{mole/g.h}$) and six pair of Helmholtz Coil ($244.72 \mu\text{mole/g.h}$). As shown in the graph, the yield percentage increases significantly when the magnetic strength was increased. It approve that magnetic field can enhance the catalytic induction and enhance the yield of reaction.

CHAPTER 5

CONCLUSION AND RECOMMENDATION

5.1 Conclusion

It is concluded that the presence of magnetic induction could enhance the yield of ammonia production as the yield for ammonia synthesis with magnetic induction using $Y_3Fe_5O_{12}$ (YIG) catalyst is $242.56\mu\text{mole/h.g-cat}$ which is much higher than yield for ammonia synthesis without magnetic induction using $Y_3Fe_5O_{12}$ (YIG) catalyst which is $10\mu\text{mole/h.g-cat}$ only. Besides, the Curie point also plays significant effect on electron spin alignment. At temperatures below the Curie point, the magnetic moments are partially aligned within magnetic domains in ferromagnetic materials. As the temperature is increased, thermal fluctuations increasingly destroy this alignment. Experiment of ammonia synthesis at different temperature of 0°C and 25°C prove that ammonia yield is higher at temperature of 0°C which is $242.56\mu\text{mole/h.g-cat}$ while $240.4\mu\text{mole/h.g-cat}$ at 25°C . High magnetic strength also contributes to the higher catalytic activity. Synthesis of ammonia at different magnetic strength shows that yield at 0.2Tesla is higher than yield at 0.1Tesla which is $249.04\mu\text{mole/h.g-cat}$ and $242.56\mu\text{mole/h.g-cat}$ respectively and addition of Helmholtz Coils at the inlet of reactant gases stream also contributes to the yield enhancement since ammonia synthesis yield is $244.72\mu\text{mole/g.h}$ with six pair of Helmholtz Coils while yield is $241.12\mu\text{mole/g.h}$ without Helmholtz Coil. Results prove that as more magnetic field applied, more effective the catalytic activity will be. Catalytic reaction giving emphasis on types of catalysts was also reviewed in this chapter. $Y_3Fe_5O_{12}$ (YIG) shows the best catalytic reaction ($242.56\mu\text{mol/g-cat.h}$) followed by Fe_2O_3 (Hematite) and MnO (Manganese Oxide) which is $241.656\mu\text{mol/g.h}$ and $239.256\mu\text{mol/g.h}$ respectively.

5.2 Recommendations

From this study, it shown that the ammonia yield is lower than the industry since we use pressure of only 1 atm. It is recommended to use higher pressure to gain higher yield of ammonia as follow to the Le Chartelier's Principle. Moreover, the reactor used in this project is limited up to 0.2Tesla magnetic strength only, study shows that it is recommended to use higher magnetic field strength up to 20Tesla for a better alignment of electron spin and for a better enhancement in yield. Other than that, to maintain the temperature of insulator, chiller is recommended to be used in industry.

REFERENCES

- [1] Chemsystems. Prospectus (September 2009/2010). (2011). *Ammonia*. Retrieved November 09, 2011 from www.chemsystem.com
- [2] *Second Industrial Revolution, 1870-1914 / New science, new materials, new power / New chemicals: Ammonia*. Retrieved November 09, 2011 from www.makingthemodernworld.org.uk
- [3] Jim Clark. (2002). *Haber Process*. Retrieved November 09, 2011 from www.chemguide.co.uk/physical/equilibria/haber
- [4] Ozzie. (2004). *Haber Process Research Site*. Retrieved November 07, 2011 from, Haberchemistry.tripod.com
- [5] *Ammonia and Urea Strategic Business Analysis*. Retrieved April 20, 2011 from, www.chemsytem.com
- [6] G.T. Austin, N. Basta. (1998). *Shreve's Chemical Process Industries Handbook*, 5th Edition, McGraw-Hill
- [7] M Appl, Dr. H L Roy (1986) *Memorial Lecture in Annual Meeting of Indian Institute of Chemical Engineers, Hyderabad*
- [8] H Bakemeier and others, (1997) *Ammonia, Ullmann's Encyclopedia of Industrial Chemistry*, Vol. A2, VCH, Weinheim
- [9] Z Kowalczyk, S Jodzic and J Sentek, 1996. *Applied Catalysis A: General*, Source 138, (pp.83)
- [10] Somorjai G.A. (1994) *Introduction to Surface Chemistry and Catalysis*, Wiley, New York
- [11] Somorjai G.A. (1981) *Chemistry in Two Dimensions: Surfaces*, Cornell University Press, Ithaca and New York
- [12] Sandra Bencic. (2001) *Ammonia Synthesis Promoted by Iron Catalysts*, Literature Report, Department of Chemistry, Michigan State University
- [13] S.M. Yunusov, B.L. Moroz, A.S. Ivanova, V.A. Likholobov, V.B. Shur. (1998) *J. Mol. Catal. A: Chem.* Source 132, (pp.263)
- [14] S.M. Yunusov, E.S. Kalyuzhnaya, H. Mahapatra, V.K. Puri, V.A. Likholobov, V.B. Shur. (1999) *J. Mol. Catal. A: Chem.* Source 139 (pp.219)
- [15] S.M. Yunusov, E.S. Kalyuzhnaya, B.L. Moroz, A.S. Ivanova, T.V. Reshetenko, L.B. Avdeeva, V.A. Likholobov, V.B. Shur. (2004), *New ammonia synthesis*

- catalysts based on supported potassium carbonyl ruthenates as precursors of catalytically active ruthenium particles and potassium promote*, Journal of Molecular Catalysis A: Chemical Source 219 (pp.149–153)
- [16] R.Kojima, H. Enomoto, M.Muhler, K. Aika (2003). *Cesium-promoted rhenium catalysts supported on alumina for ammonia synthesis*. Applied Catalysis A: General 246 (pp. 311–322)
- [17] Svend Erik Nielsen. (April 2007). *Latest Development In Ammonia Production Technology*. Haldor Topsoe A/S Lyngby, Denmark Latest Developments in Ammonia Production Technology
- [18] (2009). *Universal Industrial Gases, Inc.*
- [19] (2007). *Universal Industrial Gases, Inc.*
- [20] U.S. Department of Labor n.d
- [21] (2011). www.icis.com
- [22] FCPS Science SOL Review Booklet. (2005/2006). *Energy Transformation*. (pp.117-130). Retrieved 01 November, 2011 from www.wsanford.com
- [23] Gale Cengage.(2003), *World of Earth Science*
- [24] *Law of Thermodynamics*. Retrieved 09 November, 2011 from www-spod.gsfc.nasa.gov
- [25] *National Aeronautics and Space Administration*. Retrieved 25 october 25, 2011 from, <http://www.grc.nasa.gov/WWW/k-12/airplane/thermo1>
- [26] Ingo Muller, Wolfgang H. Müller. (2009). *Fundamentals of Thermodynamics and Applications: With Historical Annotations and Many Citations*. (pp.269-271). Germany
- [27] Yunus A. Gengel, Michael A. Boles. (2011). *Thermodynamics: An Engineering Approach*. Mc-Graw Hill. (7th Edition)
- [28] *Law of Thermodynamics*. Retrieved 10 November, 2011 from www-spod.gsfc.nasa.gov
- [29] Y. F. Han, L. Chen, K. Ramesh, Z. Zhong, F. Chen, J.Chin, H. Mook. (2008) *Catalysis Today*. (Source 131, pp. 35–41)
- [30] E.R. Calderon (2008) Thesis of University of Puerto Rico Mayaguez Campus
- [31] J. Xu, H. Yang, W. Fu, K. Du, Y. Siu, J. Chen, Y. Zheng, M. Li, G. Zou. (2007) *Journal of Magnetism and Magnetic Materials*. (Source 309, pp. 307-311)
- [32] W. R. Pilecka, E. Mi'skiewicz, D. Szmigiel, Z. Kowalczyk. (2005). *Journal of Catalysis*. (Source 231, pp.11–19)

- [33] Qin, X, Ju, Y.bernard, S and Yao, N. Flame. (2005). *Synthesis of Y₂O₃: eu nanophosphors using ethanol as precursor solvents*. Journal of Materials Research Society. (Volume 20, No 11)
- [34] R. Lepley and G. L. Closs. (1973). *Chemically induced magnetic polarization*, Wiley, The University of California
- [35] U. E. Steiner, T. Ulrich. (1989) Chem. Rev. 89, 51
- [36] H. Hayashi. (2004) *Introduction to Dynamic Spin Chemistry: Magnetic Field Effects on Chemical and Biochemical Reactions*, World Scientific, Singapore
- [37] F. Z. Tang, A. Katsuki, Y. Tanimoto. (2006) *Mol. Phys.* (Source 104, pp. 1667)
- [38] K. Maeda, K. B. Henbest, F. Cintolesi, I. Kuprov, C. T. Rodgers, P. A. Liddell, D. Gust, C. R. Timmel, P. J. Hore. (2008) *Nature* (source 453, pp. 387)
- [39] R. Kaptein, J. L. Oosterhoff. (1969). *Chem. Phys.* (Lett. 4,pp.195)
- [40] G. L. Closs. J. Am. (1969). Chem. Soc. 91, 4552
- [41] K. A. McLauchlan, U. E. Steiner. (1991). *Mol. Phys.* (Source 73, pp.241)
- [42] Hemholtz Coil. Retrieved from <http://www.universetoday.com> on December 01, 2011
- [43] *Hemholtz Coil*. Retrieved from <http://physicsx.pr.erau.edu> on December 02, 2011
- [44] *Inside the Atom, Snapshots in the Gallery of Atoms and Energy*, Retrieved from <http://www.e-missions.net/ssa/CH1-insidetheatom.htm> on December 06, 2011
- [45] Lorena Tomas Laudo. (2010). *Magnetic iron nanocatalysts*. Highlights in Chemical Science. Retrieved from <http://www.rsc.org/Publishing/ChemScience/> on December 02,2011
- [46] Lorena Thomas Laudo. (2010). *Magnetic Nanocatalyst*. Retrieved from http://www.rsc.org/Publishing/ChemScience/Volume/2010/02/magnetic_iron.asp on 31 November 2011
- [47] M. Mohapatra and S. Anand. (2010). *Synthesis and applications of nano-structured iron oxides/hydroxides*. International Journal of Engineering, Science and Technology Vol. 2, No. 8, 2010 (pp. 127-146)
- [48] P. N.Rao, (2010). *Nanocatalysis: Applications in the chemical industry*. Retrieved from <http://www.nanowerk.com/spotlight/spotid> on December 02,2011
- [49] Adem Yildirim, *Nanocatalyst*. UNAM-Institute of Materials Science and Nanotechnology MSN 532: Selected Topics in Materials Science and Nanotechnology MSN 532

- [50] Joshua Rolnitzky. (2005) *Catalyst at the Nanoscale*, Nanotechnology and Society
- [51] Somojai, G.A. (1994) Wiley-Interscience, 1, pp. 452–454
- [52] Richardson, James T. (2009). *Journal of Applied Catalyst*. Issue 3, (pp.1781–1786)
- [53] Roebuck, C.M. (2008) Exeel HSC Publisher, (pp. 35–41)
- [54] Whitten, K.N., Davis, K.E., Peck, M.L., Stanley, G.G.: Thomson Brookscole, (2003) Source 7 (pp. 813–720)
- [55] Modak, J.M. (2002). *Haber process for ammonia synthesis*. Resonance, (pp.69–77)
- [56] J.C. Ganley, E.G. Seebauer, R.I. Masel. (2004). *Development of a Microreactor for the Production of Hydrogen from Ammonia*. (Sources 137 p53-61). Journal of Power
- [57] S. K. Kundra, Ekta. (2004). *Excel With Systematic Numerical Chemistry*. Golden Bell (pp. 731-732)
- [58] Professor John Blamir. (2003). *Kjeldahl Method*. Science@a Distance. Retrieved from, <http://www.brooklyn.cuny.edu> on December 02,2011
- [59] Jessen-Hansen, H. (1932) *Johan Kjeldahl*, pp.169–172 in: Meisen, V. Prominent Danish Scientists through the Ages. University Library of Copenhagen 450th Anniversary. Levin & Munksgaard, Copenhagen
- [60] S. K. Kundra, Ekta (2004), *Excel With Systematic Numerical Chemistry*, Golden Bells. (pp.714)
- [61] W.K. Jozwiak, E. Kaczmarek. (2007). *Reduction behavior of iron oxides in hydrogen and carbon monoxide atmospheres*. Applied Catalysis A: General Volume 326, Issue 1 (pp. 17-27)
- [62] M. A. Ullmann¹, A. da C. Schneid¹, D. Bianchini. *Thermal catalytic properties of Mn supported on porous silica nanostructures*.
- [63] Wataru, U., Ning, F.C., Kenzo, (1999). *O.: Chem. Commun.*, (pp.517–518)
- [64] Yucai, Y., Ping, Y., Tao, L., Jiang, Z., Dangdong, Z.: (2007) Indian J. Chem. 46a, (pp.1270–1272)
- [65] Meisheng, L., Wenkai, K., Kechang, (2009). *J. Nat. Gas Chem*. 18, (pp. 110–113)
- [66] Oliveira, L.C.A., Fabris, J.D., Rios, R.R.V.A., Mussel, W.N., Lago, R.M. (2004): *Appl. Catal. A Gen*. 259, (pp.253–259)

- [67] Flavia, G.D., Bibiana, P.B., Luis, E.C., Cristina, R., Miguel, A.C., Jose. A.O. (2009): *Appl. Catal. B Environ.* 92, (pp.194–201)
- [68] Michael E. Flatte. (2007). *Manipulating quantum coherence in solid state systems*. Springer, (pp. 100)
- [69] M. Rajendran, S. Deka, P.A. Joy, A.K. Bhattacharya. (2005). *Size-dependent magnetic properties of nanocrystalline yttrium iron garnet powders*.
- [70] Ubizskii S B, Matkowskii A O, Mironova-Ulmane N, et al 2000 *Phys. Stat. Sol. A* 177 349. Ghasemi A, Hossienpour A, Morisako A, Saatchi A, Salehi M 2006 *J. Magn. Magn. Mater.* 302 429.
- [71] Anjum Qureshi1, Ayhan Mergen1 and Bekir Aktas. (2009). *Dielectric and magnetic properties of YIG/PMMA nanocomposites*. Journal of Physics: Conference Series 153
- [72] Qi Gang, Liu Wei, Bei Zhining.(2011) *Fe₃O₄/ZnS Hollow Nanospheres: A Highly Efficient Magnetic Heterogeneous Catalyst for Synthesis of 5-Substituted 1H-Tetrazoles from Nitriles and Sodium Azide*. Chin. J. Chem. Source 29, (pp. 131—134)
- [73] M. Mohapatra and S. Anand. (2010). *Synthesis and applications of nano-structured iron oxides/hydroxides*. International Journal of Engineering, Science and Technology Vol. 2, No. 8, 2010 (pp. 127-146)
- [74] Christopher T. Rodgers (2009). *Magnetic field effects in chemical systems*. Pure and Applied Chemistry 81, (pp.19–43)
- [75] *Molecular Orbital Theory*, Retrieved on December 10, 2011 from, <http://chemed.chem.purdue.edu/>
- [76] Masuhiro Yamaguchi, Isao Yamamoto, Kiyonori Ishikawa, and Soichiro Mizusaki. (2002). *Unified consideration on magneto-thermodynamic effects in chemical reactions*, RIKEN Review No. 44

APPENDIX A
CALCULATIONS OF YIELD PERCENTAGE

$$\begin{aligned} mN_2 (g) &= 33.33 \text{ mL/min} \times 30 \text{ min} = 0.9999 \text{ L (volume)} \\ &= 0.9999 \text{ L} \times (1.251 \text{ g/L}) \\ &= 1.2508749 \text{ g } N_2 \end{aligned}$$

$$\begin{aligned} mH_2 (g) &= 100 \text{ mL/min} \times 30 \text{ min} = 3 \text{ L (volume)} \\ &= 3 \text{ L} \times (0.08988 \text{ g/L}) \\ &= 0.26964 \text{ g } H_2 \end{aligned}$$

$$\begin{aligned} \text{Actual Yield} &= \text{Taken from mole } NH_3 \text{ in Khejdhal Method} \times (17.03 \text{ g/mol}) \\ &= X \text{ g} \end{aligned}$$

$$\begin{aligned} nN_2 (\text{initial}) &= 1.2508749 \text{ g } N_2 \times (1 \text{ mol } N_2 / 28.029 \text{ g } N_2) \\ &= 0.0446278 \text{ mol } N_2 \end{aligned}$$

$$\begin{aligned} nH_2 (\text{initial}) &= 0.26964 \text{ g } H_2 \times (1 \text{ mol } H_2 / 2.016 \text{ g } H_2) \\ &= 0.13375 \text{ mol } H_2 \end{aligned}$$

Ratio of initial amount:

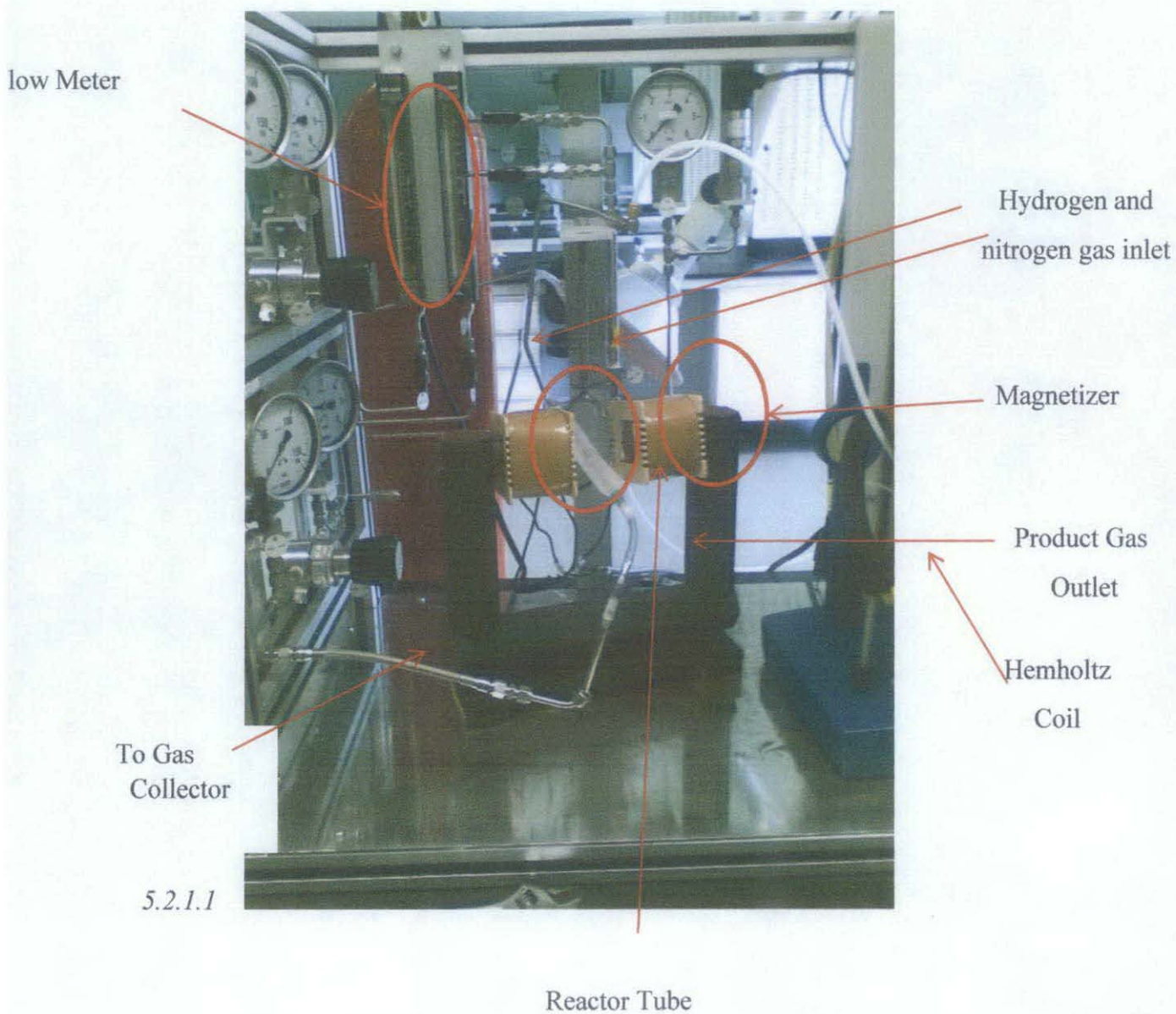
$$\begin{aligned} nH_2 / nN_2 &= 0.13375 \text{ mol } H_2 / 0.0446278 \text{ mol } N_2 \\ &= 3/1 \text{ , Hence, } N_2 \text{ is limiting reactant} \end{aligned}$$

$$\begin{aligned} nNH_3 &= 0.0446278 \text{ mol } N_2 \times (2 \text{ mol } NH_3 / 1 \text{ mol } N_2) \\ &= 0.0892556 \text{ mol } NH_3 \end{aligned}$$

$$\begin{aligned} mNH_3 &= 0.0892556 \text{ mol } NH_3 \times (17.03 \text{ g } NH_3 / 1 \text{ mol } NH_3) \\ &= 1.52 \text{ g } NH_3 \end{aligned}$$

$$\begin{aligned} \text{Percent yield} &= \text{actual yield} / \text{theoretical yield} \\ &= (X \text{ g} / 1.52 \text{ g}) \times 100 \end{aligned}$$

APPENDIX B MICRO-REACTOR



APPENDIX C
TESTING OF AMMONIA PRODUCED AT PETRONAS
FERTILIZER KEDAH BY USING DRAGGER PUMP

1) Ammonia gas is collected in gas pack



2) Dragger pump is used to test the ammonia



3) 3ppm of Ammonia Yield is noted by Dragger Tube



Ammonia presence of 3ppm is proved

APPENDIX D
FIELD TRIP TO PETRONAS FERTILIZER KEDAH



Supervisor:
Dr. Noorhana
Yahya

Author:
Norhasifah Binti Noordin